Comprehensive Proteomics of
Sorangium cellulosum So ce56

Dissertation

to obtain the academic title
Doctor of Natural Sciences
(Dr. rer. nat.)
at the Faculty of Biology
in the University of Bielefeld

by
Dipl. Biol. Aysel Alici
from
Höxter, Germany

October 2007

„Nicht das Beginnen wird belohnt,

sondern einzig und allein das Durchhalten."

Katharina von Siena (1347 – 1380)

Dedicated to my parents

Table of Contents

List of Figures

List of Tables

List of Abbrevations

ABC	ATP-binding cassette
APS	ammonium persulphate
ATP	adenosine triphosphate
BN	Blue Native
bp	base pairs
CDS	coding sequences
CHS	chalcone synthase
COG	Cluster of orthologous groups of proteins
Da	dalton (1 Da = 1.6605402 x 10-24 g)
DIGE	difference gel electrophoresis
DNA	deoxyribonucleic acid
dpi	days post inoculum
DTT	dithiothreitol
E. coli	Escherichia coli
EDTA	ethylene diamine tetra acetic acid
e.g.	exempli gratia (for example)
EPS	exopolysaccharide
ESI	electro spray ionization
et al.	et alii (and other)
Fig.	figure
g	gramm
h	hours
HPLC	high performance liquid chromatography
i.e.	id est (that means)
IEF	isoelectric focusing
l	liter
LC	liquid chromatography
MALDI	matrix-assisted laser desorption/ionization
Mb	mega base pairs
µg	microgramm
min	minute
MS	mass spectrometry
MW	molecular weight
M. xanthus	Myxococcus xanthus
NADPH	nicotinamide adenine dinucleotide phosphate
NCBI	National center for biotechnology information
nm	nano meter
NRPS	nonribosomal peptide synthetase

OMP	outer membrane protein
OMV	outer membrane vesicle
ORF	open reading frame
PAGE	polyacrylamide gel electrophoresis
PKS	polyketide synthase
PMF	peptide mass fingerprint
pI	isoelectric point
PTS	phosphoenol-pyruvate:sugar phosphotransferase system
RND	resistance-nodulation-cell division transporter superfamily
rpm	rounds per minute
SDS	sodium dodecyl sulfate
So ce	Sorangium cellulosum
sp.	species
Tab.	table
Tat	twin arginine translocator
TBS	Tris-buffered saline
TCA	tricarboxylic acid cycle
TEMED	N,N,N',N' – tetramethylethylene-diamine
TIGR	The institute for genomic research
TOF	time of flight
Tris	N-tris-(hydroxymethyl)-amino methane
V	volt
v/v	volume per volume
W	watt
w/v	weight per volume
1-D	one-dimensional
2-D	two-dimensional

Summary

In this work an extensive proteomic approach for *Sorangium cellulosum* So ce56 was developed and applied encompassing the extraction of different subproteomes: the cytoplasmic, membrane, extracellular and outer membrane vesicle fractions of So ce56. Consequently, a proteome reference map of *Sorangium cellulosum* So ce56 cytosolic proteins was established. Moreover, proteome analyzes were performed for the identification of proteins involved in the regulation of secondary metabolite biosynthesis, morphogenetic differentiation (fruiting body formation), signal transduction, transport process or gliding motility activities. A 2-D proteome map of So ce56 cytoplasmic proteins expressed during stationary phase was established and analyzed by MALDI-TOF-MS. 115 different cytosolic proteins of the 300 processed protein spots were identified and classified into COG categories. As expected, a large number of identified functionally annotated cytosolic proteins (75%) were involved in primary metabolic pathways, e.g. glycolysis, tricarboxylic acid (TCA) cycle and fatty acid degradation. This finding was supported by the analysis of tyrosine and serine phosphorylated proteins via Western Blot method resulting in the detection of many proteins activated during primary metabolism. Differentially expressed cytosolic proteins of the exponential phase and stationary phase from So ce56 were identified using DIGE technology. Additionally, the use of Blue-Native PAGE from the cytosolic and membrane fraction led to the identification of proteins belonging to protein complexes which are involved in different cellular processes, e.g. secondary metabolite production. Isolation of extracellular proteins by the phenol-extraction method resulted in the identification of 41 unique extracellular proteins which were shown to be enzymes mainly involved in biomacromolecule degradation like cellulase. To overcome analytical limitations created by the hydrophobic nature of membrane proteins a specific extraction procedure was adapted. SDS-PAGE preparation and consequent nanoLC-ESI-MS/MS analysis led to the identification of 66 proteins of the entire membrane fraction. For a detailed view, the outer membrane proteins were analyzed separately, which revealed the identification of 35 proteins from the outer membrane fraction. The identification of a putative serine histidine kinase in the membrane fraction showed a significant correlation with a sensor kinase in the jerangolid or ambruticin biosynthetic gene cluster isolated from other *Sorangium* strains. This discovery indicates further genes

nearby which might be participating in the jerangolid or ambruticin polyketide biosynthetic gene cluster. Genomic and metabolomic approaches are additionally needed to characterize this putative fifth polyketide biosynthesis. Moreover, outer membrane vesicles (OMVs) of So ce56 could be visualized via electron microscopy, which might indicate a transport system of this myxobacteria. In total about 241 different proteins originating from the different cellular localizations could be identified.

Zusammenfassung

In dieser Arbeit wurden umfangreiche Proteomanalysen von *Sorangium cellulosum* So ce56 durchgeführt, wobei Proteine aus den verschiedenen zellulären Kompartimenten untersucht worden sind: Proteine aus dem Cytosol, sekretierte Proteine, Membran- und Vesikelproteine. Diese Untersuchungen hatten zum Ziel, Proteine in So ce56 zu identifizieren, die an morphologischen Differenzierungsprozessen, wie der Bildung von Früchtkörpern, der Biosynthese von Sekundärmetaboliten, sowie an Transportprozessen, bei der Signaltransduktion und bei der Zellfortbewegung beteiligt sind. Die isolierten Proteine wurden unter konstanten Wachstumsbedingungen in der frühen stationären Phase elektrophoretisch aufgetrennt. Die Identifizierung der differentiell auftretenden Proteine erfolgte mittels MALDI-TOF-MS und nanoLC-ESI-MS. So wurden 115 differentielle Proteine aus der cytosolischen Fraktion identifiziert, die vorwiegend an Primärstoffwechselprozessen von So ce56 beteiligt sind. Desweiteren wurden Phasenspezifische Proteine (exponentielle und frühe stationäre Phase) mittels Differentieller Gelelektrophorese (DIGE) analysiert. Proteine, die in der Signaltransduktion involviert sind, wurden zusätzlich mit Westernblotanalysen detektiert, insbesondere die Phosphorylierungen an Tyrosin und Serin. Die Untersuchung des Sekretoms von So ce56 führte zur Indentifizierung von 41 verschiedenen Proteinen, die hauptsächlich hydrolytische Funktionen aufzeigen. Um die Identifizierung und Charakterisierung des So ce56 Proteoms zu erweitern, wurden neben den cytosolischen und sekretorischen Proteinen auch die Membran- und die Vesikelproteine untersucht. Mit Hilfe von 1-D Gelen und Blue-Native Gelen konnten hydrophobische Proteine und Proteine, die in Proteinkomplexen gebunden sind, detektiert und massenspektrometrisch analysiert werden. Die Analyse der Membraneproteine resultierte in 66 identifizierten Proteinen. Zusätzlich wurden durch Untersuchungen der äußeren Membran weitere 35 Proteine identifiziert. Interessant war der Fund einer Sensorkinase, die einen hohen Homologiegrad zur Sensorkinase des Jerangolid/ Ambruticin Biosyntheseclusters (So ce307 und So ce10) aufzeigte. Überdies wurden noch elektronenmikroskopische Aufnahmen von Vesikelproteinen erstellt, die möglicherweise eine wichtige Transportfunktion in So ce56 übernehmen. Durch diese Proteomarbeit von So ce56 wurden insgesamt 247 verschiedene Proteine identifiziert, die ihren funktionalen Klassen zugeordnet werden konnten.

1 Introduction

The availability of complete genome sequences allows the entire potential protein complement of different organisms to be defined. Sequence analyzes of simple organisms like bacteria (e.g. *Escherichia coli*) to more complex organisms as eukaryotes (e.g. *Saccharomyces cerevisiae*) have already been determined. Therefore, it was a matter of time to analyze the large and complex myxobacterial genomes such as *Myxococus xanthus* with 9.14 Mb and *Sorangium cellulosum* with 13.2 Mb, which are currently sequenced and annotated resulting in a vast data of genome information (Goldmann *et al.*, 2006; Schneiker *et al.*, 2007). Many cellular activities in myxobacteria like transcription and translation, post-translational modifications and protein turn over underlie changes depending on the environment, resulting in qualitative and quantitative changes detectable at different levels, e.g. the protein and/or metabolome level. Therefore, a number of different approaches are needed for the functional analysis of novel genes and products in myxobacteria. These approaches include large-scale analyze of: protein expression (proteomics) and metabolite production (metabolomics). The availability of fully sequenced genomes of myxobacteria facilitates the discovery of gene products and their functions. Proteomics complements genomics because it focuses on gene products, which are the active elements of cells (Pennington *et al.*, 1997; Wilkins *et al.*, 1996). Moreover, proteins undergo protein-protein interaction and different post-translational modifications such as phosphorylation, glycosylation, ubiquititation and acetylation, which influence their function but can not be deduced from the RNA or DNA sequence. Protein modifications and expression levels can be detected by proteomic techniques (Lottspeich, 1999; Nock & Wagner, 2000; Lohaus *et al.*, 1998; Pandey & Mann, 2000).

1.1   Myxobacteria

Myxobacteria are Gram-negative obligate aerobic bacteria. Characteristic for myxobacteria is their ability to glide in swarms, to feed cooperatively, and to form under unfavorable conditions fruiting bodies with structures of varying complexity and often brightly colored (Reichenbach & Dworkin, 1992). Another interesting feature is that myxobacteria produce a high number of bioactive secondary metabolites like

fungi or actinomycetes (Hopwood, 1997; Rawlings, 1999). Myxobacteria mainly occur in soil, dung, decaying plant material, and the bark of trees and generally prefer a neutral pH and are therefore considered as mesophilic soil microbes with a temperature optimum of 30 °C. Other reports show that myxobacteria are also able to live in extreme environments, e.g., in antarctic soils (Dawid *et al.*, 1988) and in marine environments (Reichenbach, 1999). *Polyangium vitellinum* (today *Kofleria flava*), the first myxobacterium was discovered by the German botanist H.F. Link in 1809 (Reichenbach & Dworkin, 1992). Due to its fruiting bodies, the bacteria were termed as "gasteromycete" (fungi). In 1857, the British mycologist M.J. Berkeley discovered two additional species, *Stigmatella aurantiaca* and *Chondromyces crocatus,* which he classified as hyphomycetes (fungi imperfecti) (Berkeley, 1857). The genera name "myxobacteria" was formed by the American botanist Roland Thaxter in 1892 who was the first scientist to describe their life cycle (Thaxter, 1892).

Contemporary, phylogenetic analyze, by comparison of the 16S rRNA, reveal that myxobacteria belong to the delta branch of the proteobacteria (Ludwig *et al.*, 1983). Based on morphological and physiological features and after several renamings, the order *Myxococcales* (myxobacteria) can be divided into three subgroups *Cystobacterineae, Sorangineae,* and *Nannocystineae* (Reichenbach, 2004; Shimkets *et al.*, 2005), six families, 17 genera and about 50 species (Fig.1).

Myxococcus xanthus, Corallococcus sp*., Archangium* sp. and *Stigmatella aurea* are typical members of the first subgroup and mainly obtain nutritional substrates by proteolytic or bacteriolytic activities. They feed upon other bacteria, utilizing the protein and lipid fraction as carbon and energy sources. The vegetative cells are slender and have tapering ends up to 1 µm in diameter and up to 20 µm in length. *Myxococcus xanthus* is the most extensively studied model organism among myxobacteria, and has a genome size of 9.14 Mb (Goldman *et al*., 2006).

The *Sorangineae* like *Sorangium (Polyangium) cellulosum* and the *Byssophaga* genera are cellulose degraders and use inorganic nitrogen compounds while growing on cellulose and glucose (Reichenbach & Dworkin, 1992; Reichenbach, 2004). The vegetative cells of this suborder are mainly cylindrical rods with rounded ends up to 1 µm wide and 10 µm long. In contrast, other members of the *Sorangineae* subgroup like *Haploangium* and *Chondromyces* and the subgroup *Nannocystineae* show in feeding experiments no cellulolytic activity. The analysis of *Sorangium cellulosum*

provides new insights into the biology of *Sorangium* species and also for other myxobacterial strains. Therefore, the So ce56 strain is used as model organism with favorable features compared to other strains which are presented in the next chapter.
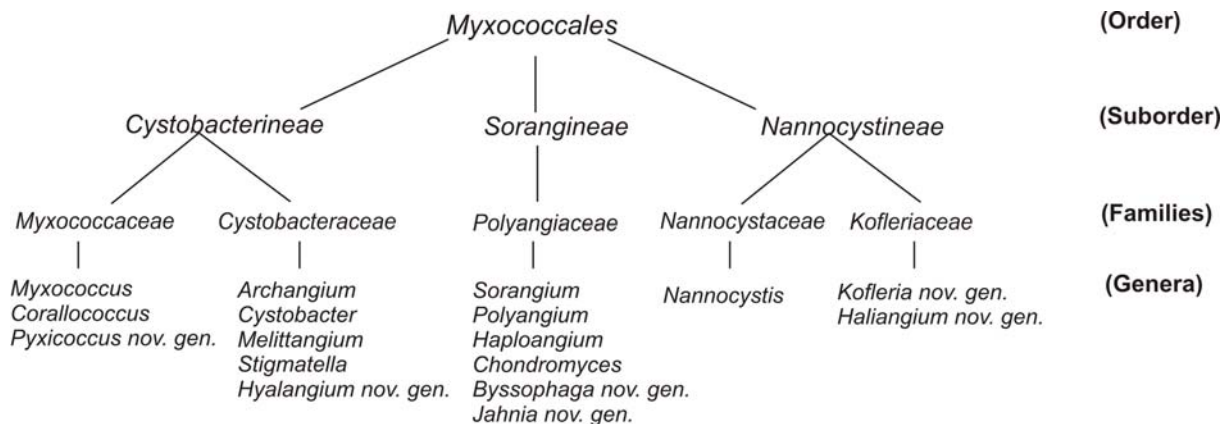
Fig. 1: Taxonomy of myxobacteria (Reichenbach, 2004; Shimkets *et al.*, 2005).

1.2 *Sorangium cellulosum* So ce56

For a better understanding of the genus *Sorangium*, the model strain *Sorangium cellulosum* So ce56 was chosen for a functional genomic approach in the "Genomik" network funded by the German Ministry of Education and Research (BMBF) in 2001. With the recent completion of the genome sequence and annotation of So ce56 (Schneiker *et al.*, 2007) a sound basis information is available to facilitate future works. Compared to other *Sorangium* strains, So ce56 exhibits features like a relatively short generation time (7 h) and a homogeneous growth in a defined liquid medium, which facilitates handling in the laboratory (Gerth *et al.*, 2003; Müller & Gerth, 2006). *Sorangium cellulosum* So ce56 colonies and fruiting bodies are orange coloured and exhibit swarming patterns like other myxobacteria (Fig.2). This bacterium harbors the largest bacterial genome (circular) known up to now (13 Mb) encoding about 9367 predicted protein coding sequences (CDS) (Schneiker *et al.*, 2007; Pradella *et al.*, 2002). It can be expected that a high number of proteins (enzymes) are needed for the regulation of the various cellular processes involved in the complex lifestyle of this bacterium. Putative functions could be assigned to 4895 (52.2%) of the encoded proteins on the basis of manual annotation. About 1224 (13.1%) are conserved hypothetical proteins showing similarities to other proteins encoded by bacterial genomes. In contrast, the remaining 3248 (34.7%) proteins

show no significant similarities to predicted proteins stored in public databases. BLASTP comparisons of So ce56 to itself display that 36% (3402) of the predicted genes constitute 772 families of paralogous genes. The largest family consists of serine/threonine/tyrosine protein kinases (eukaryotic protein kinase-like kinases (ELKs)) and histidine kinases with 498 members. The abundance of the high number of protein kinases indicates the high activity of this bacterium regulating the complex and multicellular lifestyle of this strain.
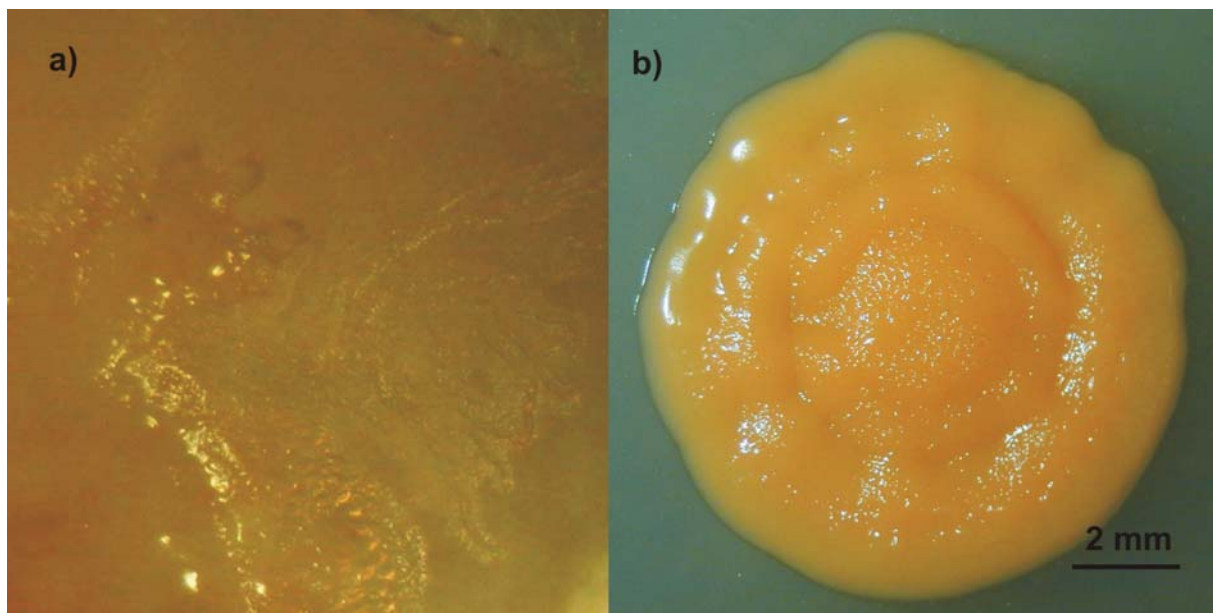
Fig. 2: a) *Sorangium cellulosum* So ce56 swarming after 7 dpi on solid P-medium. b) Colony of *Sorangium cellulosum* So ce56.

One of the interesting features of So ce56, which has to be controlled, is the ability to produce secondary metabolites mainly produced to inhibit eukaryotic and prokaryotic competitors in the habitat, e.g. fungi. Up to now, metabolic screening of So ce56 led to the characterization of three secondary metabolites of biotechnological importance: (i) chivosazol, (ii) etnangien and (iii) myxochelin.
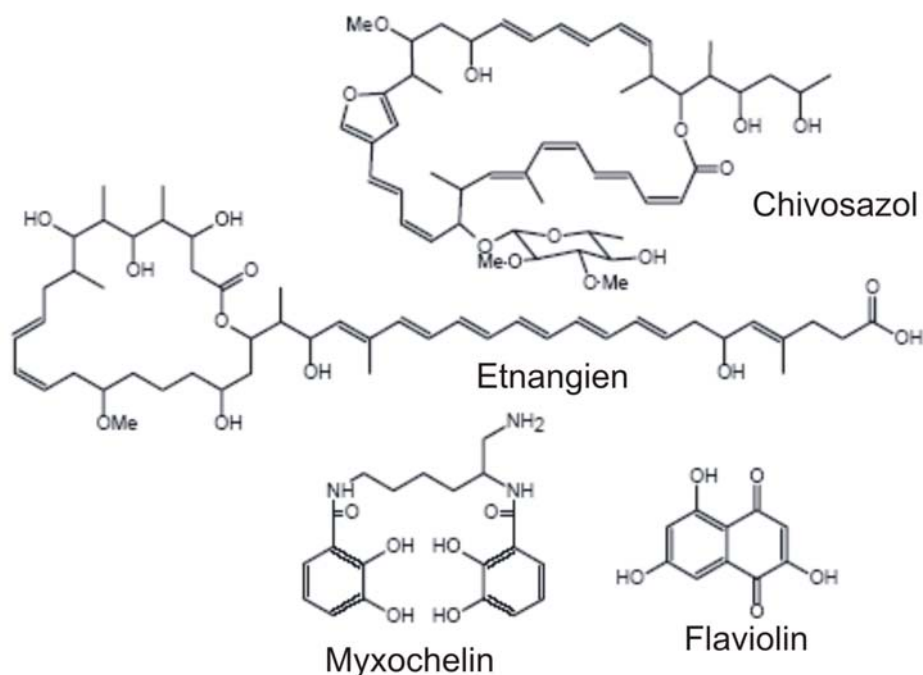
Fig. 3: Secondary metabolites of *Sorangium cellulosum* So ce56 (Schneiker *et al.*, 2007).

The macrolide chivosazol exhibits cytotoxic effects on fungi but not on bacteria (Jansen *et a*l., 1997; Irschik *et al.*, 1995, Perlova *et al.*, 2006). The secondary metabolite etnangien inhibits growth of Gram-positive bacteria by acting as a general nucleic acid polymerase (DNA, RNA, RT) inhibitor (Höfle, 1995). The third compound myxochelin (NRPS) is a catecholate-type siderophore, which belongs to a bacterial iron-uptake system that is produced by many myxobacteria (Gaitatzis *et al.*, 2005). However, the genome sequence analysis revealed also the existence of further putative biosynthetic gene clusters (17 in total). Some of them might be involved in carotenoid and terpenoid biosynthesis, but many of them are more or less still unknown. The identification and characterization of these secondary metabolites are a major goal for the investigators to find a way revealing these natural products. One successful method was the heterogeneous expression of a predicted So ce56 biosynthetic gene cluster in a *Pseudomonas* strain, which led to the production of a fourth metabolic compound named flaviolin (Gross *et al.*, 2006; Bode & Müller, 2006). This experiment showed that unknown biosynthetic gene clusters of So ce56 have the potential to produce new compounds with interesting activities. For the analysis of these and further biosynthetic gene clusters, a gene transfer system (Pradella *et*

al., 2002; Kopp et al., 2004) and a quantitative gene expression system (Kegler *et al.*, 2006) for *S. cellulosum* So ce56 have already been established.

1.3   Molecular and biochemical characterization of myxobacteria

As *Sorangium* strains provides no or less information concerning major biological processes like the (i) gliding system, (ii) fruiting body formation and cell-to-cell interaction, these studies mainly deal with the investigation of the model organism *Myxococcus xanthus*. The reciprocal BLASTP comparison of the two genomes shows that only 2857 of the predicted CDS (30.5%) in the So ce56 genome are homologous to predicted CDS of *M. Xanthus* (Goldman *et al.*, 2006; Schneiker *et al.*, 2007). The production of (iii) secondary metabolites was characterized chemically upon different *Sorangium* strains, *Myxococcus xanthus* and other myxobacterial species. Due to the progress in genomics of myxobacteria, many of the secondary metabolite biosynthetic gene clusters can be characterized easily with molecular approaches.

1.3.1 Gliding motility of myxobacteria

The surface gliding motility of myxobacteria are controlled by two multigene systems, the A-system (adventurous system), which is responsible for the movement of single cells and groups of cells, while the S-system (social system) mediates only the movement of group translocation, which is essential during swarming, aggregation and fruiting body formation (Spormann, 1999). The mechanism of A-motility is proposed to be slime extrusion from cell ends through nozzle-like structures. For the S-motility the cells use type IV pili to pull themselves on solid surfaces (Fig. 4) (Kaiser, 1979, 2000; Wolgemuth *et al.*, 2002) and extracellular fibrils to mediate cell to cell contact (Kim *et al.,* 1999; Yang *et al.,* 2000).
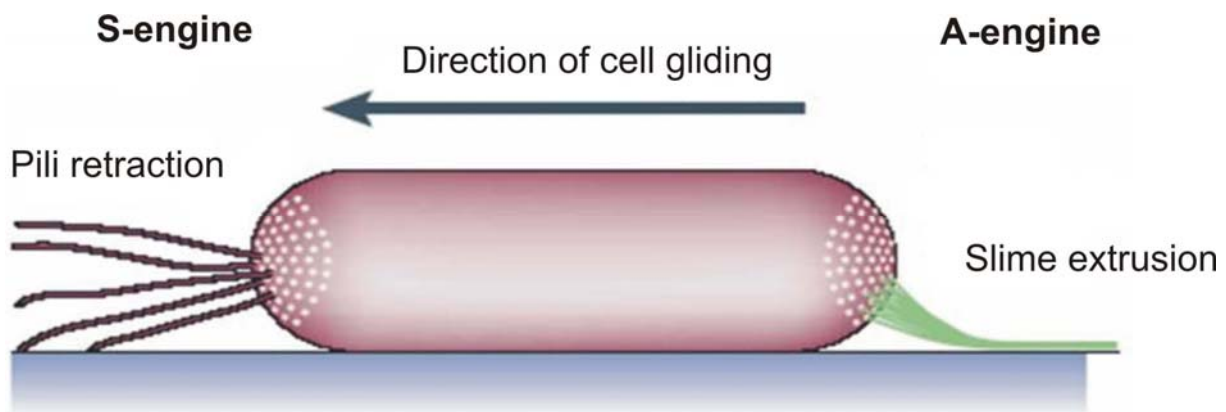
Fig. 4: Modell of the myxobacterial gliding system: the S-motility engine uses pili to pull the cells on solid surfaces, whereas the force for A-motility is generated by slime extrusion pushing the cell forward (Wolgemuth *et al.*, 2002; Kaiser, 2000).

Furthermore, the cytoplasmic Frz (frizzy) signal transduction system that interacts with the A- and S-machinery controls the directed movement of *Myxococcus xanthus* by modulating their cell reversal frequency (Blackhart & Zusman, 1985; Spormann, 1999). Frz proteins show homologies to proteins involved in chemotaxis in other bacteria. Another chemosensory signaling system is encoded by the *dif* (defective in fruiting) genes, which show also similarity to chemotaxis proteins. The DiF proteins are necessary for S-motility, fibril production and fruiting body formation (Yang *et al.*, 1998, 2000; Lancero *et al.*, 2005). Studies from Kearns and Shimket (1998) revealed that the chemoattractant phosphatidylethanolamine (PE), which is a component of the bacterial cell membrane, cause chemotactic excitation in *Myxococcus xanthus* of the Dif and the Frz system. During this reaction, the cells are able to distinguish between the different PEs: from itself by migrating to an aggregation centre during fruiting body formation and from prey to feed upon this (Kearns *et al.*, 2000, 2001). Further chemosensory machineries in *M. xanthus*, like Che3 and Che4 were characterized, which are chemotaxis-like two-component signal transduction systems (Kirby & Zusman, 2003; Vlamakis *et al.*, 2004). Moreover, there are still 4 more chemosensory systems, which are not fully characterized yet (Epperson & Kirby, 2006).

1.3.2 Fruiting body formation and cell-to-cell interaction

Under starvation conditions the myxobacterial cells undergo a remarkable cooperative morphogenesis involving 10^5-10^7 cells to produce fruiting bodies. These

fruiting bodies are resistant to several stress conditions such as desiccation, sonication and UV radiation. The morphology of fruiting bodies varies between different myxobacterial species. Whereas the *Stigmatella* and *Chondromyces* spp. form sophisticated multiple tree-like sporangioles, *Sorangium* strains produce simple knobs consisting of slime and myxospores (Fig. 5).
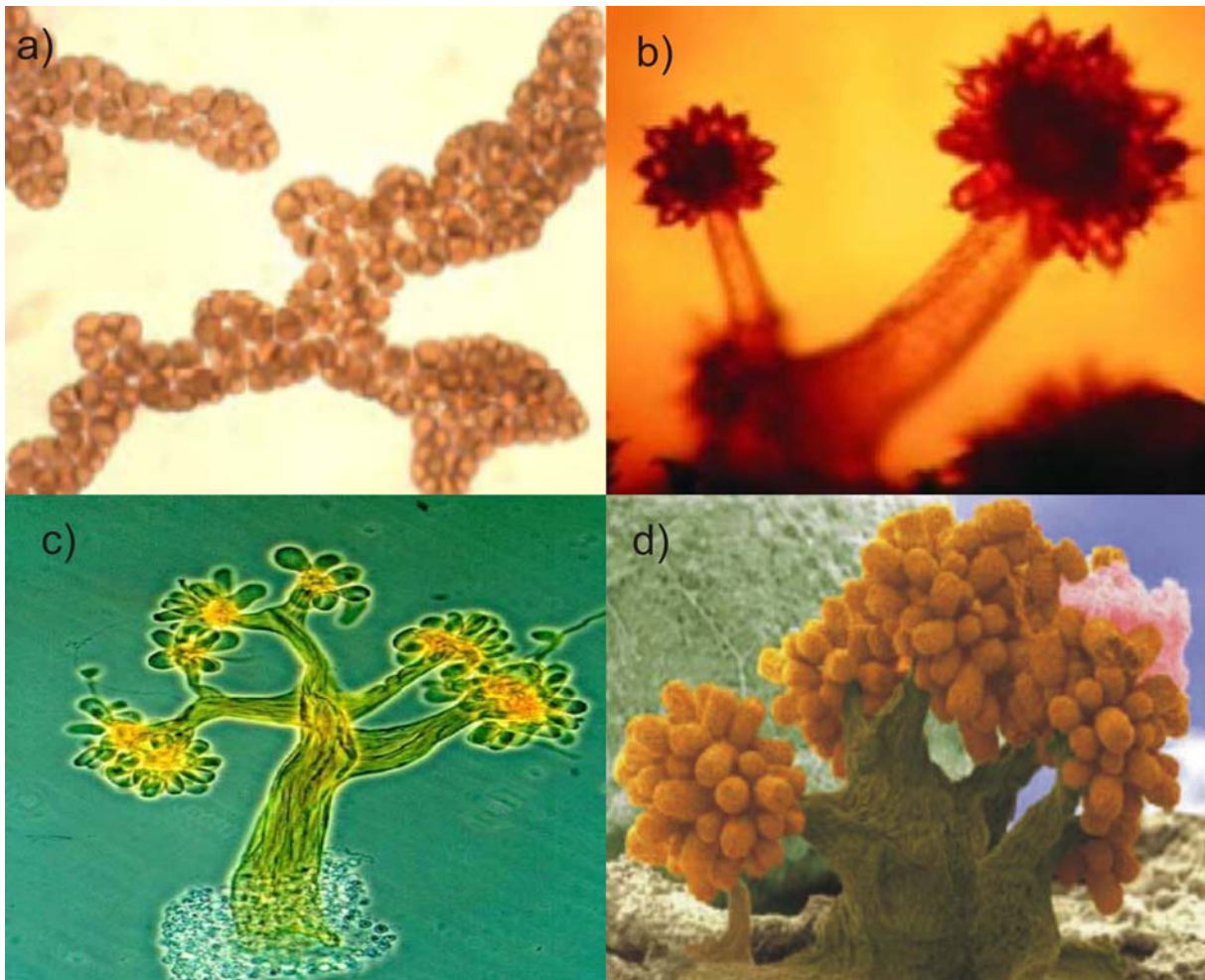
Fig. 5: Fruiting bodies of different myxobacterial species: a) *Sorangium cellulosum* So ce56 (Gerth *et al.*, 2003); b) *Chondromyces apiculatus* (Reichenbach, DSMZ); c and d) *Chondromyces crocatus* (Reichenbach & Dworkin, 1992; Manfred Rohde).

During fruiting body formation the cells interact with each other by using 5 intercellular signals (A to E), from which only signals A and C have been characterized biochemically. It is supposed that the B-, A-, D- and E-signals are essential for progression through the first 5 h of development: A- and B-signals are important in an earlier developmental state, whereas the signals D- and E-signals appear after 3-5 h (Dworkin, 1996; Kaiser, 2004). Fruiting body formation is induced

by starvation, and the extracellular A-signal helps the myxobacteria to sense the density of starving cells. The A-signal consists of a subset of amino acids and represents a typical quorum sensing signal. The C-signal is mediated by a 17 kDa extracellular protein, which occurs after 6h of starvation, inducing aggregation and subsequent sporulation (Kaiser, 2004). The functions and biochemical nature of the B-, D, and E-signals are still not determined and have to be investigated. It is assumed that amino acids, peptides, and lipids are critical for the development revealed by experiments with sporulation defective mutants (*bsg, dsg* and *esg* mutants). For example the *bsgA* gene encodes an ATP-dependent Lon protease (LonD), which might be essential to make amino acids available for the synthesis of new proteins during starvation-induced development. The sporulation defect can be rescued by the transfer of amino acids and peptides from wild type donor cells to a *bsgA* mutant by cell contact (Sogaard-Andersen *et al.,* 2003; Kaiser, 2004). The starvation process starts with the accumulation of a large number of vegetative cells, where the vegetative growth of the bacteria ceases and the cells begin to migrate in traveling wave patterns, called "ripples" (Welch & Kaiser, 2001). Later, cells leave these ripples and stream into nascent aggregates. Aggregation leads to an unstructured agglutination of cell masses whereof 65 - 90% will be autolysed. The maturing phase starts with the formation of special structural elements of fruiting bodies, like sporangiole walls or stems. During this period some of the vegetative rod cells transform into myxospores, which are resistant to several stress challenges. When nutrients are available these spores germinate to produce vegetative cells (Fig. 6) (Reichenbach, 1974; Reichenbach & Dworkin, 1992, Dworkin, 1996).
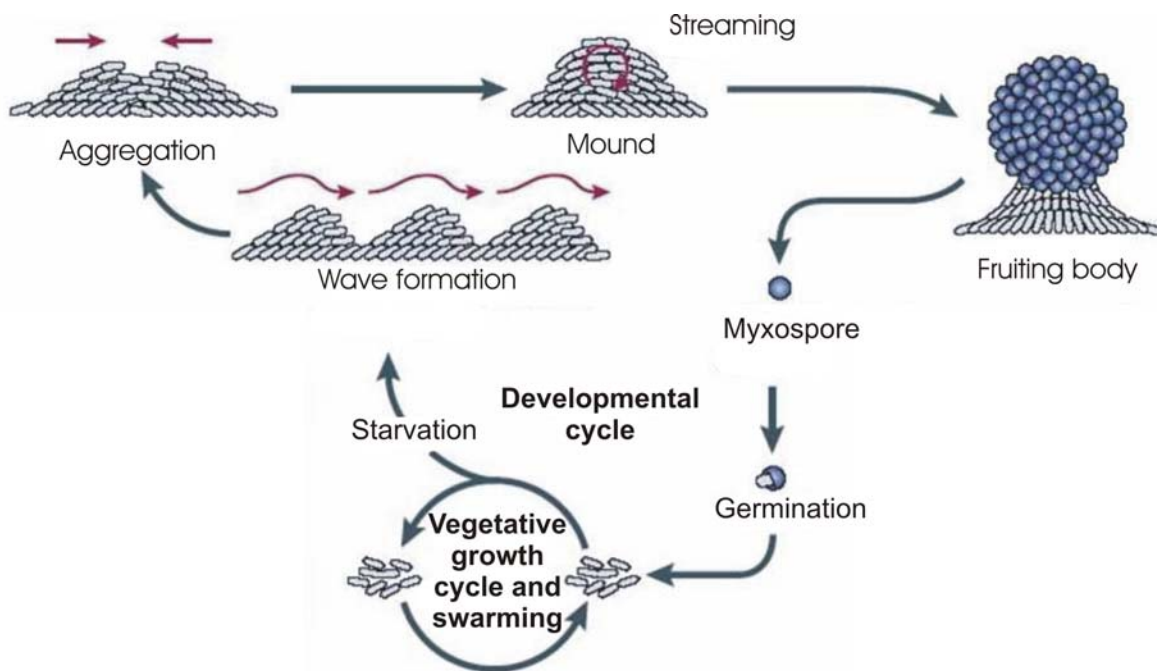
Fig. 6: Modell of morphogenesis of multicellular fruiting bodies in myxobacteria (Reichenbach & Dworkin, 1992; Sogaard-Andersen *et al.*, 2003).

The first genetic element of the gliding motility system of myxobacteria was reported in the suborder *Sorangineae* in 2004 (Zirkle *et al.*) for *Sorangium cellulosum* So ce26, a producer of the agricultural fungicide soraphen A. An *mglA* gene of *M. xanthus* was used to identify and clone an *mglA* homolog from So ce26. The disruption of this gene led to a non-swarming strain as observed in *M. xanthus* (Stephens *et al.*, 1989). The *mglA* homolog encodes a small GTPase of the Ras superfamily (Hartzell & Kaiser, 1991). In *M. xanthus,* MglA interacts with proteins of the serine, threonine and tyrosine kinase family and is proposed to be the intracellular switch that coordinates A- and S-motility (Thomasson *et al.*, 2002).

1.4   Secondary metabolites

Many plants, animals and microorganisms produce a wealth of unusual secondary metabolites for different purposes like self-defence or intercellular communication. For mankind, natural products have been playing an important role due to their chemical diversity and various bioactivities against diseases (Fig. 7).
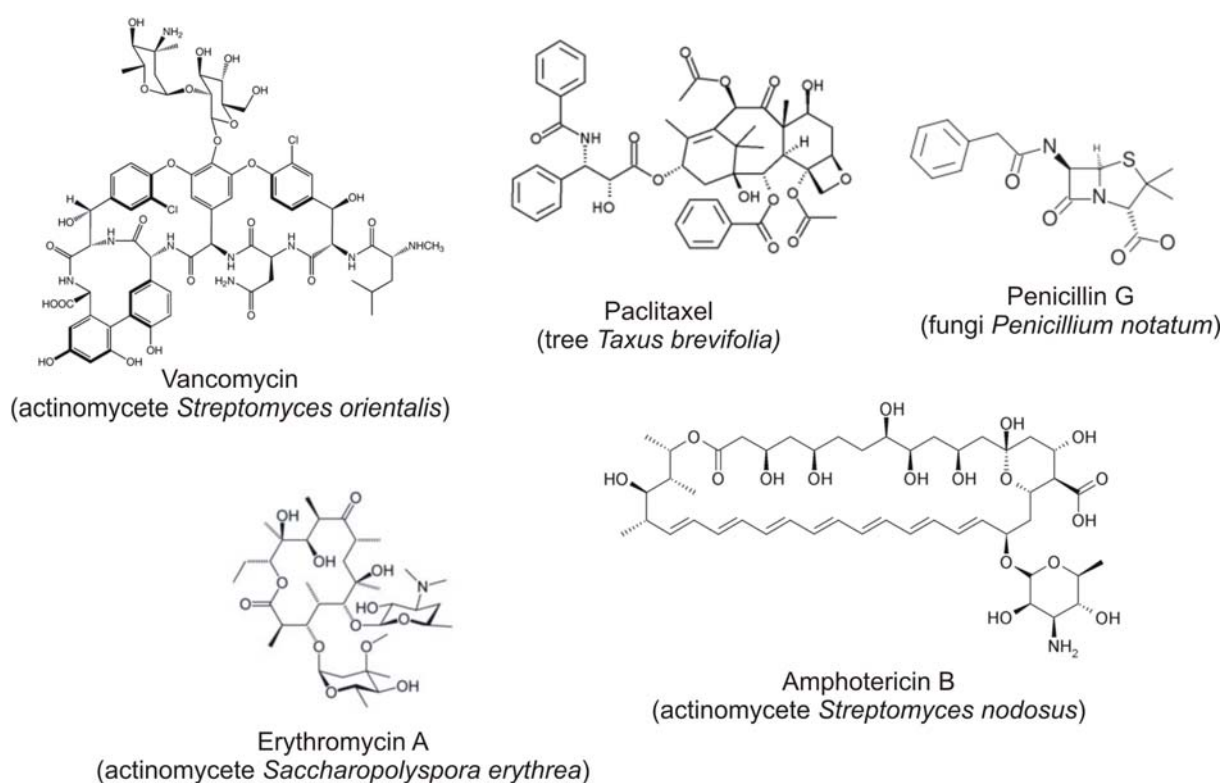
Fig. 7: Some known secondary metabolites from different organisms used in clinical medicine: Vancomycin (antibacterial); Paclitaxel (Taxol®, anticancer); Penicillin G (antibacterial); Erythromycin A (antibacterial); Amphotericin B (antifungal) (Frank, 2007).

In order to discover new bioactive compounds with improved therapeutic effects different sources and antibiotics were screened. Microorganisms like actinomycetes, *Bacillus* sp., pseudomonads, cyanobacteria and myxobacteria are known to synthesize antibacterial, antiviral, antitumoral compounds (Grabley & Thiericke, 1999, Reichenbach, 2001).

Myxobacteria are known to be prolific producers of interesting and novel bioactive substances applied in biotechnology and pharmacology (Gerth *et al.*, 2003; Bode & Müller, 2006; Reichenbach & Höfle 1993, 1999). About 7500 different myxobacteria have been isolated and many of them were screened for secondary metabolites. This way, nearly 500 derivatives from 100 core structures were found forming several novel core structures (Gerth *et al.* 2003). In figure 9, only some medically interesting examples out of a huge stock of myxobacterial metabolites are shown. Most of the isolated natural products are produced by different strains of *Sorangium cellulosum* (Fig.8).
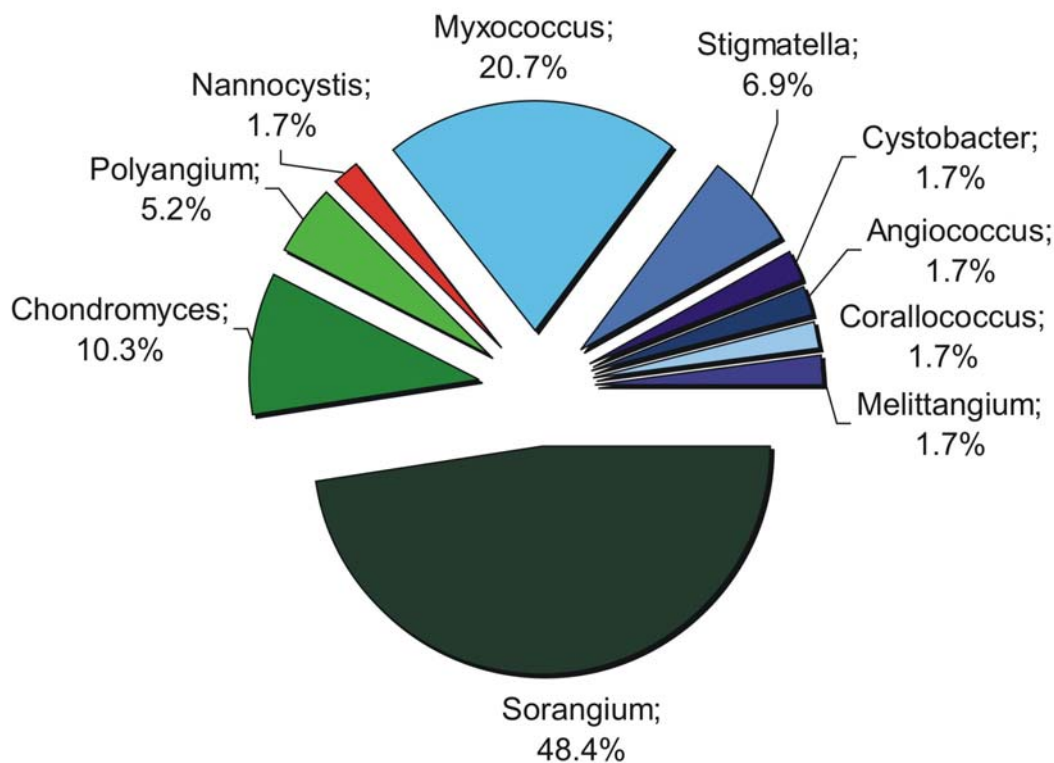
Fig. 8: The myxobacterial secondary metabolite producers given in percentages (Gerth *et al.*, 2003). Approximately, 50% of secondary metabolites are synthesized by different *Sorangium* sp.

The antifungal soraphen A inhibits the fungal acetyl-CoA carboxylase (Gerth *et al.*, 1993) and the cytotoxic substances chondramides, disorazoles, tubulysins and epothilones interact with actin filaments or influence the microtubule network. Chondramides stabilize the actin fibers by binding to F-actin (Grabley & Thierke, 1999). The disorazoles and tubulysins inhibit the polymerization of tubulin; they are in preclinical studies for antitumoral studies (Kopp *et al.*, 2005; Sandmann *et al.*, 2004).
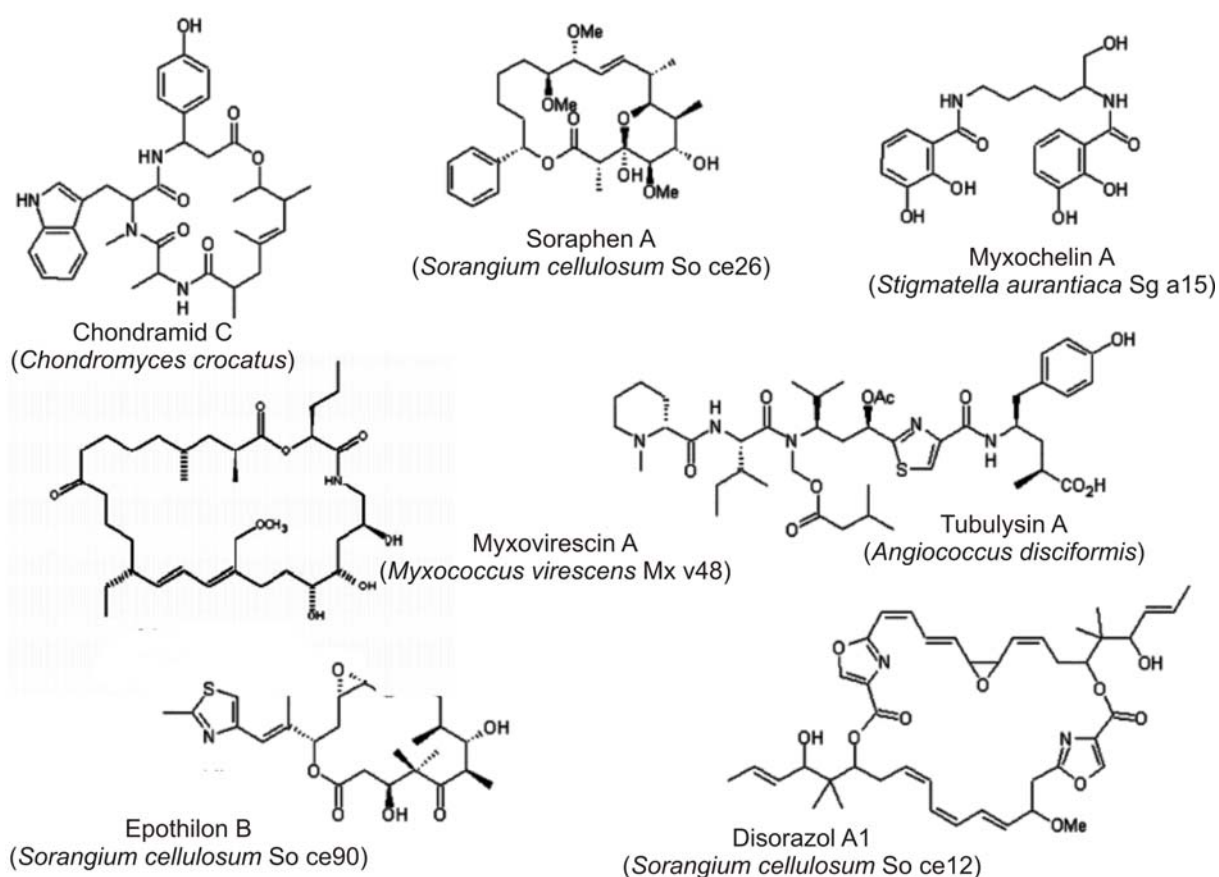
Fig. 9: Secondary metabolites of Myxobacteria: Soraphen A (antifungal); Myxochelin A (iron siderophore); Chondramid C (anticancer); Epothilone B (anticancer); Tubulysin (anticancer); Myxovirescin A (antibacterial); Disorazol A1 (anticancer) (Bode & Müller, 2006).

In contrast, the epothilones, which are in phase III of clinical studies, stabilize microtubules in a way similar to paclitaxel (Taxol®) used in chemotherapy (Gerth *et al.*, 1996; Bollag *et al.*, 1995). Many of these compounds belong to the polyketide and nonribosomal peptide families. Multimodular enzymatic systems known as polyketide synthases (PKS) and non-ribosomal peptide synthetases (NRPS) encoded by biosynthetic gene clusters are responsible for the production of this large number of interesting secondary metabolites. In many cases NRPSs and PKSs are working together giving hybrid products, e.g. chivosazol from So ce56. The biosynthetic gene cluster of chivosazol (Fig.10) was currently described by Perlova *et al.* (2006).

Tab. 1: Secondary metabolite biosynthetic gene clusters identified from myxobacteria (Bode & Müller, 2006). PKS: polyketide synthase; NRPS: non-ribosomal peptide synthetase

Compound	Synthase type	Producer
Soraphen	PKS	*Sorangium cellulosum* So ce 26
Myxochelin	NRPS	*Stigmatella aurantiaca* Sg a15
Chondramide	PKS/NRPS	*Chondromyces crocatus* Cm e5
Tubulysin	PKS/NRPS	*Angiococcus disciformis* An d48
Chivosazol	PKS/NRPS	*Sorangium cellulosum* So ce56
Disorazol	PKS/NRPS	*Sorangium cellulosum* So ce12
Epothilone	PKS/NRPS	*Sorangium cellulosum* So ce90

Three types of PKS multienzyme complexes are known: the type I, type II and the type III PKSs (Hopwood, 1997, Staunton & Weissman, 2001, Austin & Noel, 2003). Type I PKSs are modularly organized giant synthases, each module of which usually contains a β-ketoacyl synthase (KS), an acyltransferase (AT), and an the acyl carrier protein (ACP) as basic domains that may be complemented by a variable set of additional domains. These additional domains lead to the structural diversity of the products synthesized by PKSs. Different modifications of the growing acyl chain can occur with domains from ketoreductase (KR), enoyl reductase (ER) or dehydratase (DH), when starter and extender units (CoA thioesters) are bound within the PKS *via* an acyl carrier protein (ACP). The completed polyketide chain is then released from the enzyme complex by a thioesterase (TE) domain (Staunton & Weissman, 2001).
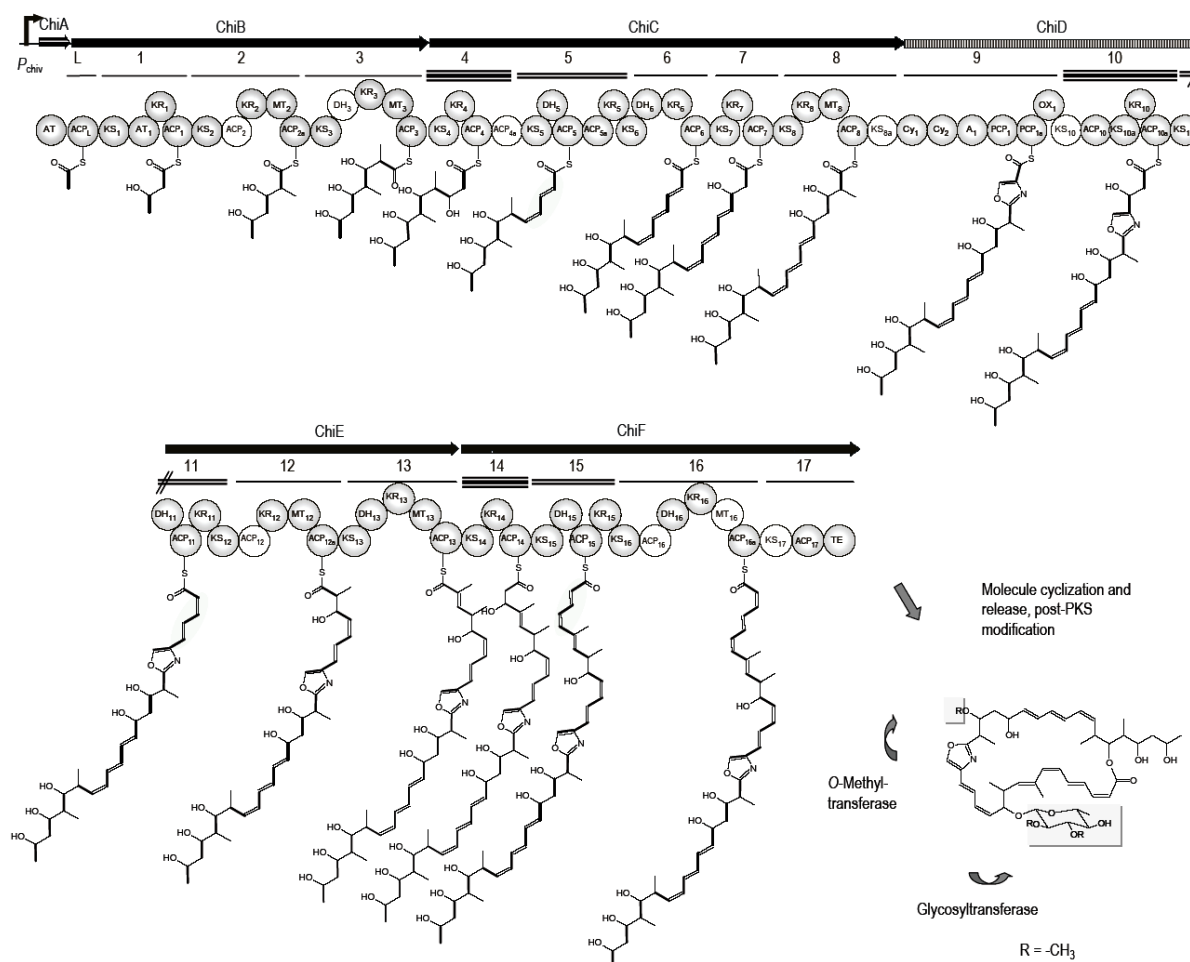
Fig. 10: Model of the chivosazol biosynthetic gene cluster of *Sorangium cellulosum* So ce56. The biosynthetic gene cluster spans 92 kbp on the chromosome and contains four polyketide synthase genes (*chiA*, *chiB*, *chiC*, *chiE* and *chiF*) encoding type I PKSs and one hybrid polyketide synthase/nonribosomal peptide synthetase gene (*chiD*). The five polypeptides having two to five distinct modules. Each module catalyzes one condensation of the growing chain with an extender unit, and subsequent reduction. The polypeptide ChiD contains one module of NRPS and one module of PKS. The NRPS part of the molecule forms an oxazole ring derived from serine (Perlova *et al.*, 2006).

Type II PKS systems are analogous to bacterial Fatty Acid Synthases. The active sites of these synthases are distributed among several smaller monofunctional polypeptides. Type II synthases catalyze the formation of compounds that require aromatization and cyclization, but not extensive reduction or reduction/dehydration cycles, e.g. actinorhodin. The type III PKSs or chalcone synthase-like PKSs (CHSs) are structurally and mechanistically quite different from type I and type II PKSs (Moore & Hopke, 2001). They are relatively small proteins and are involved in the synthesis of precursors for flavonoids. This synthase is a homodimer of identical β-ketoacyl synthase (KS) monomeric domains using free CoA substrates without the

involvement of 4'-phosphopantetheine residues on ACPs. In general, PKS multienzymes maintain a very high molecular weight, typically above 250 kDa. Another class of enzymes for secondary metabolite production is the large multidomain enzyme, the NRPS that catalyzes the assembly of complex natural peptide products like the prominent bioactive compounds vancomycin and penicillin (ACV tripeptide, Fig. 11) (Mootz *et al.*, 2002; Sieber & Marahiel, 2003). At least three domains are required for the synthesis of the peptide backbone: the A (adenylation) domain for coordinated recognition and activation the PCP (peptidyl carrier protein) domain for covalent binding and the C (condensation) domain for incorporation of a certain amino acid into the peptide chain. In addition to these so-called core domains, optional domains catalyze the modification of the incorporated residues, e.g. the MT (N-methylation) domain. Product release is normally achieved by a thioesterase (TE), catalyzing the formation of linear, cyclic, or branched cyclic nonribosomal peptides.
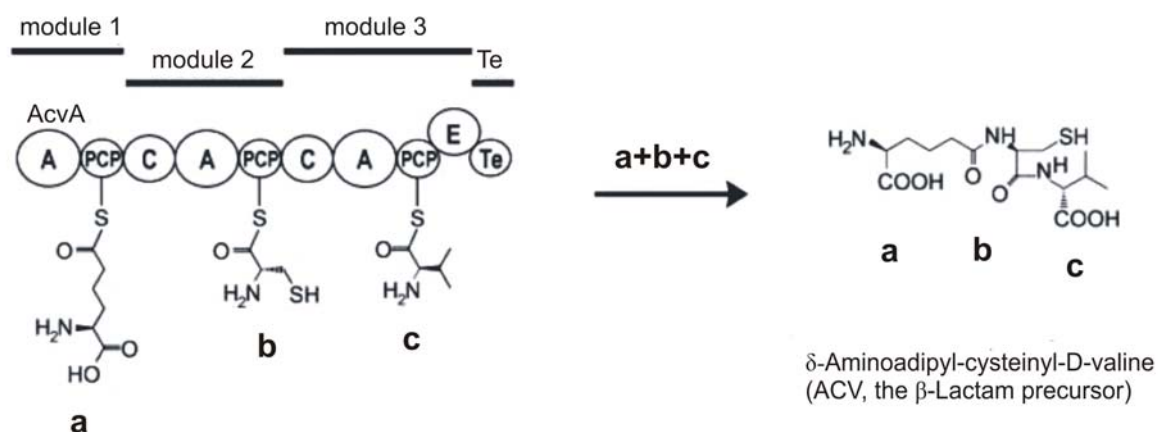
Fig. 11: Organization of a linear NRPS illustrated in the example of the biosynthesis of the tripeptide ACV (penicillin and cephalosporin precursor). The three core domains are in the order C-A-PCP in the elongation module. The first amino acid is incorporated by the initiation module which lacks a C domain. The terminal module contains a Te domain to release the full-length peptide chain from the enzyme (Mootz *et al.*, 2002).

1.5   Proteomics of So ce56

This proteomic approach was performed to complement the So ce56 genome project, which was recently completed (Schneiker *et al.*, 2007).

The methodological approach of proteomics is based on the separation of the whole cell proteome by isolating individual proteins via two-dimensional gel electrophoresis

or by liquid chromatography subsequently followed by protein identification by mass spectrometry (Aebersold & Mann, 2003).

1.5.1 Two-dimensional gel electrophoresis (2-D PAGE)

Two-dimensional gel electrophoresis (2-DE) was introduced by O'Farrell and Klose (1975) and is usually performed as a combination of isoelectric focusing (IEF) and sodium dodecyl sulphate-polyacrylamide gel electrophoresis (SDS-PAGE) for resolving complex protein mixtures (O'Farell, 1975; Klose, 1995; Klose & Kobalz, 1995). The IEF (first dimension) separates proteins according to their isoelectric points (pI). Normally, commercially available acrylamide strips (IPG gel strips) with an immobilized pH gradient formed with a mixture of ampholytes are used (Corbett *et al.*, 1994; Görg *et al.*, 1988, 2000). There, the proteins move to the position of their isoelectric point in between the pH gradient. In the second dimension, the proteins are separated in an SDS-PAGE according to their molecular weights (M$_r$). SDS is an anionic detergent that denatures proteins, masks the charges and moves in a negative SDS-protein-complex into the direction of the electrophoresis anode. Thus the proteins are separated in the polyacrylamide matrix proportional to their size. To ensure transfer of the proteins from the first dimension matrix to second dimension gels, equilibration of the IPG gel strips with a buffer containing SDS and a reducing agent is necessary to cleave the disulfide bonds between cysteine residues by, e.g. dithiothreitol (DTT) (Görg *et al.*, 2000). The protein spots on the 2-D gel can be visualized by several different gel staining methods: silver staining, fluorescent staining (e.g. SYPRO) and Coomassie Blue staining. Silver staining is a very sensitive method limited to protein concentrations between 1 and 10 ng. The Ag$^+$ ions form complexes with glutamine, asparagine and cysteine residues (Collgan *et al.*, 1995). The application of new silver staining protocols in which the silver reducing agent formaldehyde is used instead of glutaraldehyde allows a MALDI compatible analysis (Shevchenko *et al.*, 1996). Coomassie Blue is an organic dye (anionic triphenylmethane) that binds non-covalently to the lysyl residues of proteins, which are stained in proportion to the amount of their basic and aromatic amino acids and the amount of protein in the spot. In contrast to the silver staining method at least 0.1 µg of protein per spot is required. The colloidal Coomassie staining reveals increased sensitivity (ca. 30 ng per band) and shows no background staining (Neuhoff *et al.*, 1985). Fluorescence staining methods are less sensitive than silver staining (2 - 8 ng

protein), but compatible with subsequent mass spectrometric analysis (Berggren *et al.*, 2002). The Difference gel electrophoresis (DIGE) is a powerful technique for quantitative proteomics that allows simultaneous visualization of multiple protein extracts (Unlu *et al.*, 1997). This method is based on fluorescence pre-labelling of different protein pools using spectrally resolvable, size and charge-matched fluorescent dyes known as CyDye DIGE fluors (Marouga *et al.*, 2005).

1.5.1.1 Blue-Native PAGE gels from protein complexes

In contrast to the denaturing SDS electrophoresis, the Blue-Native technique obtains the natural form of protein complexes isolated from membranes (Schägger & Jagow, 1991). Using BN-PAGE, electrophoretic mobility of proteins is obtained through the binding of negatively charged amphiphilic Coomassie Blue. This technique separates complexes without dissociating them in contrast to SDS. Blue-native gels were formerly developed for the characterization of the respiratory complexes in mitochondria (Schägger *et al.*, 1994, 2001; Jänsch *et al.*, 1996), but it is also applied successfully for the analysis of the prokaryotic membrane complexes (Stenberg *et al.*, 2005). Eubel *et al.* (2005) describe in a review the capabilities and the use of BN-PAGE in proteomics to investigate protein:protein interactions.

1.5.2 Phosphoprotein analysis

Proteomics is a good method to analyze posttranslational modifications, for example the detection of protein phosphorylation. In this work, the phosphoproteome analysis plays a major role as So ce genome annotations reveal more than 400 protein kinase (Schneiker *et al.*, 2007). Protein phosphorylation has been shown in the regulation of a number of processes in prokaryotic organisms including chemotaxis, sporulation, differentiation, coordination of nitrogen and carbon metabolism and synthesis of secondary metabolites (Kennelly, 2001). The phosphorylation status of proteins is controlled by two different classes of enzymes: protein kinases which catalyze the transfer of phosphoryl groups from a high-energy compound (e.g. ATP or GTP) to a nucleophilic acceptor on an amino acid side-chain of proteins, and protein phosphatases which catalyze water-driven hydrolysis of phosphoester bonds (Hunter, 1995). These amino acid residues are mainly serine, threonine, tyrosine, histidine/aspartate (represent a two-component signal transduction system), where the phosphorylated and the dephosphorylated state act as a switch to turn on or off a

protein activity by changing their conformational structure (Cozzone, 1998). Most kinases act on serine and threonine, others on tyrosine, and a number of dual specifity kinases act on all three. Protein phosphorylation can principally be detected on 2-D gels by a gel shift in a spot position resulting into a mass increase of 80 daltons. Phosphorylation of proteins can be detected by labeling the cells with radioactive isotopes such as ^{32}P or ^{33}P, where inorganic phosphate is taken up by cells and metabolized to ^{32}P-γ-ATP which leads to a transfer of ^{32}P on proteins during phosphorylation. However, inorganic phosphate is also incorporated into other molecules like DNA, RNA, phospho-lipids and sugars, which decreases the incorporation rate into proteins (Link, 2006). Therefore, further methods are chosen to detect phosphorylated proteins. One sensitive method is the Western Blotting analysis using antibodies raised against the phosphoamino acids (Towbin *et al.*, 1979). The proteins can be easily transferred from the SDS-PAGE onto a blotting membrane (e.g. PVDF, nitrocellulose). After the application of specific antibodies, visualization of the targeted proteins can be achieved by using a chemiluminescent detection method (ECL).

1.5.3 Mass spectrometry

Mass spectrometry is a powerful tool in proteome analysis where hundreds of different proteins can be identified and modifications can be screened for from a crude protein extract separated by 2-D PAGE gels. Two techniques proved to be very useful in the proteome analysis: the MALDI-TOF-MS and the ESI-MS/MS (Fig.12) (Mann *et al.*, 2001; Aebersold & Mann, 2003). These are soft ionization techniques which are used to volatilize and ionize the proteins or peptides for mass spectrometric analysis and to determine the mass-to-charge ratios *(m/z)* of gas-phase ions.

Generally, a mass spectrometer has three components: a source of ions, a mass analyzer and a detector (Fig. 12). The sample must first be ionized and vaporized in a vacuum and exposed to a high voltage, where the produced ions are accelerated and separated due to their mass-to-charge ratio by the mass analyzer. Finally, the detector records the impact of individual ions, displayed as peaks on a mass spectrum. Thus, the mass of a molecule can be calculated from the m/z ratio of its derivative ions.

1.5.3.1 Matrix-Assisted Laser Desorption/Ionization Time of Flight mass spectrometry (MALDI-TOF-MS)

MALDI, introduced by Karas and Hillenkamp (1988), is an efficient method, which ionizes and sublimates the samples out of a dry and crystalline matrix via laser pulses usually from nitrogen lasers with a wavelength of 337 nm. Matrices like α-cyano-4-hydroxycinnamic acid have a strong absorption at this laser wavelength. The irradiation by the laser induces a rapid heating of the crystallized sample matrix mixture which causes localized sublimation and ionization (i.e. protonation). Matrices minimize the high sample fragmentation by absorbing the incident energy and increase the efficiency of energy transfer from the laser to the biomolecules. To accelerate the ions into the mass analyzer a high potential electric field is applied between the sample slide and a sampling orifice (Kussmann & Roepstorff, 2000). MALDI mainly produces singly charged ions (Karas *et al.*, 2000) (Fig. 12a).

1.5.3.2 Electrospray Ionization (ESI)

ESI, developed by Fenn *et al.* (1989), is an atmospheric pressure method that transfers analyte ions from solution into the gas-phase (Mann *et al.*, 2001), whereby a fine spray of the sample of highly charged droplets in the presence of a strong electric field produce ions of the sample in the gas phase. With the coat of nitrogen gas the liquid sample evaporates and is then moved into the mass analyzer (e.g. Ion Trap). In a proteomic workflow, this ion source is usually directly coupled to a liquid chromatography system (LC, HPLC) to introduce the separated and concentrated peptide mixtures to the ESI-MS/MS, also called on-line method. The generated MS/MS spectra contain information about amino acid sequences which increases the database search specificity.
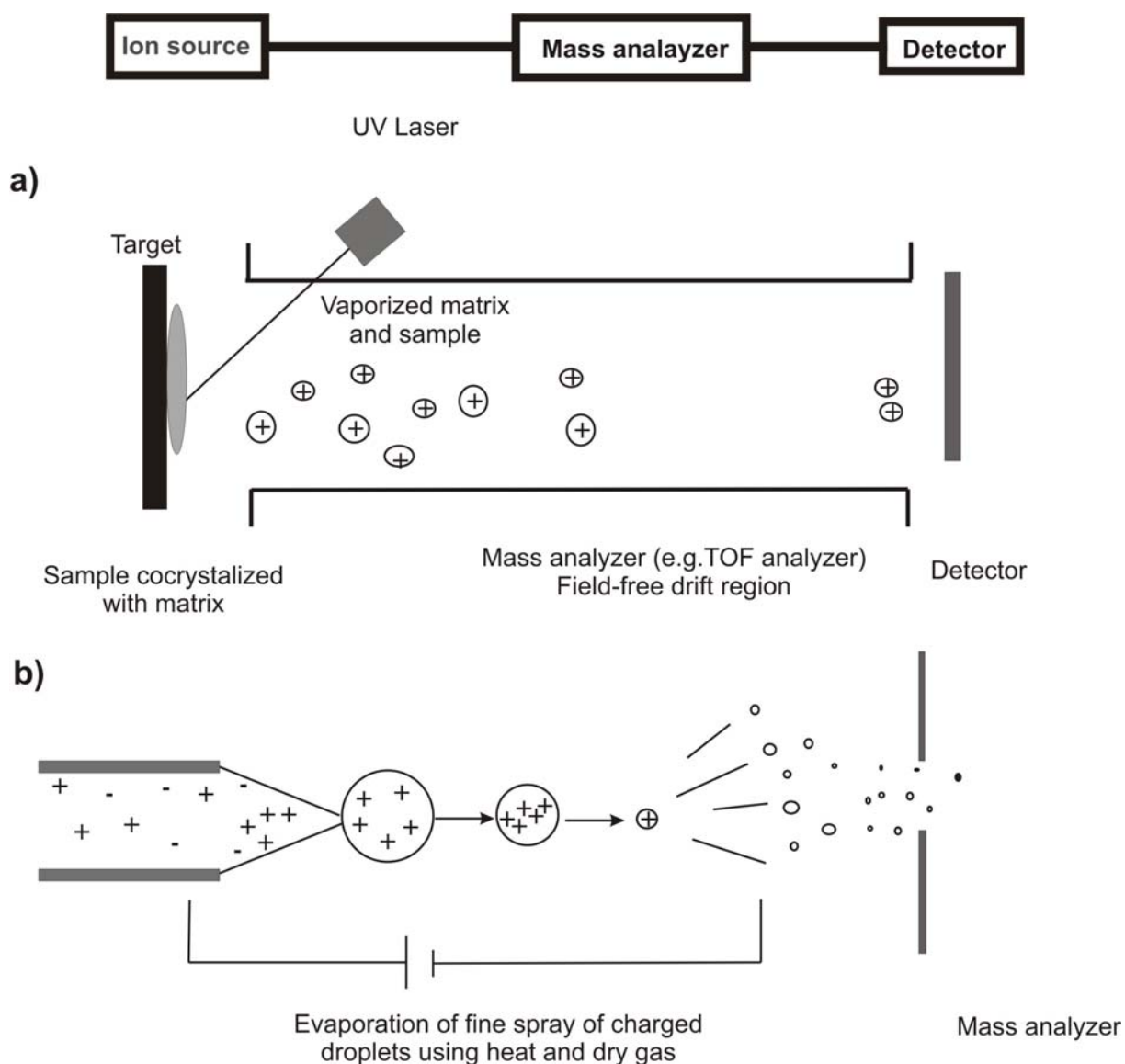
Fig. 12: a) Schematic of the MALDI ionization method: Laser pulses sublime and ionize the crystalline mixture on the target surface. The ionized analyte pulsed into the mass spectrometer for analysis; b) Schematic of the electrospray ionization method: Electric field forces the charged liquid at the end of the tip to form a cone (Taylor cone), that minimize the charge/ surface ratio. Droplets from the end of the cone move towards the entrance of the mass analyzer (Mann *et al.*, 2001; Lottspeich, 2006)

1.5.3.3 Protein identification

Peptide mass fingerprinting (PMF) is a high throughput method for protein identification by MALDI-TOF-MS to measure the masses of proteolytic peptide fragments (e.g. tryptic digested fragments). The PMF is characteristic for each protein, and thus can be used for protein identification by comparison with predicted peptide masses (Pappin *et al.*, 1993; Mann *et al.*, 1993). A search algorithm such as

MASCOT, www.matrixscience.com, (Perkins *et al.*, 1999) compares the theoretically digested proteins of the organism of interest in the database with the experimentally analyzed and digested proteins. From this comparison a list of possible proteins is generated with MOWSE (MOlecular Weight SEarch) scores and probabilities (e.g. sequence coverage) to determine the confidence of the identification. If protein and genomic sequence are not available for an organism, proteins can be identified by sequencing and comparison to sequence databases (e.g. MASCOT and Sequest). The tandem mass spectrometry (MS/MS) is a second set of information that can be used to identify a protein. The advantage of sequencing by MS/MS in combination with liquid chromatography (LC-MS/MS) is that several sequence fragments are obtained. Similar to PMF, individual proteins subjected to LC-MS/MS are first digested and a fragment spectrum is produced. Finally, the deduced sequences are compared with protein or genome sequence databases to identify the protein homology.

1.6   Aim of this work

This work aims to perform an extensive proteomic approach for *Sorangium cellulosum* So ce56 encompassing the extraction of the cytoplasmic, membrane, extracellular and outer membrane vesicle subproteomes in order to analyze the different So ce56 proteins. For this purpose it was necessary to firstly develop methods to isolate secreted proteins and outer membrane vesicles from the culture supernatant as well as a method to extract cytosolic and membrane proteins. Furthermore, a proteome reference map of *Sorangium cellulosum* So ce56 cytosolic proteins had to be established and an extensive proteome analysis under standard conditions to identify proteins involved in the regulation of secondary metabolite biosynthesis, differentiation, signal transduction, or gliding motility and methods such as one- and two-dimensional electrophoresis (1-D and 2-D electrophoresis) had to be applied.

2 Material

2.1 *Sorangium cellulosum* strain

Strain	Characteristics	Literature
So ce56	Wild type, Kan^R	Pradella *et al.*, 2002 Müller and Gerth, 2006

2.2 Growth media

2.2.1 P-medium (solid)

0.1%	Probion
0.2%	Peptone
0.5%	Starch
0.2%	Glucose
0.05%	CaCl$_2$ x 2H$_2$O
0.05%	MgSO$_4$ x 7H$_2$O
50 mM	Hepes (11.9 g/l)
1.2%	Select agar

pH 7.6; autoclaved

2.2.2 SG-medium (synthetic medium with glucose)

100 mM	Hepes (23.8 g/l)
0.5%	Asparagine
0.05%	MgSO$_4$ x 7H$_2$O
10mg/l	Fe-EDTA

pH 7.2, autoclaved

Separately autoclaved supplements as stock solutions (concentrations given in brackets) added per 100 ml:

1 ml	CaCl$_2$ x 2H$_2$O (5%)
1 ml	K$_2$HPO$_4$ x 3H$_2$O (0.6%)
5 ml	Glucose (20%)
100µl	ZnSO$_4$ (1mg/ml)

Antibiotics

100µg/ml	Kanamycin
10µg/ml	Gentamycin

2.3 Buffers and solutions

2.3.1 Buffers and solutions for the extraction of proteins

Cytosolic proteins

Washing buffer	50 mM	Tris (pH 7.2)

Lysis buffer	50 ml	Washing buffer
	1 tablet	Complete EDTA free for protease inhibition

Rehydration buffer	8 M	Urea
	2% (w/v)	CHAPS
	0.01% (w/v)	Bromophenol Blue

(Solution without Bromophenol Blue is used, when the protein concentration was determined with Bradford (Bio-Rad)

Extracellular proteins

SDS solution	0.5%	Sodium dodecyl sulfate
Tris buffer	0.5 mM	Tris (pH 6.8)
DTT solution	1 M	Dithiothreitol
Precipitating solution	8 M	Ammonium acetate

Membrane proteins

Membrane-extraction buffer	50 mM	Hepes
	5 mM	EDTA
	150 mM	Sucrose
	0.5%	Triton X
	1 mM	$MgCl_2$
	0.6%	PVP
	1 mM	DTT
	1 tablet	Protease inhibitor cocktail

Outer membrane proteins

SM buffer	100mM	NaCl
	10 mM	$MgSO_4$
	20 mM	Tris
	pH 7.5	

OMP washing buffer	10 mM	Tris-HCl (pH 8.0)
	2%	Lauroyl-sarcosine

Lysis buffer for OMPs	10 mM	Tris (pH 8.0)
	1 mM	EDTA

Vesicle proteins

Sample buffer for OMVs	0.02%	CHAPS
	0.4%	SDS
	0.5%	Triton X

2.3.2 Buffers and solutions for the 2-D PAGE gels (Bio-Rad system)

Tricine gel buffer
3 M	Tris
0.3%	SDS

pH 8.45, HCl (37%)
(First dissolve Tris and then add SDS and HCl)

Anode buffer
0.2 M	Tris

pH 8.9

Cathode buffer
0.1 M	Tris
0.1 M	Tricine
0.1%	SDS

pH 8.25 (normally fits)

Overlay solution
1 M	Tris
0.1%	SDS

pH 8.45

Agarose sealing solution
100 ml	Tricine gel buffer
0.5%	Agarose
0.01%	Bromophenol Blue

DTT solution
28%	Dithiothreitol

SDS solutions
10%	Sodium dodecyl sulfate

Equilibration buffer
50 mM	Tris (pH 8.8)
6 M	Urea
30% (v/v)	Glycerol (87%)
2% (w/v)	SDS
0.01%	Bromophenol Blue

EB 1
5 ml	Equilibration buffer
2%	DTT

EB 2
5 ml	Equilibration buffer
2.5%	Iodoacetamide

2.3.3 Buffers and solutions for the 1-D PAGE gels

4x stacking buffer
500 mM	Tris
0.1%	SDS

pH 6.8

4x resolving buffer
1.5 M	Tris
0.1%	SDS

pH 8.8

Protein sample buffer
100 mM	Tris
4%	SDS
0.2%	Bromophenol Blue
20% (v/v)	Glycerol (87 %)

Cathode buffer (10x)
250 mM	Tris
1.9 M	Glycine
1%	SDS

Anode buffer (10x)
250 mM	Tris

pH 8.4

28

2.3.4 Buffers and solutions for Blue-Native gels (BN-PAGE)

5x Cathode buffer

250 mM Tricine
75 mM Bis-Tris
0.1% Coomassie 250 G
pH 7.0 at 4°C

6x Anode buffer

300 mM Bis-Tris
pH 7.0 at 4°C

6x BN gel buffer

1.5 M 6-amino-n-caproic acid (ACA)
150 mM Bis-Tris
pH 7.0 at 4°C

Solubilization buffer

30 mM Hepes
150 mM K-acetate
10% Glycerin (87%)

Digitonin solution

10 ml Solubilization buffer
1% Digitonin
(Digitonin dissolve at high temperature, then keep at
-20°C)

5 % Serva Blue G

750 mM ACA
5% Coomassie 250 G

2.3.5 Buffers and solutions Western Blot analysis

TB buffer

50 mM Tris (60.57g)
50 mM Boric acid (30.91g)

TBS buffer

10mM Tris (12.11g)
150mM NaCl
pH 7.4

Blocking buffer

1% (w/v) BSA in TBS buffer

Tab. 2: Antibodies against phosphorylated serine and tyrosine.

Antibodies	Used antibody concentrations
Monoclonal Anti-Phosphotyrosine Clone PT-66 (mouse) Biotin Conjugate (B1531, SIGMA)	1:3,000
Monoclonale Anti-Phosphoserine Clone PSR-45 Biotin Conjugated (P3430, SIGMA)	1:3,000
Streptavidin-biotinylated horseradish peroxidase complex (217511, Amersham Biosciences, UK)	1:20,000 or 1:4,000

VECTASTAIN® ABC Kit

2 drops REAGENT A (Avidin DH)
2 drops REAGENT B (Biotinylated Horseradish
Peroxidase H)
(mix in 30 ml of TBS buffer and incubated for 30 min at
4°Cprior to use)

Developing solution (DAB) (100 ml)	5 ml	2 M Tris-HCl, pH 7.4
	93 ml	H_2O_{dist}
	0.5 ml	$NiCl_2$ (stock 80 mg/ ml)
	1.5 ml	DAB (diaminobenzidine tetrachloride)
	30 µl	H_2O_2 (30%)

2.3.6 Staining buffers and solutions

2.3.6.1 Coomassie Blue staining

Fixing solution	10% (v/v)	Acetic acid
	30% (v/v)	Ethanol
	60%	H_2O_{dist}

Staining solution	2g/l	Coomassie brillant blue CBB-G250 (Roth)
	0.5/l	Coomassie brillant blue CBB-R250 (Roth)
	5%	Methanol
	42.5%	Ethanol
	10%	Acetic acid
	42.5%	H_2O_{dist}

2.3.6.2 Colloidale Coomassie staining (Blue Silver)

Solution A	2% (w/v)	O*rtho*-phosphoric acid (85%)
	10%	Ammonium sulfate $(NH_4)_2SO_4$

Solution B	5%	CBB-G250

Fixation solution	40%	Methanol
	10%	Acetic acid
	50%	H_2O_{dist}

Staining solution	98%	Solution A
	2%	Solution B

shaking over night and adding:	80%	Staining solution
	20%	Methanol

2.3.6.3 Silver staining for protein gels (MS compatible)

Silver staining solution (prepared fresh)	0.4 g	$AgNO_3$
	200 ml	H_2O_{dist}
	150 µl	Formaldehyde (37%)

Developer (prepared fresh)	15 g	Na_2CO_3
	1 mg	$Na_2S_2O_3$ x 5 H_2O
	250 ml	H_2O_{dist}
	125 µl	Formaldehyde (37%)

Sensitizing solution (prepared fresh)	0.1 g	$Na_2S_2O_3$ x 5 H_2O
	500 ml	H_2O_{dist}

Fixation solution	50%	Ethanol
	10%	Acetic acid
	40%	H_2O_{dist}
	0.5 ml/l	Formaldehyde (37%)

| **Washing solution** | 50% | Ethanol |
| | 50% | H_2O_{dist} |

Stopping solution	44%	Ethanol
	44%	H_2O_{dist}
	12%	Acetic acid

2.3.6.4 DIGE staining for protein gels (GE Healthcare)

DIGE labeling buffer	8 M	Urea
	4%	CHAPS
	30 mM	Tris
	pH 8.5 (cold 1 N HCl)	

| **DIGE stopping solution** | 10 mM | Lysine |

| **CyDye solution** | 12.5 µl/ 5 nmol | DMF (>99.8%) |
| | (keep at -20°C in the dark) | |

2.3.6.5 LIVE/ DEAD® BacLight™ viability staining (Molecular Probes)

| **Component A** | 2.5 ml | sterilized H_2O |
| | (1 pipet of STYO® 9 dye) | |

Component B	2.5 ml	sterilized H_2O
	(1 pipet of propidium iodide)	
	(keep solutions at -20°C in the dark)	

2.3.7 Buffers and Solutions for tryptic digest

| **Washing solution** | 0.1% | Trifluoracetic acid (TFA) |
| | 60% | Acetonitrile (CH_3CN) |

| **Solution A** | 50% | CH_3CN |
| | 50% | H_2O |

| **Solution B** | 50% | CH_3CN |
| | 50 mM | NH_4HCO_3 |

| **Solution C** | 50% | CH_3CN |
| | 10 mM | NH_4HCO_3 |

| **Solution D** | 10 mM | NH_4HCO_3 |

Trypsin solution (SIGMA)		
proteomic grade	100 µl	HCl (1 mM)
1 vial (20 µg/ml)	900 µl	NH_4HCO_3 (10 mM)

3 Methods

3.1 *Sorangium cellulosum* So ce56 strain

Sorangium cellulosum So ce56 was isolated in 1985 from a soil sample from Indonesia (Pradella *et al.*, 2002) by Dr. Gerth and his group in Braunschweig (former GBF, now Helmholtz Centre for Infection Research). Growth adaptation of the wild strain was made first in M medium using increasing concentrations of peptone. For further experimental approaches, a So ce56 variant from 2002 with enhanced cultivation conditions was used (Müller & Gerth, 2006). In order to establish a comprehensive proteome map of *S. cellulosum* So ce56 cultivation of the bacteria was optimized and adapted to the technical needs of a proteome study. *S. cellulosum* So ce56 has a slow generation time of about 7 hours and requires high cell numbers for sub-cultivation. In addition, these bacteria prefer complex media (Müller & Gerth, 2006) containing starch and protein-hydrolysates that interfere with protein isolation and identification. For this reason, bacteria were grown on solid and complex P-medium, and subsequently transferred to liquid minimal S-medium. Beside the good compatibility with proteome studies, the chosen S-medium supports biosynthesis of secondary metabolites (Müller & Gerth, 2006).

3.1.1 Cultivation of So ce56 cells in medium P

To prepare the inoculum for the liquid medium, *S. cellulosum* So ce56 cells were cultivated on solid P-medium at 30°C, which is a rich and complex medium containing starch, peptone and probion. Single cells are able to regenerate on this solid medium and additionally, it is also a good detection system for contaminations. The generation time of So ce56 is about 7 h and it can therefore easily be overgrown by unwanted microorganisms. After one week orange colonies (clumps) appear on the agar surface. These colonies were scratched completely with an inoculation needle from the solid medium and transferred to 10 ml S-medium, a defined synthetic medium developed by Müller and Gerth (2006) consisting of: hepes buffer, glucose and asparagine as sole carbon and organic nitrogen sources, respectively, plus the trace element zinc, in 50 ml Erlenmeyer flasks.

3.1.2 Cultivation of So ce56 cells in medium SG

The cell cultures were incubated at 30°C in a shaking incubator at 170rpm (GFL, Hamburg, Germany). To avoid contaminations the flasks were covered with autoclavable cellulose steri-stoppers (Omnilab, Bremen, Germany). Due to the long generation time, the clumped cells need about 5-7 days until a homogeneous orange cell suspension is reached. After adding an additional 10 ml S-medium, the So ce56 culture was incubated for another 5-7 days to increase the cell count for inoculation. After about 2 weeks in total, the 20 ml culture broth was centrifuged carefully and, the cell pellet was transferred into 100 ml S-medium in 250 ml Erlenmeyer flasks and incubated at 30°C in the shaking incubator at 170 rpm. The cell counts were detected after 2 h of inoculation and after that every 24 hours for the next 7 days using a haemocytometer and additionally a spectrophotometer to measure the optical density (λ=600 nm) of the population. Growth rates were monitored each day over seven days and additionally at 10 and 14 dpi.

3.1.3 Detection of cell viability

Viability of the cells was detected using the two-color fluorescence dye LIVE/DEAD[®] BacLight[TM] Viability Kit (Molecular Probes, Oregon, USA) at a fluorescence microscope with a longpass and dual emission filter for simultaneously viewing of STYO[®] 9 and propidium iodide stains. The green fluorescent nucleic acid stain labels all bacteria, whereas the red-fluorescent nucleic acid stain propidium iodide labels only bacteria with damaged membranes causing a reduction of STYO[®] 9 stain when both dyes are present. The excitation/emission maxima are about 480 nm/500 nm for STYO[®] 9 and 490 nm/635 nm for propidium iodide. Both dyes were mixed together according to the manufacturer's protocol to a final concentration of 6 µM STYO[®] 9 stain and 30 µM of propidium iodide. Sample preparation was then carried out by incubating 40 µl of the cell suspension with 40 µl of the mixed stock solution 15 min in the dark. 5 µl of the stained cell suspension was transferred onto a glass slide. Ten fluorescence frames were made of different positions on the slide. From these pictures the living and the dead cell numbers were determined and the resulting viability was evaluated in percentage.

3.2 Isolation of proteins from *Sorangium cellulosum* So ce56 for 1-D, 2-D and Blue-Native PAGE gels

3.2.1 Protein extraction of cytoplasmic fraction

To isolate the proteins from the cytoplasmic fraction, 100 ml of bacterial suspension culture was centrifuged for 25 min at 10,000 x *g* (6K 15, SIGMA Laborzentrifugen, Osterode, Germany) at 4°C. The cells were washed three times with cold 50 mM Tris washing buffer (pH 7.2) and centrifuged for 15 min at 10,000 x *g* at 4°C. The cell pellet was resuspended in 1ml lysis buffer including a protease inhibitor cocktail (Complete, EDTA free, Roche, Mannheim, Germany) and subsequently disrupted with 0.8 g glass beads (SIGMA, Taufkirchen, Germany) in a ribolyser (Thermo Fisher Scientific, Waltham, MA, USA) for 20 sec at 6.5 m x s^{-1}. The cells were centrifuged at 20,000 x *g* (5417R, Eppendorf, Hamburg, Germany) at 4°C for 20 min, the supernatant was incubated at 37°C for 30 min with 1-2 µl benzonase (250 units/µl, SIGMA) and centrifuged again at 20,000 x *g* for 15 min at 4°C. For protein precipitation, cold acetone was added to a final concentration of 80% (v/v) and samples were incubated over night at -20°C. The precipitate was collected by centrifugation at 20,000 x *g* for 20 min at 4°C. The pellet was dried and dissolved in rehydration buffer. The protein content was determined by a Bradford protein assay (Bio-Rad Laboratories, Richmond, CA, USA).

3.2.2 DIGE analysis of cytosolic proteins

Two types of So ce56 growth conditions - the exponential and stationary phase - were compared using Differential Gel Electrophoresis (DIGE, GE Healthcare). For each condition 50 µg of protein was independently dissolved in DIGE labeling buffer according to the manufacturer's protocol (GE Healthcare). The proteins of the exponential phase were labelled with 1 µl of Cy3^{TM} and for the stationary phase the equal amount of Cy5^{TM} Dye was used. Finally the two labeling reactions were mixed and focussed isoelectronically on one IPG strip (18 cm) as described above. For spot detection, quantitation and matching the Delta2D 3.1.2 software (DECODON, Greifswald, Germany) was used.

3.2.3 Isolation of extracellular proteins

The extracellular proteins were isolated according to an adapted protocol for phenol extraction (Watt *et al.*, 2005). First, the supernatant of the 100 ml centrifuged culture broth (early stationary phase) was filtered in a cross-flow system (Vivaflow 200, 0.2 µm polyethersulfone membrane, Vivascience AG, Germany) on ice. After filtration, the sample was lyophilized and solubilized in protein extraction buffer (0.5% SDS, 250 µl 1 M DTT and 1 ml 0.5M Tris-HCl, 12.5 ml MilliQ, pH 6.8). Protein samples were incubated at room temperature for 30 min. After adding 5 ml of phenol, samples were carefully mixed and centrifuged at 10,000 x g for 30 min at 4°C. 10 ml of cold methanol, 100 µl 1 M DTT and 150 µl 8 M ammonium acetate were added to the phenol phase and this fraction was precipitated over night at -20°C. Proteins were harvested by centrifugation at 10,000 x g for 20 min at 4°C. The resulting pellets were washed twice with 70% (v/v) of cold ethanol. The proteins were dissolved in rehydration buffer for a 2-D SDS-PAGE.

3.2.4 Membrane protein extraction

50 ml cells were harvested after 7 days and centrifuged for 15 min at 10,000 x g at 4°C. The pellet was dissolved in a membrane extraction buffer and sonicated (Bandelin Sonoplus, Berlin, Germany) 6 times at maximum speed for 30 sec. Between each step, the sample was cooled on ice for 1 min. The disrupted cell fractions were centrifuged at 10,000 x g for 40 min at 4°C to remove cell debris. The supernatant was ultracentrifuged at 100,000 x g (Optima L-90K, Beckman Coulter, Krefeld, Germany) for 2 h to separate the membrane protein fraction from the cytoplasmic protein fraction. The membrane fraction was dissolved in a solubilizing buffer (30 mM HEPES, 150mM potassium acetate, 10% glycerol and 1% digitonin). After adding 4% SDS (w/v), 1 mM DTT and 0.005% (w/v) Bromophenol Blue, electrophoretic separation was carried out on a 12.5% SDS-PAGE gel at 15 W.

3.2.5 Isolation of Outer Membrane Proteins (OMPs)

The cell extract of So ce56 was harvested after centrifugation of the bacterial suspension culture at 8000 x g for 45 min at 4°C. The resulting cell pellet was washed twice with SM buffer for 15 min and centrifuged again as described before. The pellet was resolved in 10 mM Tris HCl (pH 8.0) and 1 mM EDTA and sonicated

on ice 10 times for 6 seconds at 80% intensity. Between the sonification steps the sample was cooled for 30 seconds. The disrupted cells were centrifuged at 8,000 x g for 30 min at 4°C to remove the cell debris. The supernatant was then ultracentrifuged at 100,000 x g for 90 min at 4°C, followed by an incubation step of the pellet with 10 mM Tris-HCl (pH 8.0) and 2% lauroyl-sarcosine for 30 min at 30°C. Finally, the sample was centrifuged at 15,000x g for 60 min at 4°C. The resulting pellet with the outer membrane proteins was dissolved in rehydration buffer with 0.5% Triton X.

3.2.6 Extraction of Outer Membrane Vesicle proteins

The isolation of the outer membrane vesicle (OMV) from the supernatant of the cell fraction was carried out using a modified method from Wai *et al.* (1995, 2003). For this purpose, the supernatant was centrifuged two times at 6000 x g for 45 min at 4°C. The cell free supernatant was filtered on ice with the Vivaflow 200 cross-flow system (Vivascience) as described before, followed by an ultracentrifugation step at 100,000 x g for 3 h at 4°C.

For electrophoretic separation, the pellet was dissolved in sample buffer (0.02% CHAPS, 0.4% SDS and 0.5% Triton X) and loaded onto a 12.5% SDS-PAGE gel.

3.3 One-dimensional (1-D), two-dimensional (2-D) and Blue-Native (BN) Polyacrylamide Gelelectrophorese (PAGE) gels of *Sorangium cellulosum* So ce56 proteins

3.3.1 One-dimensional SDS-PAGE gels for membrane proteins, outer membrane proteins and outer membrane vesicle proteins

The 1-D SDS-PAGE gel (size: 18 x 16 x 1.5 mm) was prepared in the Hoefer600 gel casting system (GE Healthcare). Protein fractions were separated in a 12.5% SDS-PAGE (Laemmli, 1970), which was prepared as followed (Tab.3):

Tab. 3: Components of the one dimensional 12.5% SDS-PAGE for protein separation

	Resolving gel	**Stacking gel**
Acrylamide (40/1)	12.5 ml	1.55 ml
4x resolving buffer	10 ml	-
4x stacking buffer	-	2.75 ml
H$_2$O	17.4 ml	8.25 ml
TEMED	20 µl	25 µl
APS (10%)	75 µl	60 µl

SDS-PAGE was performed for 3.5h at 5-15 W.

3.3.2 Two-dimensional gel electrophoresis of the cytosolic and extracellular proteins

For isoelectric focussing (IEF), 18 cm immobilized dry strips (IPG strips) with linear pH gradients 3 – 10 (GE Healthcare, Uppsala, Sweden) were rehydrated with rehydration buffer containing 600 µg of isolated protein according to the manufacturer's protocol. The IEF was carried out in an IPGphor with voltages from 30 to 8,000 V for 24h.

IPGphor running protocol for 18 cm strips:

20°C, max. 50 µA per strip	1h	0V (Rehydration)
	12h	30V (Step&Hold)
	2h	500V (Step&Hold)
	1h	1,000V (Gradient)
	4h	8,000V (Gradient)
	6h	8,000V (Step&Hold)
		Total: 67610Vhs

For the second dimension, a 13% SDS-Tricine-PAGE gel was carried out in a Bio-Rad gel system (PROTEAN^{TM} II xi Cell).

Tab. 4: 13% Tricine-PAGE gel, the Bio-Rad glass plate size is 20 x 20 x 1 mm

SDS-Tricine-PAGE gel	
H$_2$O dest.	24.39 ml
Tricine gel buffer	30 ml
Glycerol (87%)	12 ml
Acrylamide (49.5/3)	23.61 ml
APS (10%)	300 µl
TEMED	300 µl

This combination of the Amersham and Bio-Rad system was described previously (Colditz *et al.*, 2004). Before the IEF strips were embedded on the SDS-Tricine PAGE gel, they were first equilibrated for 15min in equilibration buffer 1 with 2% (w/v) DTT and in the second equilibration step, the strips were incubated 15 min in equilibration buffer 2 supplemented with 2.5% (w/v) iodoacetamide. Electrophoresis was performed at 30 mA/ mm gel for 24h.

3.3.3 Blue-Native PAGE (BN-PAGE) proteins from the cytosol and membrane fraction

First dimension (BN-PAGE):

To analyze soluble and membrane protein complexes in *S. cellulosum,* the protein extracts from the cytosol and from the membrane (4.2.1 and 4.2.3) were used for Blue-Native PAGE. The preparation of the gradient Blue-Native PAGE was carried out according to the protocol of the Plant Proteomics group of Prof. H.P. Braun in Hannover (Eubel *et al.*, 2003, 2005). An acrylamide gradient from 4.5% to 16% was chosen to maximize the resolution of the BN-gel for protein complexes with high molecular weights (> 300kDa). The gradient was prepared with a two-chamber gradient mixer using the components listed in table 5:

Tab. 5: Components for the BN gradient PAGE gel for the separation of protein complexes.

BN resolving gel	Mixing chamber (Light solution)	Reservoir (Dense solution)
	4.5%	16%
H$_2$O$_{dist}$	15.6 ml	6 ml
6x BN gel buffer	3.5 ml	3 ml
Acrylamide (49.5/3)	1.9 ml	6 ml
100% Glycerol	-	3.5 ml
Σ Total volume	21 ml	18.5 ml
APS (10%)	95 µl	61 µl
TEMED	9.5 ml	6.1 µl

The gel solution was pumped slowly from the gradient mixer upwards into the electrophoresis chamber (Hoefer SE 600, glass plate size 18 x 16 cm, Amersham). For this purpose, a needle was injected between the glass plates to load the gel chamber. After polymerization of the gradient BN gel, a 4% stacking gel was loaded onto the gradient gel.

Tab. 6: Components for the stacking gel of the BN gradient PAGE.

BN stacking gel	
H$_2$O$_{dist}$	11.3 ml
6 x BN-gel buffer	2.5 ml
Acrylamide (49.5/3)	1.2 ml
TEMED	6.5 µl
APS (10%)	65 µl

Solubilization of the protein complexes was carried out using the mild non-ionic detergent digitonin prepared as followed:

- dried protein pellets from the membrane and cytosolic fraction (max. 1 mg protein) was dissolved in solubilization buffer containing 1% digitonin (100 µl solubilization buffer used for 1 mg protein)

- samples were incubated on ice for 20 min and then centrifuged at 14,000 for 10 min at 4°C

- the supernatant was mixed then with 5 µl of 5% Serva Blue G stain.

Before loading the protein samples, cathode and anode buffers were filled into the gel chamber and incubated for 25 min at 4°C. Electrophoretic separation of the BN gels was carried out at 4°C (100 V, max. 15 mA, 45 min; 500 V, max 15 mA, 11-13 h).

Second dimension (Tricine-SDS-PAGE):

For the second dimension a lane of the BN-gel was cut out and placed horizontally on an SDS-Tricine-Gel. Before loading, the cut out gel lane was incubated in 1% SDS and 1% β-mercaptoethanol for 30 min to denaturate the protein complexes for subsequent separation of their subunits. The lane was then washed for 30-60 sec with H_2O_{dist} as β-mercaptoethanol inhibits the acrylamide polymerization. Finally, the lane was placed between the glass plates as shown in Fig. 13. For a better transition of the proteins from the first into the second dimension, an additionally spacer gel was prepared. The stacking gel was then casted around the BN lane.

Tab. 7: Components of the second dimension of the BN analysis.

	Resolving gel 16.5%	Spacer gel 10%	Stacking gel 10%
Acrylamide (49.5/3)	10 ml	2 ml	2 ml
H$_2$O$_{dist}$	6 ml	4.6 ml	3.4 ml
Tricine gel buffer	10 ml	3.4 ml	-
6 x BN gel buffer	-	-	3.4 ml
Glycerol (100%)	-	-	1 ml
Glycerol (87%)	4 ml	-	-
SDS (10%)	-	-	100 µl
APS (10%)	100 µl	34 µl	83 µl
TEMED	10 µl	3.4 µl	8.3 µl
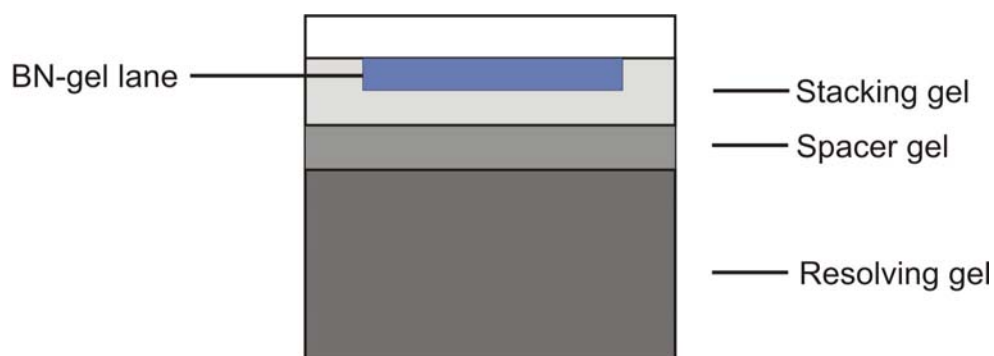
Fig. 13: Casting the second dimension for the BN gel.

Electrophoresis was performed at room temperature starting with 30 mA for 1 h and 50 mA over night (max. 500 V).

3.4   Protein staining methods

3.4.1 Coomassie Blue

Gels were incubated in fixing solution for at least 45 min and Coomassie stained overnight. Destaining was performed for 2 h with fixing solution and then overnight with 7% acetic acid.

3.4.2 Colloidale Coomassie Blue (Blue Silver)

Gels were incubated for 1 h with fixing solution and then stained with colloidale Coomassie for 3 h or over night. Destaining was carried out only with H_2O_{dist}.

3.4.3 Silver staining method

The low abundant proteins in 2-D SDS-PAGE gels were visualized with the MALDI compatible silver staining method based on the protocol from Shevchenko *et al.* (1996). The MALDI-TOF-MS analysis was carried out immediately after the staining process, because of the reducing agent formaldehyde, which leads to cross-linking of proteins. The silver staining process was carried out as followed:

- fixing: 1 h or over night, washing: 2 x 25 min with washing solution

- sensitizing: 1 min with sensitizing solution, washing: 3 x 20 sec with H_2O_{dist}

- staining: 20 min in silver staining solution, washing: 3 x 20 sec with H_2O_{dist} (changing of the staining tray)

- developing: gel was shaken until spots were visible (3-5 min), washing: 20 sec with H_2O_{dist}

- stopping: 10 min with stopping solution, washing: 3 x 10 min with H_2O_{dist}

- keeping the gel at 4°C in 1% acetic acid

3.5 Western Blot analysis of phosphorylated proteins from the cytosolic fraction of *Sorangium cellulosum* So ce56 strain

Detection of phosphorylated proteins was carried out by Western Blot analysis using antibodies against phosphoamino acids (tyrosine and serine). Therefore, separated proteins from the 2-D SDS-PAGE gel were transferred electrophoretically onto a hydrophobic, microporous polyvinylidine (PVDF) membrane (Roth), which was chosen for its high binding capacity for proteins and its mechanical stability compared to other membranes. Due to its hydrophobic character, the membrane had to be activated prior to usage with methanol; the membrane maintains a hydrophilic character. For protein transfer, a vertical tank-blot system (Hoefer) was used, where the gel and blotting membrane was clamped in grids between filter papers (Whatman 3 MM) and sponge pads suspended in the tank filled with TB buffer (Fig. 14). Before loading the tank-blot, the blotting membrane and the 2-D gel were prepared as followed:

- cutting the membrane and the filter papers according to the size of the 2-D gel

- incubation of the unstained gel with TB buffer for 15 min

- activation of the PVDF membrane by wetting 15 sec in methanol, 2 min in H_2O_{dist} and 5 min in TB buffer
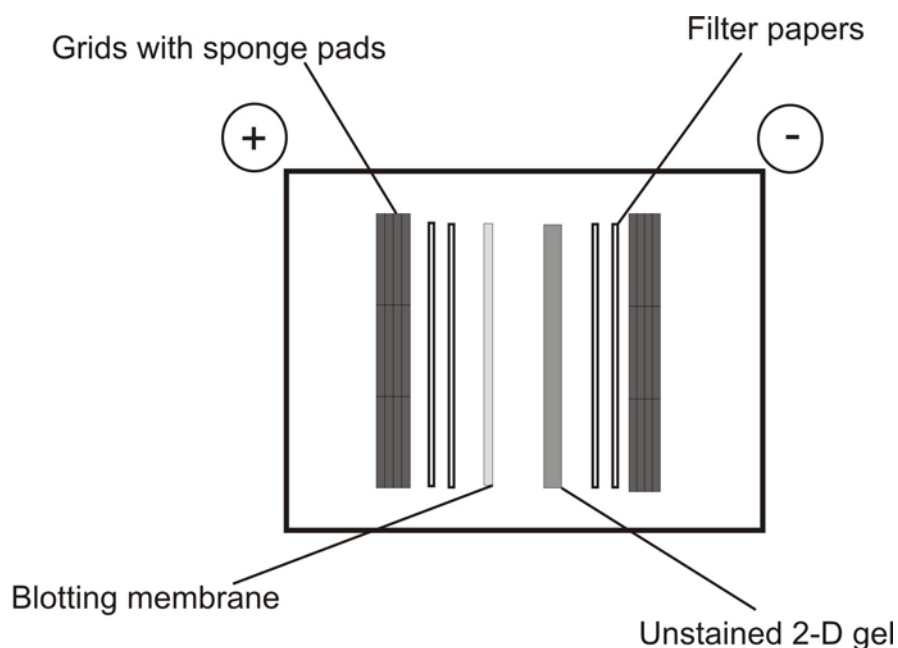
Fig. 14: Diagram of a vertical tank-blotting system setup.

After blotting the membrane, a blocking-step was carried out over night at 4°C in 1 % BSA (in TBS). The membrane was then washed three times for 10 min with TBS. The primary antibody (Anti-Phosphotyrosine, 1:3000) was incubated for 2 h or over night at 4°C and washed 20 min with 2 changes of TBS. The secondary antibody (Streptavidin-biotinylated horseradish peroxidase complex) was incubated for 30 min and washed three times for 15 min with TBS. Detection of the phosphorylated antigens conjugated to Horseradish Peroxidase (HRP) labeled antibodies was carried out using the ECL™ Plus detection reagents (Amersham Biosciences). Chemiluminescent signals were detected on autoradiography films (Hyperfilm™ ECL, Amersham Biosciences). Alternatively, detection of the proteins with the primary antibody Anti-Phosphoserine was carried out directly on the Blotting membrane using the VECTASTAIN® ABC Kit (Burlingame, CA, USA). For this technique, the blot was washed after the incubation with the primary antibody two times à 10 min with TBS. The secondary antibody (1:4000) was incubated for 2 h and twice à 10 min with TBS and then incubated for 2 h with Vectastain® Complex. Detection of Avidin-HRP was carried out with the chromogen diaminobenzidine tetrahydrochloride (DAB) for 5-15 min as brown signals on the membrane. The reaction was stopped with TBS buffer.

3.6 Mass spectrometry

3.6.1 Tryptic digest

After staining the gel, the bands/spots of interest were excised and digested with trypsin as described in the protocol on the KECK home page (http://info.med.yale.edu/wmkeck/prochem/geldig3.htm). The protein gels were washed 5 min with 50% acetonitrile in prewashed tubes. In the next step, the gel pieces were washed with solution B for 30 min, another 30 min with solution C and dried in a vacuum centrifuge (Speedvac). 15 µl of a digestion buffer containing solution D and trypsin (Proteomic grade, Sigma) was added to the small gel pieces (1 mm^2) and samples incubated 1h at 4°C. After adding another 15 µl of solution D, the enzymatic cleavage was carried out at 37°C for 24h on a shaking incubator.

3.6.2 MALDI-TOF analysis of proteins

For protein MS analysis the digested samples were mixed with a matrix solution containing 33% (v/v) acetonitrile, 0.1% (v/v) trifluoroacetic acid (TFA),and α-cyano -4-hydroxy-trans-cinnamic acid (Sigma) and loaded on anchor chip targets. Mass spectrometric analysis was performed on a MALDI-TOF Ultraflex (Bruker, Bremen Germany) mass spectrometer. MALDI-TOF settings: the N2-laser is operating at a wavelength of 337 nm with a laser frequency of 20 Hz (pulse ion extraction: 100ns; shots: 50 (sum 200) in a positive mode)

MASCOT database queries (www.matrixscinece.com) were performed spectra analysis. The MASCOT settings: monoisotopic; peptide tolerance: 50 – 150 ppm; missing cleavages: max 2; fixed modifications: carbamidomethyl.

3.6.3 NanoLC-ESI-MS/MS analysis of membrane proteins and outer membrane proteins

The digests of membrane proteins were analyzed using an online nanoLC-ESI-MS/MS, an automated nano-electrospray (Eksigent Technologies, USA) coupled with a Thermo Finnigan LCQ Deca ion trap mass spectrometer (Thermo Electron Corporation, USA). After adding 200 µl 60% acetonitrile and 0.1% TFA the samples were kept at room temperature for 60 min. This step was repeated after samples had

been transferred into prewashed tubes and the mixtures had been dried in a Speedvac. The dried samples were dissolved in 10 µl 5% acetonitrile, 0.05% TFA. 2 µl of this solution was separated chromatographically on an RP-18 capillary column (50 µm i.d., Dionex, USA) at a flow rate of 200 nl/ min. The gradient profile consisted of a linear gradient from 98% A (acetonitrile/H_2O/formic acid, 5/95/0.1) to 50% B (acetonitrile/H2O/formic acid, 80/20/0.1) over 40 min followed by a linear gradient to 98% B over 5 min. The eluted peptides were analyzed by nano-spray MS/MS using the LCQ Deca ESI-ion trap MS. The MS instrument was operated with the following settings: spray voltage 1.3 kV, heated capillary voltage and temperature 14 V and 165°C, respectively. Collision energy was set to 35%. Upon a full scan a zoom scan was recorded to determine the charge state of the peptide, followed by the isolation of the particular mass and an MS/MS scan. The instrument executed one full scan, followed by a zoom in scan and MS/MS scan of each one of the three most intense peaks from the MS scan. The generated peptide sequence tags were analyzed by the MASCOT database query. Proteins were identified by two or more tryptic peptide matches and MOWSE scores of more than 40 were reported.

3.6.4 Protein annotations/online resources/databases

All predicted open reading frames (ORFs) of *Sorangium cellulosum* So ce56 were used to establish a So ce56-database (Schneiker *et al.*, 2007). The search engine MASCOT was used to compare the peptide mass fingerprints obtained by MALDI-TOF-MS and the sequence data for peptides obtained by nanoLC-ESI-MS/MS with this database. MALDI-TOF-MS analyzed proteins were regarded as identified if their MOWSE score was higher than 50%, with sequence coverage of at least 10%. The two open source systems GenDB 2.4 (Meyer *et al.*, 2003) and ProDB (Wilke *et al.*, 2003) were used for automated and manual gene prediction and "post-genomic" analysis, respectively. The system ProDB handles data conversion from the mass spectra software and automates data analysis. The genome annotation system, GenDB, automatically categorizes the annotated genome into functional classes supported by different schemes, like GO, TIGR, COG, SWISS-PROT, TMHMM, HTH, Signal P, BLASTP. Almost 40 – 60% of the genes on the new genome sequence can be classified automatically based on sequence similarity (Fraser *et al.*, 2000). This sequence similarity is the first step for assigning function to new proteins. With the Signal P, TMHMM and HTH search tools the topology and signal peptides of the

gene products were predicted based on Hidden Markov Models (HMM). The prediction of N-terminal signal peptide cleavage sites in amino acid sequences was carried out with the Signal P software. The analysis of the first 60 amino acids started from the N-termini (Nielsen *et al.*, 1997). The TMHMM software predicts putative transmembrane domains in amino acid sequences (Sonnhammer *et al.,* 1998; Krogh *et al.*, 2001). This software combines hydrophobicity, charge bias, helix lengths of integral membranes, and grammatical constraints in one algorithm. Different BLAST programs were used automatically to compare the So ce56 database with other available databases, also to other myxobacterial strains like *Myxococcus xanthus* DK 1622 (NC_008095), *Anaeromyxobacter dehalogenans* 2CP-C (NC_007760), *Stigmatella aurantiaca* DW4/3-1 and also to the database of the actinomycete *Streptomyces coelicolor* A3(2) (NC_003888). Tools like KEGG (Kyoto Encyclopedia of Genes and Genomes), GO (Gene Ontology) and COG (Clusters of Orthologous groups) were shared to predict physiological functions and probable biochemical pathways of the putatively encoded proteins. To obtain good results, the automatically collected data from databases and the human expert annotation is combined. Therefore, manual comparisons and searches were performed to identify bacterial lipoproteins from the DOPOL database (Babu *et al.,* 2006). All identified proteins with signal peptides were scanned for the presence of lipobox sequences [LVI]-[ASTVI]-[GAS]. Furthermore, FASTA files from identified proteins were blasted with the PRIAM (Claudel-Renard *et al.*, 2003) Database and the Transport Classification Database (TCDB, Saier *et al.*, 2006). The PRIAM database was used for the automated enzyme detection in a fully sequenced genome, based on the classification of enzymes in the ENZYME database (Bairoch, 2000). The results of this detection can be visualized on KEGG graphs in order to facilitate the interpretation of metabolic pathways. The data of the TC database (www.tcdb.org) is a compilation of published information from over 10,000 references encompassing nearly 3,000 representative transporters and putative transporters, classified into >400 families.

4 Results

4.1 Cultivation of *Sorangium cellulosum* So ce56

All approaches described in the present work were carried out with a *Sorangium cellulosum* So ce56 strain obtained from Dr. K. Gerth in Braunschweig at the Helmholtz Centre for Infection Research.
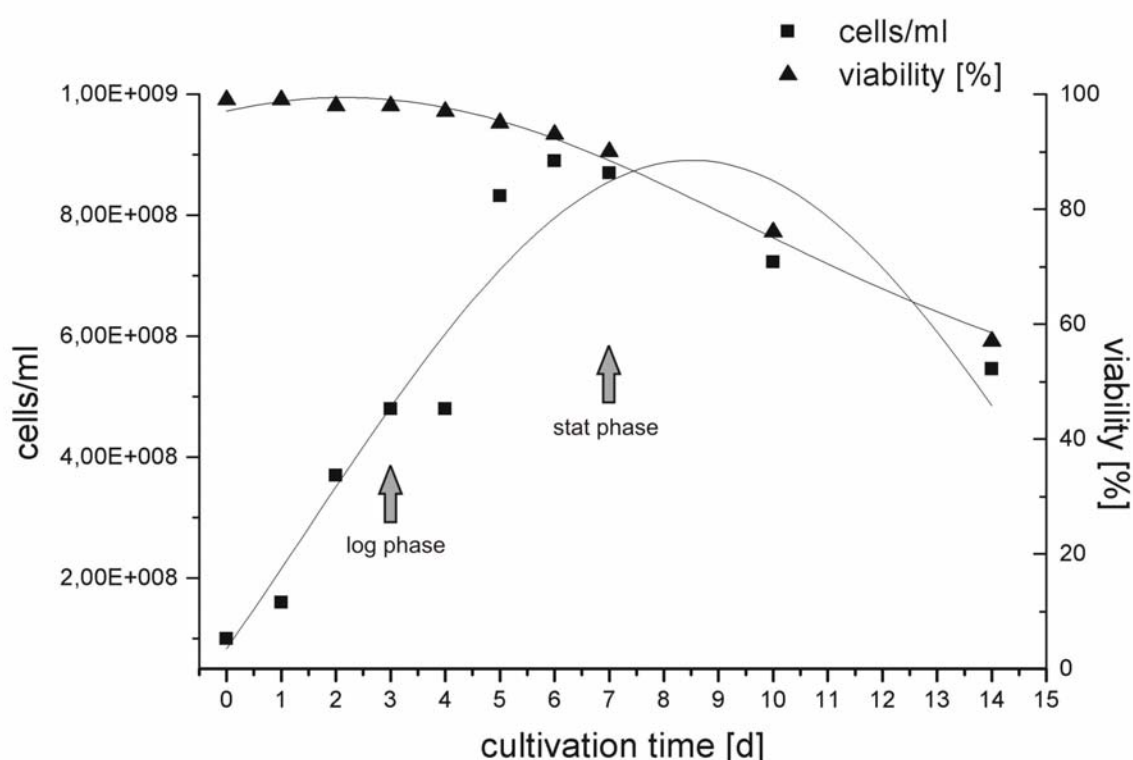
Fig. 15: Growth and viability of *Sorangium cellulosum* So ce56 cells. The upper curve indicates the viability of the cells during the cultivation given in percentages. Cell viability was detected via the LIVE/DEAD fluorescence dye. The cultivation of the cells were carried out in 100 ml liquid S-medium and incubated at 30°C at 170 rpm. Proteins were harvested from the exponential phase (3 dpi) and early stationary phase (7 dpi).

For stable growing conditions and in order to increase the synthesis of secondary metabolites, *Sorangium cellulosum* So ce56 was cultivated in synthetic medium with glucose as carbon source (SG medium). Similar same culture conditions for reproducible protein expression and proteomic analysis were achieved and cells were grown under nearly constant conditions. Two time points were chosen for all harvest and subsequent protein extraction procedure: (i) after 3 days (4x 10E8 cells/

ml) in exponential phase of growth for DIGE analysis or (ii) after 7 days (9x10E8 cells/ ml) in an early stationary phase of growth, respectively. Growth rate was determined by counting the cells each day during a time period of seven days and additionally at days 10 and 14 as displayed in the graph (Fig. 15). Additionally to the cell counting, the optical density of the cell culture was determined, which facilitates later the sampling at the right time point.

Starting with a high inoculum of about 1x10E8 cells, bacterial growth started immediately and reached its maximum at day 7 with approximately 9x10E8 cells (Fig. 11). At 10 and 14 days after inoculation (dpi), the cell number was decreased to 7x10E8 and 5x10E8 cells, respectively, indicating cell turn over and lysis. For this reason, cell viability was detected using the two-colour fluorescence dye LIVE/DEAD® *Bac*Light™ Viability Kit (Fig.16).
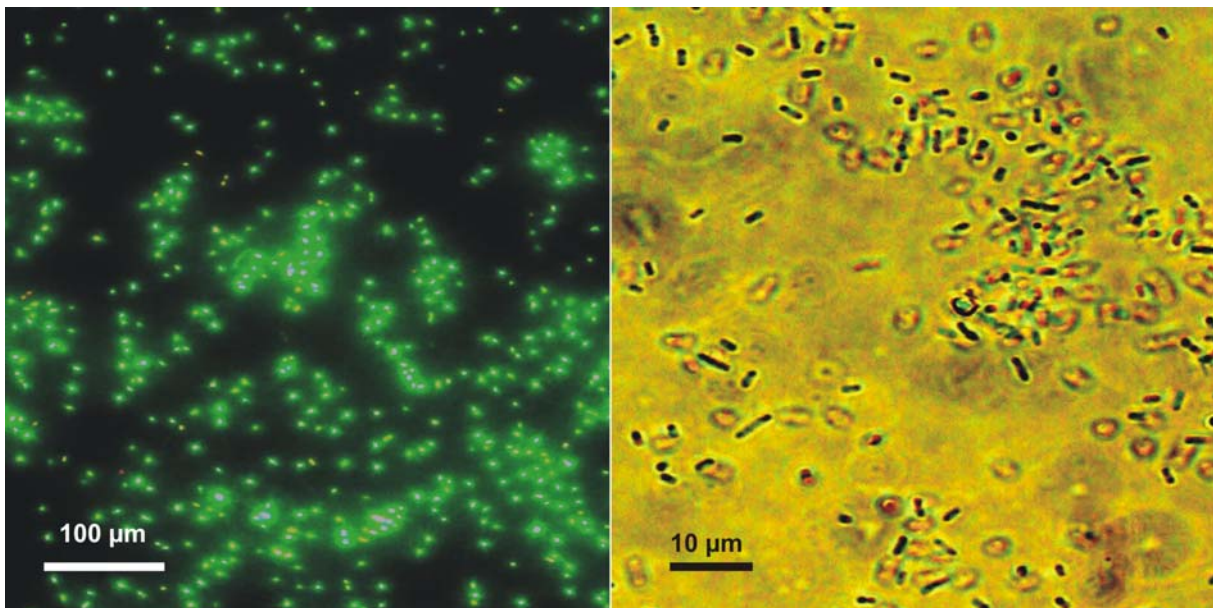
Fig. 16: *Sorangium cellulosum* So ce56 cells: Cell culture samples from the early stationary phase. On the left picture the cells were stained with the LIVE/DEAD Viability Kit and on the right picture a microscopic view of the So ce56 cells.

Further cell detection and counting was carried out via fluorescence microscopy. The viability of cells was highest at the beginning of cultivation and stayed constant for four days (Fig. 15). Afterwards, cell viability decreased to 90% living cells as compared to the initial cell viability at day 7 and was subsequently reduced to 70% and 50% living cells at day 10 and 14, respectively. For this reason, cells were harvested at 7 dpi, when a high cell number combined with good cell viability was

given. Under the cultivation conditions applied, this time point can be assigned as early stationary growth phase since no substantial growth occured during the last 24 hours. Generally, the determined growth rate for So ce56 indicates a typical bacterial growth curve in a closed system. The lag phase, the log and the stationary phase are well depicted. In the lag phase, cells adjusted to the new medium and cell population was maintained at a constant level. Exponential phase was reached between the second and the fourth day: the cells divided at a logarithmic rate depending upon the composition of the growth medium and the conditions of incubation. After 6 dpi, cell growth was retarded indicating the stationary phase. In this phase, the nutrients are consumed. In the stationary phase, So ce56 secondary metabolite production is initiated (Müller & Gerth, 2006). Furthermore, depletion of nutrients also induces the expression of genes involved in sporulation processes (Reichenbach & Dworkin, 1992). The period between 10 and 14 dpi to represents the death phase, where the viable cell population clearly decline.

4.2 Comprehensive analysis of the cytosolic proteome of So ce56

4.2.1 Gel-based analysis of *Sorangium cellulosum* So ce56 cytosolic proteins

For the proteomic analysis of So ce56, cells were harvested in the stationary phase at 7 dpi (Fig.15). This phase was chosen for protein extraction because protein samples led to nearly constant protein expression patterns in the 2-DE. Moreover, a relatively high number of viable cells were given during this period. In contrast, gels of protein mixtures extracted in the exponential phase revealed high deviations in protein expression patterns (data not shown). The cytosolic proteins were extracted by mechanic disruption of the cells and precipitation with acetone. 600 µg of proteins were loaded onto a gel. The genome sequence of So ce56 predict that nearly 80% of proteins exhibit a p*I* value between 3 to 10, therefore IEF was set between this p*I* range in order to resolve a maximal number of proteins on one gel. This experimental setup led to the separation of approximately 300 proteins in Coomassie colloidal stained gels (Fig.17).
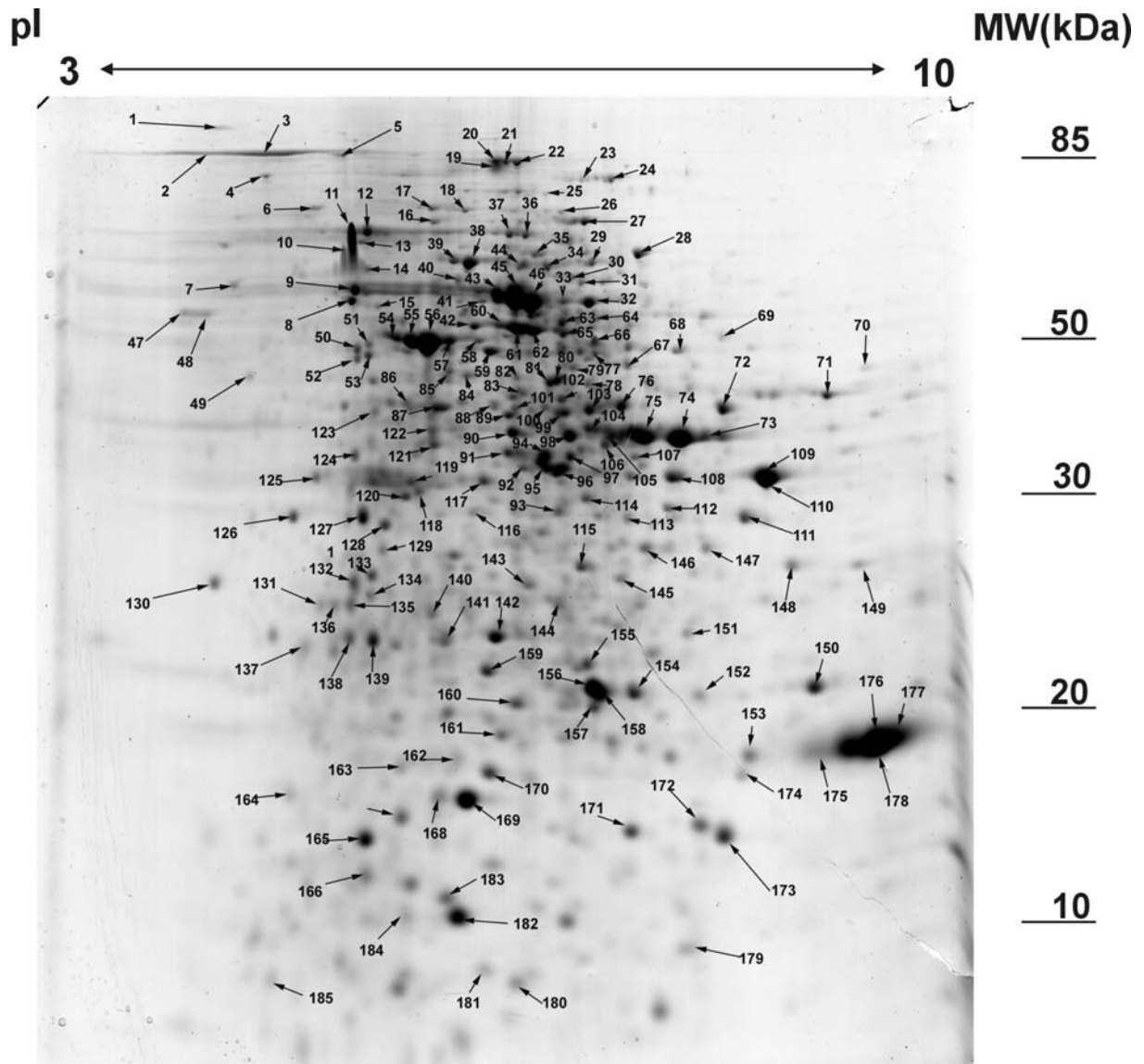
Fig. 17: 2-D map of cytosolic proteins of *Sorangium cellulosum* So ce56. Proteins were electrophoretically separated within a p*I* range of 3-10. 600 µg of protein was applied. A 12.5% SDS-tricine-polyacrylamide gel was used. Protein spots are stained with Coomassie colloidal and numbered as listed in table 1.

Tryptic digestions of excised protein spots and subsequent peptide mass fingerprint (PMF) analyzes via MALDI-TOF-MS led to the identification of 185 proteins out of 300 protein spots using the MASCOT database query. Proteins were considered to be identified, when: (i) the same proteins excised from three different 2-D gels gave the same identification; (ii) the resulting MOWSE score exhibited at least values of 50 and therefore considered as significant; and (iii) the experimentally determined p*I* and M*r* values of the proteins matched the theoretical values calculated from the predicted amino acid sequence. Some protein spots were identified as isoforms from one protein leading to the identification of 115 different proteins in total (Tab. 8)

representing the cytoplasmic proteome. These 115 proteins were further clustered into 12 groups according to their homologous relationship (COG classification). As expected, the majority of the classified proteins could be assigned to functions in the primary metabolic pathways: Assignation to amino acid (14 proteins), carbohydrate (13 proteins), lipid (6 proteins) and nucleotide metabolism (6 proteins). (Fig.18)
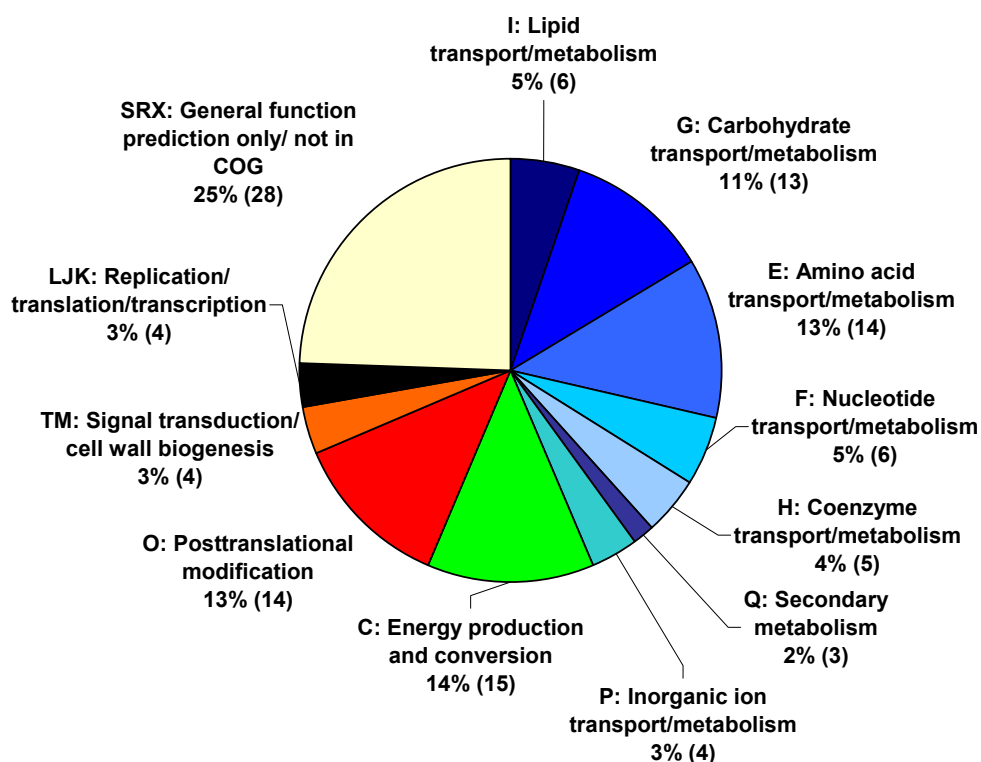
Fig. 18: Classification of 115 identified cytosolic proteins (early stationary phase) of *Sorangium cellulosum* So ce56 according to COG categories. The percentages and numbers are given with respect to the total number of identified proteins. The functional categories are as follows: G, carbohydrate transport and metabolism; I, lipid transport and metabolism; E, amino acid transport and metabolism; F, nucleotide transport and metabolism; H, coenzyme transport and metabolism; P, inorganic transport and metabolism; Q, secondary metabolites transport and metabolism; C, energy production and conversion; O, posttranslational modifications; T, signal transduction mechanisms; M, cellwall biogenesis; L, replication; J, translation; K, transcription; R, general function prediction only; S, function unknown; X, no functional category.

In order to illustrate the functional role of the detected enzymes, KEGG pathway schemes were generated using the Enzyme Classification (EC) numbers of the identified proteins.

4.2.1.1 Identified enzymes involved in the glycolytic pathway

Nine identified proteins belong to the glycolytic pathway (COG G) starting with glucose-6-phosphate isomerase (sce5669, EC 5.3.1.9) and then go further with the enzymes 6-phosphofructokinase (sce3426, EC 2.7.1.11); fructose-bisphosphate aldolase (sce1923, EC 4.2.1.13); triose-phosphate isomerase (sce7348, EC 5.3.1.1); glyceraldehydes-3-phosphate dehydrogenase (sce7350, 1.2.1.12); phosphoglycerate kinase (sce7349, EC 2.7.2.3); phosphoglycerate mutase (sce4502, EC 5.4.2.1); phosphopyruvate hydratase (sce7698, EC 4.2.1.11) and pyruvate kinase (sce4540, EC 2.7.1.40), which catalyze the final step in glycolysis, the conversion of phosphoenol-pyruvate to pyruvate.

Also proteins from the fermentation process were detected: alcohol dehydrogenase (sce3952, EC 1.1.1.1); lactate dehydrogenase (sce1050, EC 1.1.1.27); aldehyde dehydrogenase (sce0676, EC 1.2.1.3).

4.2.1.2 Identified enzymes involved in the tricarbon cycle acid (TCA) cycle

Many proteins of the TCA cycle were detected in the cyctosolic fraction and also from the pyruvate dehydrogenase reaction. Two subunits of the pyruvate dehydrogenase complex were identified, which converts the endproduct of glycolysis for the TCA cycle pathway: pyruvate dehydrogenases sce3800 and sce3801 (EC 1.2.4.1). Moreover, four identified proteins were involved in the TCA cycle: Isocitrate dehydrogenase (sce5773, EC 1.1.1.41); aconitate hydratase (sce8137, EC 4.2.1.3); succinate-CoA ligase (sce9141, EC 6.2.1.5) and malate dehydrogenase (sce1050, EC 1.1.1.37).

4.2.1.3 Identified enzymes involved in amino acid metabolism

A high percentage (13%) of the identified proteins belongs to the category of amino acid metabolism. These include the histidine (sce8010; sce8855), glutamate (sce7210), alanine/aspartate (sce5046), glycine/serine/threonine (sce6587) and valine/leucine/isoleucin metabolic pathways (Fig.33) with the identified enzymes: ketol-acid reductoisomerase (sce3732), branched-chain amino acid transaminase (sce6015) and 3-isopropylmalate dehydrogenase (sce3735).

4.2.1.4 Identified enzymes involved in lipid metabolism

The identified enzymes of the category group lipid metabolism are participating in the β-oxidation pathway of fatty acids like acyl-CoA dehydrogenase (sce2673) or butyryl-CoA dehydrogenase (sce1166; sce3575); enoyl-CoA hydratase (0250) and thiolase (sce7554) (Fig.22). The 3-oxoid CoA-transferase (sce5785) is involved in the ketone metabolism.

4.2.2 The detection of differently regulated proteins from the exponential and early stationary phase of So ce56 cytosolic proteins via Differential Gel Electrophoresis (DIGE)

Different growth phases of So ce56 are accompanied by differential metabolic fluxes, which is reflected by up- and down- regulation of proteins. The Differential Gel Electrophoresis (DIGE) technique allows the seperation of two proteomes on one gel using fluorescent dyes. In this experiment, the cytosolic proteins of *Sorangium cellulosum* So ce56 from the exponential and stationary phase were compared in order to identify the up- and down-regulated proteins which might play a role in the different metabolic pathways. For subsequent protein identification, DIGE gels were stained after visualization of the fluorescence-labeled proteins additionally with a MALDI-compatible silver-stain. The CyDye labeled gel image revealed a similar protein spot pattern as the silver stained gel (Fig. 19).
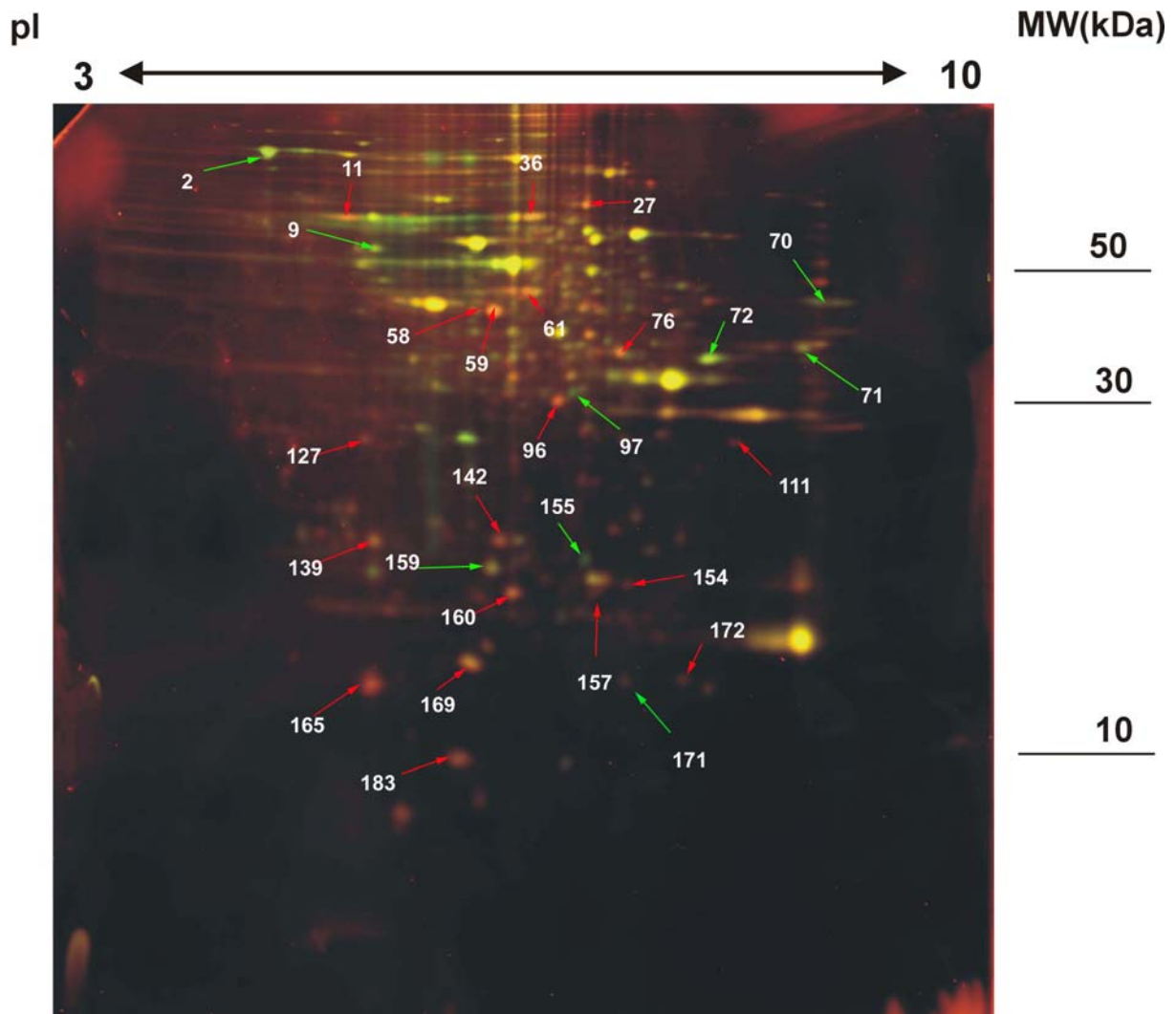
Fig. 19: Comparison of the So ce56 proteome in exponential and stationary growth phase. The cytosolic proteins were labelled with CyDyes (total protein content 100 μg) and separated on a 2-D gel (Biorad). Proteins isolated from the exponential phase labelled with Cy3™ (red spots, red arrows). The proteins of the stationary phase marked with Cy5™ (green spots, green arrows) following the numeration of the proteome map (Fig. 17 and Tab. 8).

For quantifications of protein abundances in both samples the Delta2D image analysis software was used. This led to the detection of 90 differentially expressed proteins in total, whereof 40 proteins appeared to be up-regulated in the stationary phase and 50 up-regulated in the exponential phase. However, overlay images with gels from previous experiments and the MALDI-TOF-MS analysis of the silver-stained 2-D DIGE gel (data not shown) reveal only the detection of 28 differentially regulated proteins (Tab. 9 and Fig. 19). Protein identification was assumed to be significant in case the PMF analysis of the silver stained gel and the according predictions of the proteome map as a second affirmation were coincident. Thus, 16

different proteins were identification from the up-regulated proteins in the exponential phase, whereas 9 up-regulated proteins from the stationary phase were identified (Tab. 9). The identified proteins are grouped according to the different COG classes.

4.2.3 Western blot analysis of the So ce56 phosphoproteome from the cytosolic fraction

The complex life cycle of *Sorangium cellulosum* So ce56 and the annotation of about 498 members of serine/threonine/tyrosine kinase and histidine kinase families (the majority are eukaryotic kinase-like kinases (317 ELKs)), implies that this bacterium requires broad regulation mechanisms for multiple signaling pathways (Schneiker *et al.*, 2007). Therefore, it was of interest to detect So ce56 proteins that are involved in different signaling cascades during the early stationary phase.

4.2.3.1 Anti-phosphotyrosine analysis of tyrosine phosphorylated proteins and anti-phosphoserine analysis of serine phosphorylated proteins

For the detection of tyrosine and serine phosphorylated proteins, Immuno- (Western) Blot analysis of the 2-D PAGE gels was performed using antibodies against the phosphorylated amino acids. For the detection of the proteins the 2-D Blots were compared to the 2-D proteome map of cytosolic proteins (Fig.24). Western Blot analysis led to the identification of 23 serine-phosphorylated and 28 tyrosine-phosphorylated proteins listed in table 10.12 proteins are proposed to be phosphorylated on both serine and tyrosine phosphorylation sites. Additionally, neural network predictions for serine, threonine and tyrosine phosphorylation sites of the proteins were performed using the NetPhos 2.0 database (Blom *et al.*, 1999).
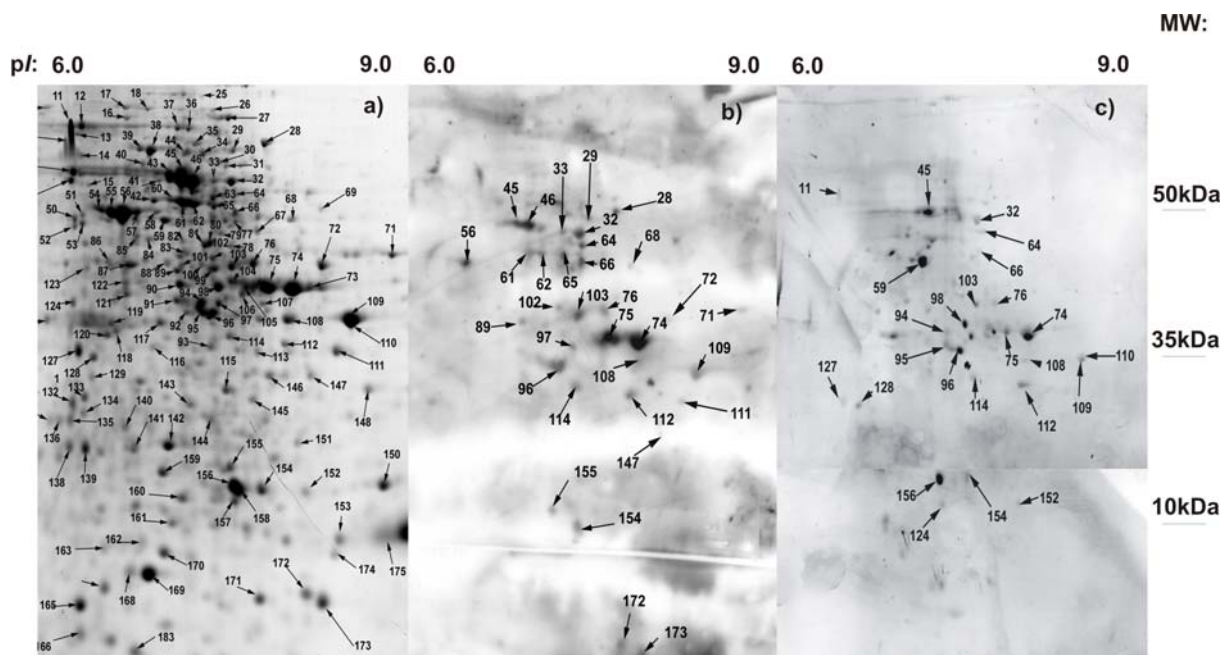
Fig. 20: Western Blot analysis of So ce56 cytosolic proteins with antibodies against phosphorylated serine and tyrosine. The numbering was according to the So ce56 proteome map as shown in a) (Fig. 17). b) Detection of tyrosine phosphorylated proteins. c) Detection of serine phosphorylated proteins.

4.2.4 Blue-Native PAGE of So ce56 for the identification of protein complexes in the cytosolic fraction

The Blue-Native PAGE was initially performed to analyze polyketide synthases (PKSs) of high molecular weight (>300 kDa). As no exact information was documented about the localization of these huge multienzymes, the cytosolic and the membrane fractions were investigated here with this method. 1 mg of cytosolic proteins was loaded per BN gel lane. The separated proteins from the first and the second dimension of the Blue-Native PAGE were analyzed with MALDI-TOF-MS. Mass spectrometric analyzes led to the identification of 5 proteins in the first dimension and of 24 different proteins from the second dimension (Fig. 21). The detected proteins were classified into their specific COG categories (Tab. 11).
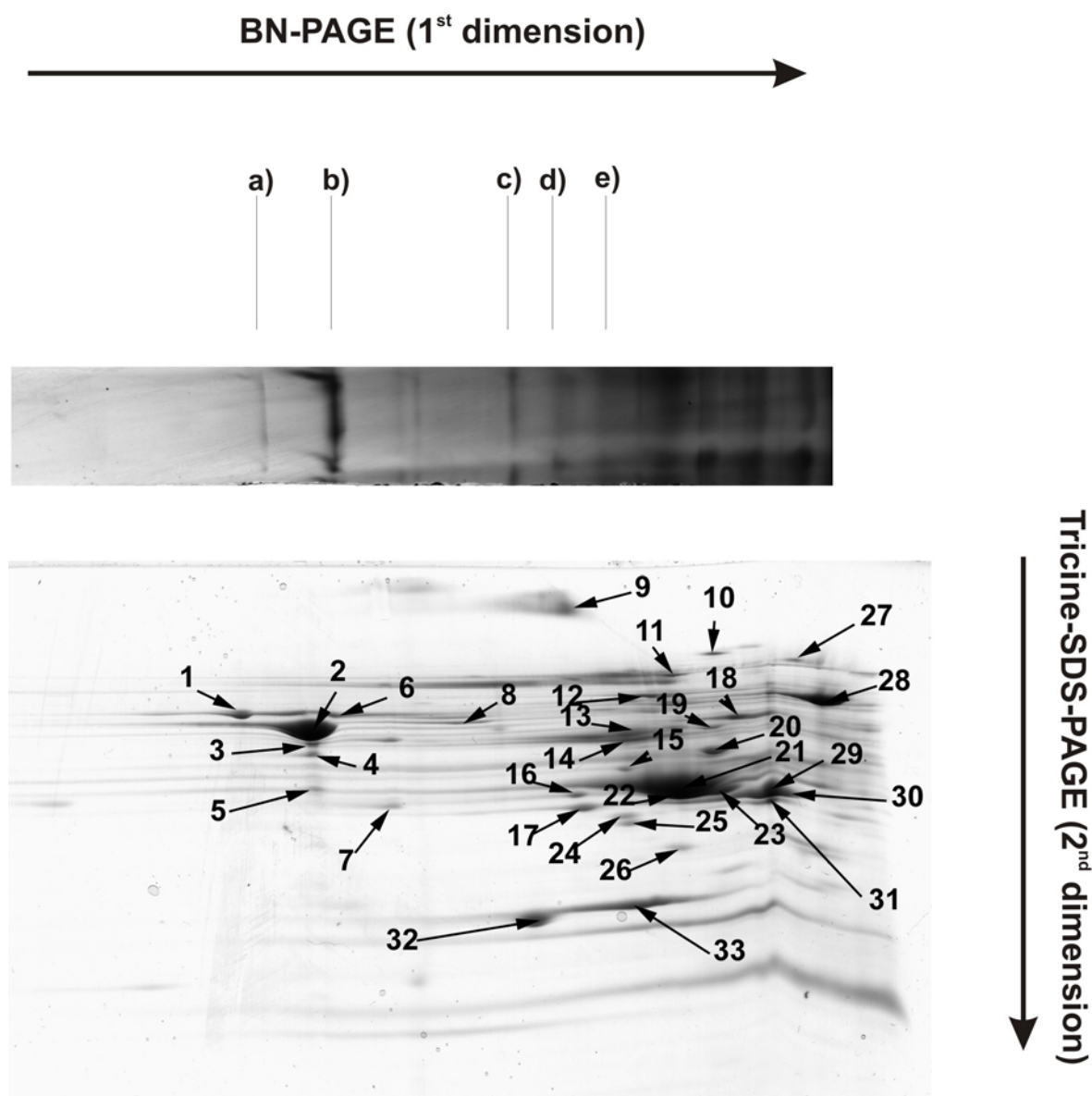
Fig. 21: Blue-Native PAGE of cytosolic proteins of So ce56 from the early stationary phase. The 5 identified proteins of the BN gel lane were given in letters (a-e) and the detected proteins of the Tricine-SDS-PAGE approach, which led to the identification of 33 proteins, were given in numbers (1-33).

4.3   Proteomic analysis of the So ce56 extracellular proteins (secretome)

The extracellular proteins of the cellulose degrading *Sorangium cellulosum* So ce56 were extracted in the stationary growth phase from the cell-free culture supernatant. To eliminate polysaccharides and lipids present in the extracellular fraction, a phenol-extraction method was applied (Watt *et al.,* 2005). After Coomassie staining, protein

spots were excised and analyzed by MALDI-TOF-MS. The resulting peptide mass fingerprints were used for MASCOT database queries, which resulted in the identification of 82 extracellular proteins (Fig. 22). As some proteins occur as isoforms on different positions in the gel, a total of 41 different proteins could be detected (Tab. 12).
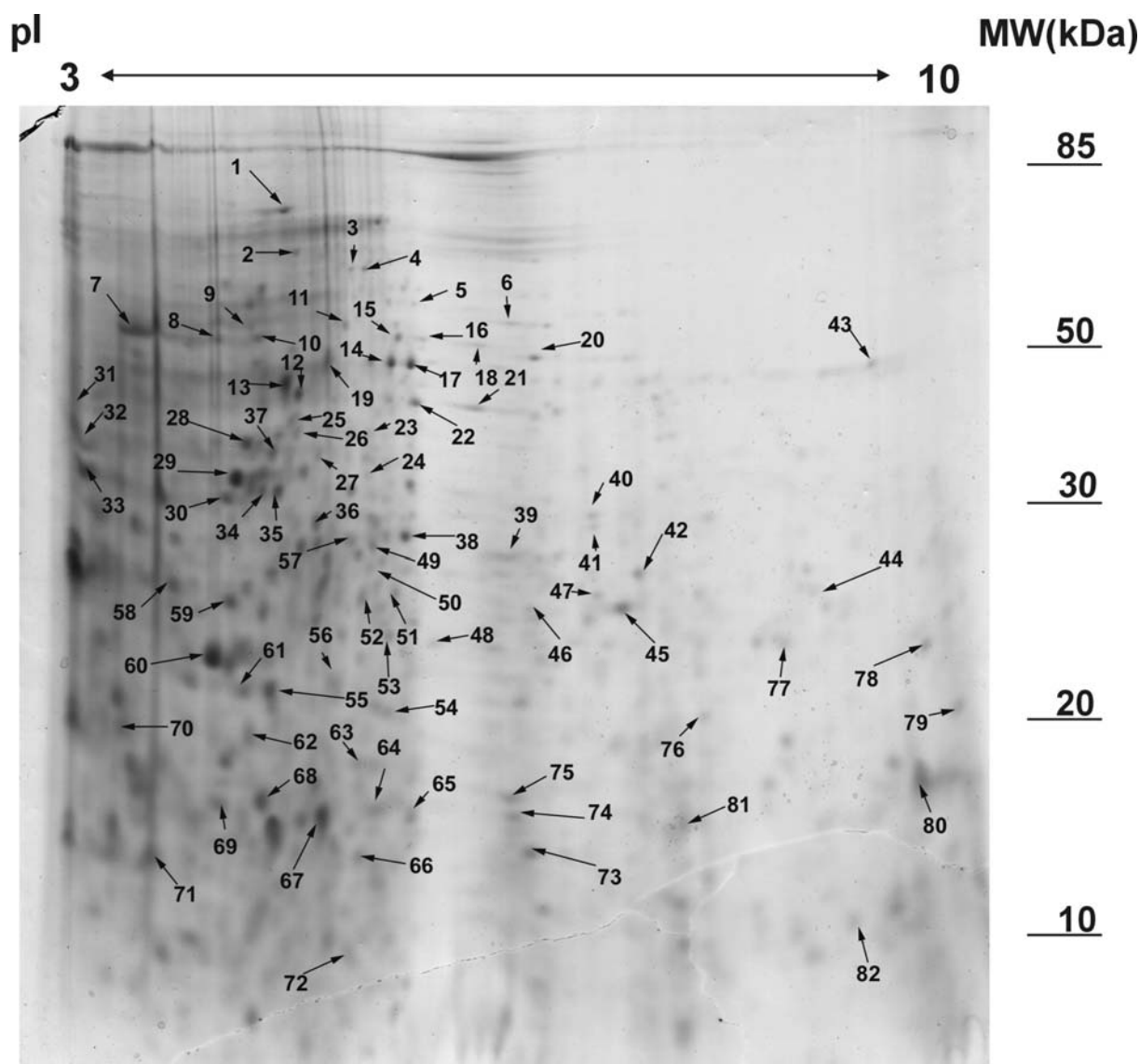
Fig. 22: Extracellular proteins of *Sorangium cellulosum* So ce56. Coomassie Blue stained 2-D gel of 500µg phenol extracted So ce56 secreted proteins in a p*I* range of 3-10 (GE Healthcare). Identified protein spots are numerated and listed in table 12.

The identified proteins could be classified into 7 functional groups according to their function or cellular localization (Tab. 12). As expected, the majority of the identified proteins (24%) are predicted as extracellular proteins. This functional group contains mainly secreted enzymes involved in degradation and cell protection processes, like

the predicted exoprotease (sce3910). Also with a high number found in the extracellular fraction are the membrane proteins (22%) assumed to derive from the inner membrane, periplasm and outer membrane. Interesting are the identification of proteins from the functional groups "DNA-interacting proteins" (7%), "protection" (10%) and "protein folding" (12%), which are known to be localized in the cytosol or in the periplasm. Only one hypothetical protein (sce1224) could not be assigned to a functional category.
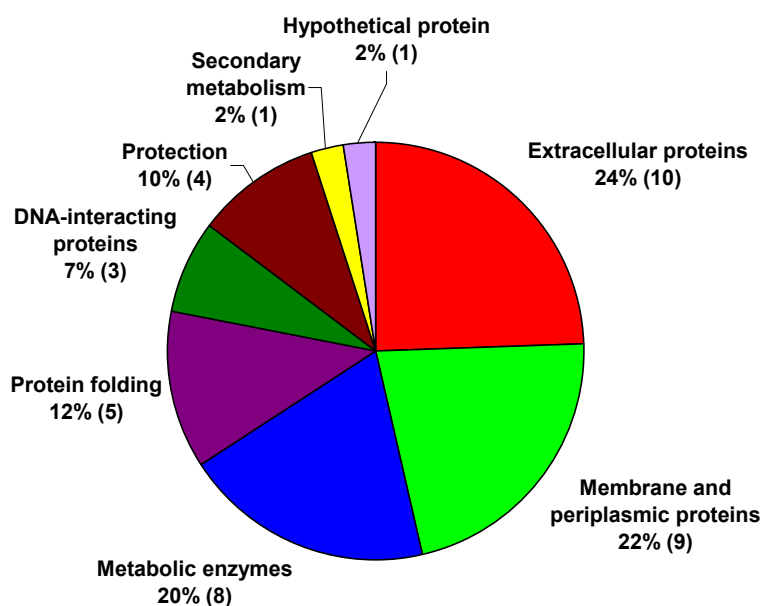
Fig. 23: Identified extracellular proteins of So ce56 grouped into seven functional subgroups represented in a pie chart diagram. The number of identified proteins is given in numbers and percentages, which relate to the 41 different extracellular proteins. The classification was carried out according to the protein's predicted function (metabolic enzymes; DNA-interacting proteins; protective enzymes; protein folding; proteins involved in the secondary metabolism) or proposed cellular occurrence (extracellular proteins; membrane and periplasmic proteins).

The presence of an N-terminal signal sequence was checked for each identified protein by the Signal P software to estimate the amount of proteins secreted to the extracellular space. Signal peptides are necessary in order to initiate protein export via the Sec translocation system. Signal peptides generally consist of three distinct domains: a basic amino-terminal n-region followed by a hydrophobic h-region and then a hydrophilic c-region containing the recognition site for the signal peptidase (Nielsen *et al.*, 1997). The destinations of the identified proteins with predicted signal

peptides might be the periplasm or the outer membrane (OM). Approximately 22% (about 2083) of the annotated proteins (9367) contain a potential signal peptide. Nevertheless, the signal sequence prediction reveals that 11 proteins of the 41 identified proteins contain a signal peptide and thereof 4 proteins reveal a t̲win-a̲rginine t̲ranslocation (Tat) signal peptide, which indicates that proteins may be transported in a folded way (Tab. 12). The Tat signal peptides resemble somehow to the Sec signal peptides. In contrast the Tat signal peptides contain a conserved amino acid sequence motif at the n-region/h-region boundary. This motif can be defined as S-R-R-x-F-L-K, where the consecutive arginine residues are almost invariant (Palmer & Berks, 2003). While the Sec system only transports unstructured substrates, the function of the Tat pathway is to translocate folded proteins. Furthermore, proteins with a helix-turn-helix motif (sce3479) and a transmembrane domain (sce1365; sce1531) were detected indicating that these proteins interact with the DNA or are integrated into the membrane, respectively. Additionally, all predicted signal peptides in So ce56 were manually screened for the presence of lipobox sequences [LVI]-[ASTVI]-[GAS]-C by using the DOPOL database (Babu *et al.*, 2002). Two lipoproteins were identified with this tool: the putative lipoproteins sce5067 and sce4343. The identification of possible transport proteins of So ce56 was carried out with the Transport Classification (TC) Database, the significantly identified transport proteins in So ce56 were assigned with TC numbers, e.g. Cyanate ABC transporter (TC 3.A.1.16.2) (Tab. 18).

4.4 Comprehensive analysis of So ce56 membrane proteins, outer membrane proteins and outer membrane vesicle proteins

In the following, proteomic analysis of So ce56 membrane proteins, outer membrane proteins and outer membrane vesicle proteins are presented. In addition to the proteomic results of the outer membrane vesicle proteins, electron microscopy studies of the vesicles were carried out.

4.4.1 Identification of membrane proteins of So ce56

Similar to other Gram-negative bacteria, the envelope of So ce56 is composed of inner (cytoplasma) and outer membranes separated by the periplasm that contains a

thin peptidoglycan layer (Duong *et al.*, 1997). The So ce56 membrane acts as a barrier against external influences in the soil, where many proteins were integrated or associated to the membrane. In order to obtain insights into the functional role (e.g. transport processes, cell-signaling and gliding motility) of the So ce56 membranes, proteins integrated into or associated to the membrane were analyzed. Their hydrophobic nature makes them difficult to solubilize and resolve on gels, resulting in a consistently underrepresentation in 2-D gel based proteomic analyzes. Therefore, a membrane extraction protocol for So ce56 membrane proteins was developed.

The membrane proteins from *Sorangium cellulosum* So ce56 cells were extracted from the early stationary phase. After extraction, the membrane proteins were solubilized with 1% digitonin and separated on a 1-D SDS-PAGE. After Coomassie staining, the gel was excised in segments containing approximately 10 visible protein bands each (Fig. 24). The gel-pieces were digested with trypsin and the peptides were loaded onto a nanoLC system coupled to an ESI-IonTrap instrument. MS/MS spectra were generated from peptides with a high signal to noise ratio to gain sequence tags. The peptide fragments were used together with its parent mass to query the sole protein database utilising the MASCOT software. Proteins were regarded as identified peptides with a MOWSE score of > 40.
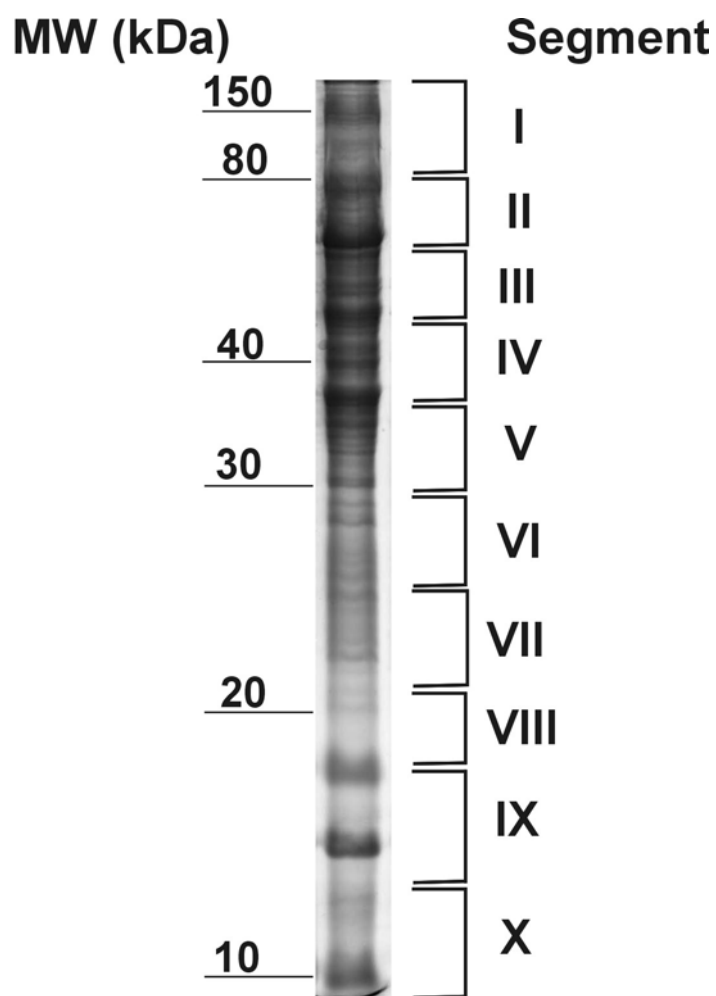
Fig. 24: Separation of *Sorangium cellulosum* So ce56 membrane proteins by 1-D SDS-PAGE, which is stained with Coomassie Blue and analyzed with nanoLC-ESI MS/MS. The gel was cut into 10 segments (I – X) containing at least 2 - 10 visible protein bands. Proteins were tryptically digested and analyzed by nanoLC-ESI-MS/MS. The identified proteins of each segment are listed in table 13

A total of 66 different proteins were identified from the membrane extract and are listed in table 13, each gel-segment revealed at least 5 different proteins.

The identified proteins from the membrane fraction were divided into eight functional classes considering their functionality and their localization in the cell (Fig. 25).
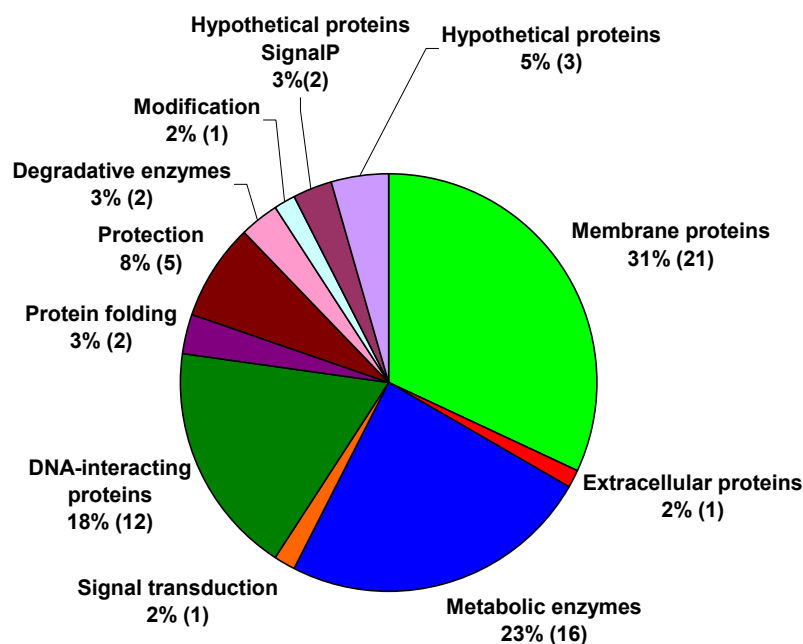
Fig. 25: Pie chart diagram representing the identified 66 So ce56 membrane proteins (given in numbers and percentages) which were divided into nine functional subgroups. Classification: DNA-interacting proteins; protective enzymes; metabolic enzymes; protein folding; degradative enzymes; protein modification; extracellular proteins; membrane proteins; hypothetical proteins.

The majority of the identified proteins (31%) could be assigned to membrane or membrane-associated proteins. TMHMM analysis reveals the detection of only one protein with three transmembrane domains, which is probably involved in potassium transport at the inner membrane (sce0244). 9 of 21 membrane proteins have a secretion signal and seven proteins of them contain a putative twin-arginine motif. The analysis of the signal sequences reveals the detection of one putative lipoprotein (sce5067), which might belong to the outer membrane. Additionally, the identified proteins were blasted in the Transport Classification (TC) Database to identify possible transport proteins in So ce56 listed in table19. Thus, the identification of many "DNA-interacting proteins" (18%) and "metabolic enzymes" (23%) from the membrane fraction reveals no apparent association to the membrane components known so far, they might belong to the cytosolic fraction.

4.4.1.1 Membrane protein analysis of So ce56 with the Blue-Native PAGE method

As described in section 4.2.4, the extracted membrane proteins were analyzed from protein complexes, which are associated to the membrane. The main focus of this analysis was the identification of multienzyme complexes such as the polyketide synthases and the transport protein integrated in the So ce56 membrane. The extracted membrane proteins were solubilized with 1% digitonin and 500 µg proteins were loaded onto the BN gel. The resolved protein complexes were then separated in a second dimension, the Tricine-SDS-PAGE, to identify individual proteins (Fig. 26). 4 proteins from the first dimension and 37 proteins of the second dimension were identified by MALDI-TOF-MS analysis. The identified proteins were classified into their COG categories. Signal sequence analysis reveals the detection of 3 out of 37 proteins with an N-terminal signal peptide. Only one protein with a transmembrane domain was detected with the TMHMM software (Tab. 14). As described before, the TC and the DOPOL database searches was also applied in this case.
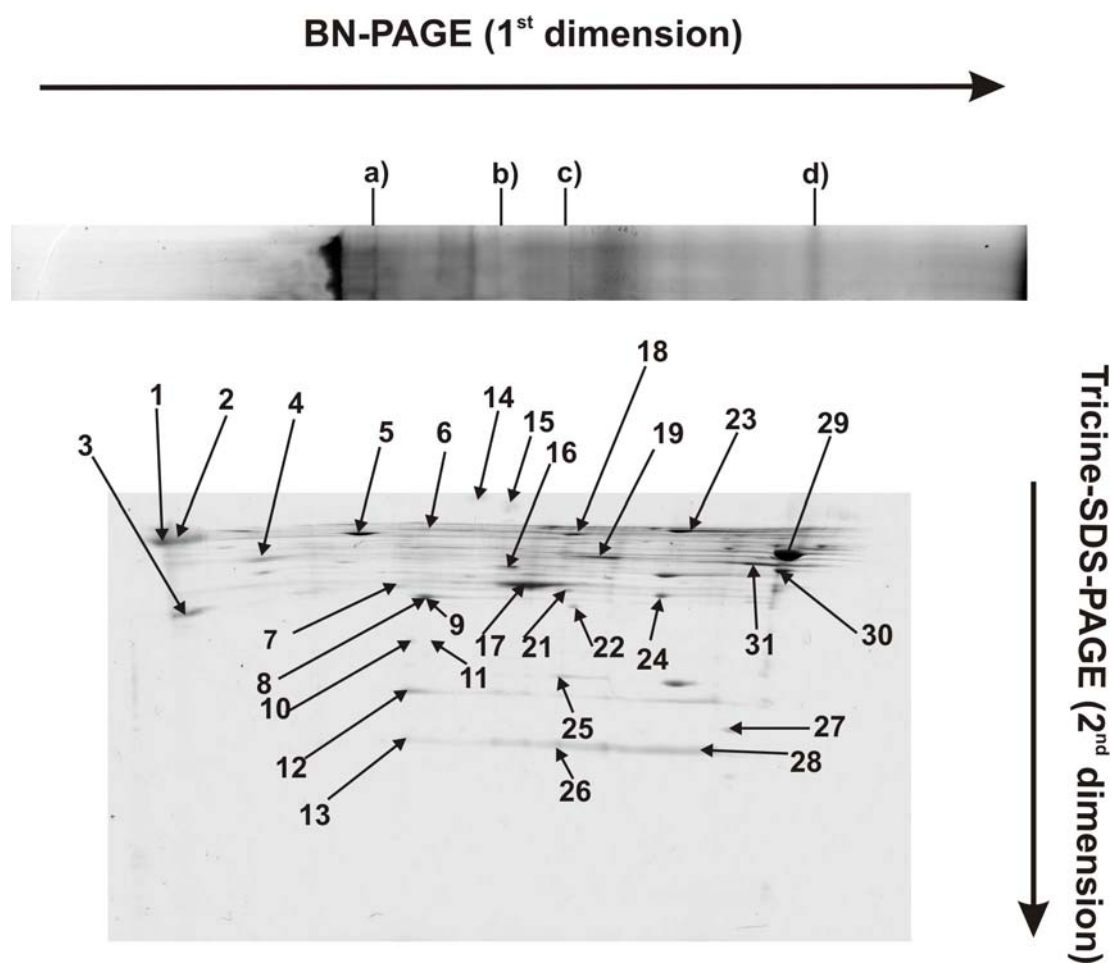
Fig. 26: Blue-Native PAGE of So ce56 membrane proteins extracted from the early stationary phase. Identified proteins from the BN gel lane were given in letters (a-d) and the detected proteins of the Tricine-SDS-PAGE were given in numbers (1-30).

4.4.2 Identification of outer membrane proteins of So ce56

Additional analysis of the outer membrane proteins might reveal detailed information about outer membrane vesicle formation and further transport systems. Therefore, the outer membrane proteins of So ce56 were extracted using cells from the early stationary phase for ultrasonification. To isolate the outer membrane proteins from the cell-free supernatant, an ultracentrifugation step was carried out. After protein separation with an SDS-PAGE, tryptically digested gel segments (I-VII) were analyzed with nanoLC-ESI-MS/MS (Fig. 27). MASCOT analysis leads to the identification of 36 proteins from the outer membrane fraction. Furthermore, all predicted signal peptides were manually screened for the presence of lipoproteins by

using the DOPOL database revealing two putative lipoproteins (sce2691 and sce4176) transported by the Tat-signalling pathway (Tab. 15).
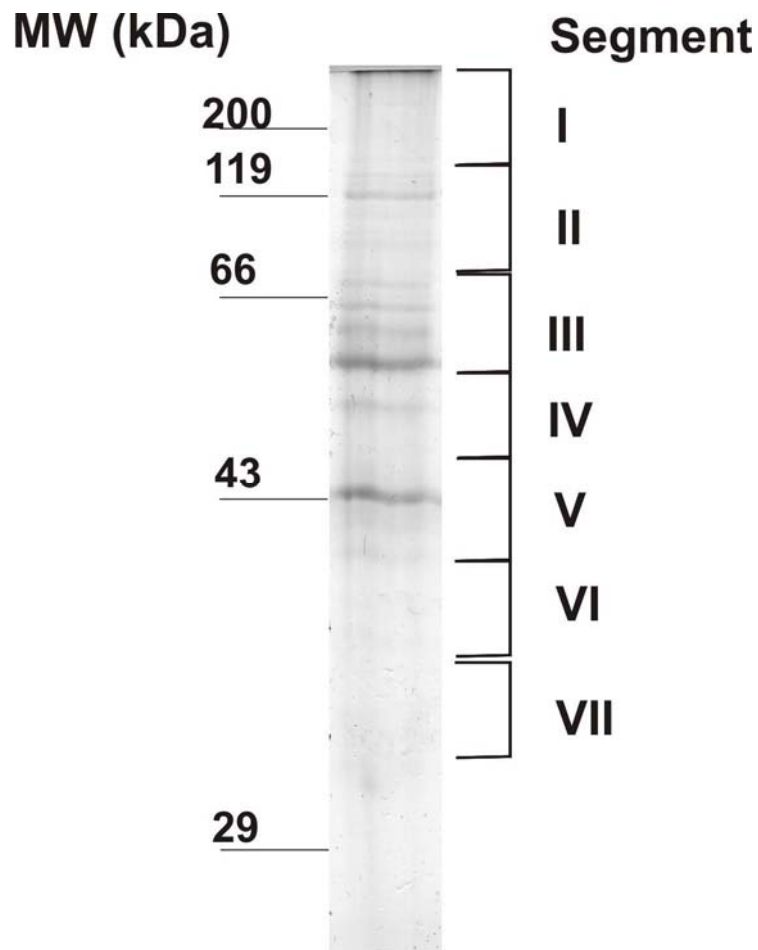
Fig. 27: 1-D SDS-PAGE of outer membrane proteins (OMPs) of So ce56 analyzed by nanoLC-ESI-MS/MS. To obtain OMPs of So ce56 the bacterial cell was ultrasonificated and centrifuged to remove the cell debris. The pellet, which was obtained after ultracentrifugation of the supernatant at 100,000 x *g*, was washed with 2% Lauryl-Sarcosine and ultracentrifuged again. The washed pellet was then separated on a SDS-PAGE and stained with Coomassie Blue. As described before, the gel was cut into 7 segments (I-VII) and digested with trypsin. The analysis of the tryptic digests was carried out with nanoLC-ESI-MS/MS. The identified proteins of each segment were shown in table 15.

The identified proteins were divided into eight different functional subgroups relating to their functionality and their locality.
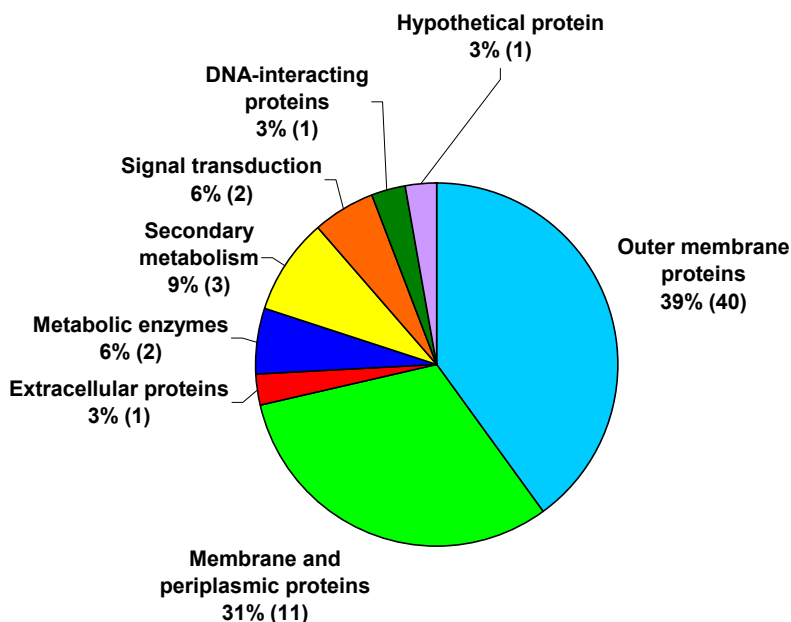
Fig. 28: The 35 identified So ce56 outer membrane proteins (OMPs) were divided into eight different functional groups. The sorting of the proteins was carried out according to the following functionalities or cellular compartments: signal transduction, secondary metabolism, metabolic enzymes, DNA-interacting proteins, hypothectical proteins without any function, extracellular proteins, inner membrane/periplasmic proteins and outer membrane proteins. The number of identified proteins was given in numbers and percentages (Tab. 15).

As expected, the main part of identified proteins (39%) belongs to the functional group of putative outer membrane components. Nearly each of them contains a signal peptide with a twin-arginine motif. The identified proteins occurring in the outer membrane are mainly transport or receptor proteins. The TC database query detect about 12 transport proteins compared to characterized and published from other organisms (Tab. 20).

But of main interest are the identified proteins from the outer membrane fraction occuring also in the outer membrane vesicle fraction, which may indicate the origin of vesicle formation. These are two components of the outer membrane: a putative maltoporin (sce7619) and a phosphate selective porin (sce7966). Another protein, which occurs in both compartments, is a predicted phosphatase (sce0936) normally active in the periplasm.

A large number of the extracted outer membrane proteins were inner membrane and periplasmic proteins (31%). The main part of these proteins were putative ABC transporters or ATPases located in the inner membrane or in the periplasm, like the identified putative ABC dipeptide transporter (sce7548) or a probable cation transporting ATPase (efflux, sce2485), which contains 10 transmembrane domains predicted by TMHMM. The identified putative nitrogen sensor histidine kinase (sce7800) from the outer membrane fraction shows homologies to Jer3/Amb3 (identity of 85%/ 81%) (Tab.21). Jer/Amb proteins belong to the jerangolid and ambruticin polyketide synthase clusters produced by *Sorangium cellulosum* strains So ce307 and So ce10, respectively. Jer3/ amb3 genes encode also a putative sensor kinase component. These results imply that So ce56 has a putative jerangolid or ambruticin biosynthetic gene cluster.

4.4.3 BLASTP comparisons to proteins involved in the jerangolid/ambruticin biosynthesis

In order to validate this finding and to find further genes which might be also involved in the jerangolid/ ambruticin, the genome sequence of So ce56 was blasted against the jerangolid/ ambruticin biosynthetic gene clusters of the *Polyangium (Sorangium) cellulosum* database (NCBI). BLASTP search reveals more genes with high similarities (>60) shown in table 21. Furthermore, the BLASTP search engine was used to scan predicted polyketide synthases of So ce56 with putative homologies to jerangolid/ ambruticin polyketide synthases from the *Polyangium cellulosum* database. But the predicted PKSs from So ce56 revealed no significant identities (less than 50%) to PKSs encoded by the jerangolid/ ambruticin biosynthetic gene cluster from *P. cellulosum*.

4.4.4 Characterization of the outer membrane vesicle proteome

A number of Gram-negative bacteria naturally produce extracellular outer membrane vesicles (OMVs). Similar to the outer membrane, OMVs contain lipopolysaccharides, outer membrane and/or periplasmic proteins, and phospholipids. Possible functions of these vesicles are cell-to-cell signalling, protein and DNA transfer between bacterial cells and transporting toxins (Mashburn-Warren *et al.,* 2006). Since so many outer membrane proteins could be identified in the extracellular proteome from the culture supernatant of So ce56 was analyzed for the existence of OMVs and their

protein content. The analysis of outer membrane vesicles (OMVs) from the cell-free culture supernatant of So ce56 was carried out in two steps described in 4.4.4.1 and 4.4.4.2:

4.4.4.1 Electron microscopic analyzes of outer membrane vesicles of So ce56

The existence of membrane vesicles in the culture supernatant of So ce56 was investigated by electron microscopy. Visualization of OMVs was achieved by negative staining of the OMV-fraction with 1% uranyl acetate. The electron micrographs of the outer membrane vesicle preparation of So ce56 displayed spherical structures with a mean diameter ranging from 30-120 nm (Fig. 30). These micrographs indicate that So ce56 extrude OMVs from its outer membrane into the culture supernatant.
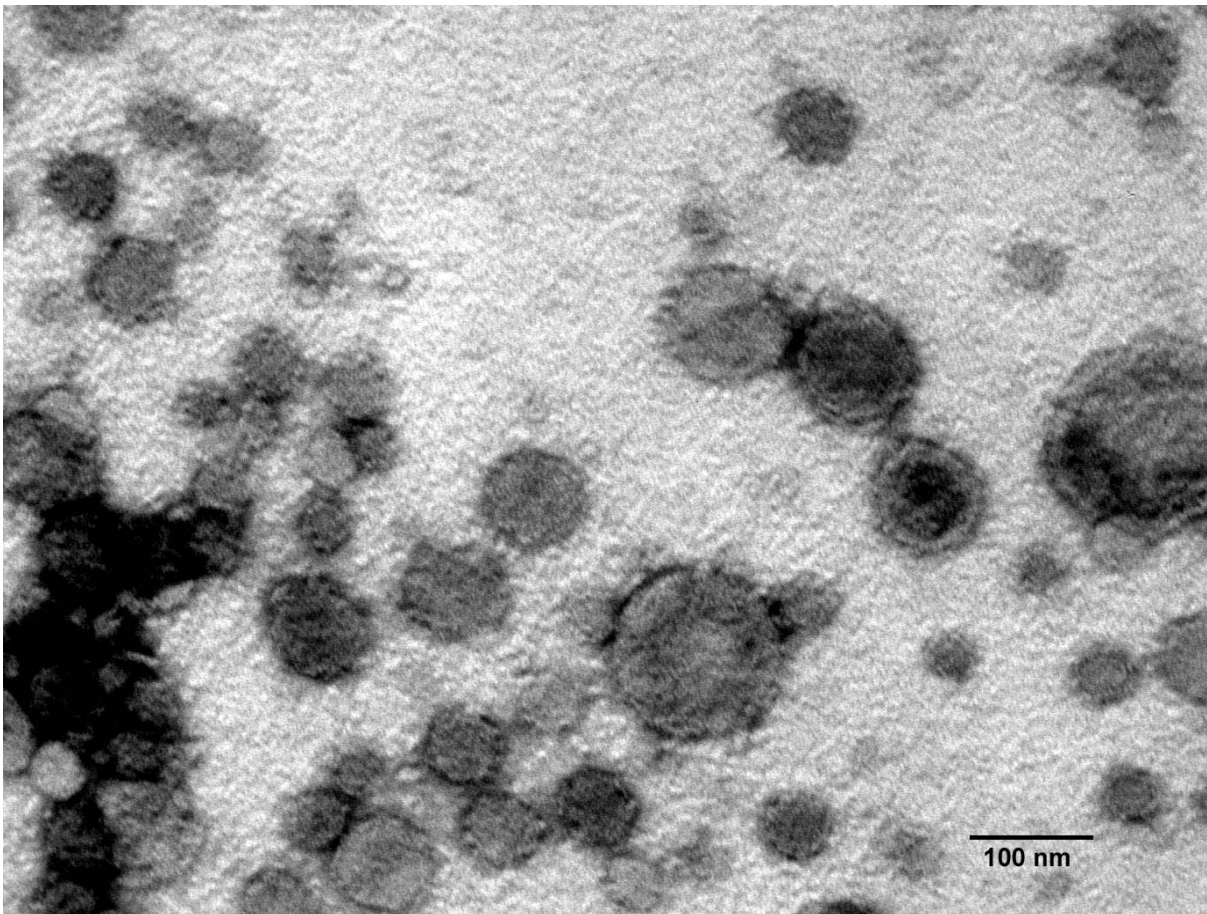
Fig. 29: Electron microscopy of 1% uranyl acetate stained outer membrane vesicles extracted from cell free supernatant of *Sorangium cellulosum* So ce56 at 27,000 fold magnification.

4.4.4.2 Proteome analysis of outer membrane vesicle proteins of So ce56

In a second approach, the outer membrane vesicle proteins of So ce56 were analyzed. Therefore, the outer membrane vesicle proteins were separated on a 1-D SDS-PAGE and the resulting protein bands (Fig. 30) were analyzed by MALDI-TOF-MS and MASCOT database query of the So ce56 genome sequence.
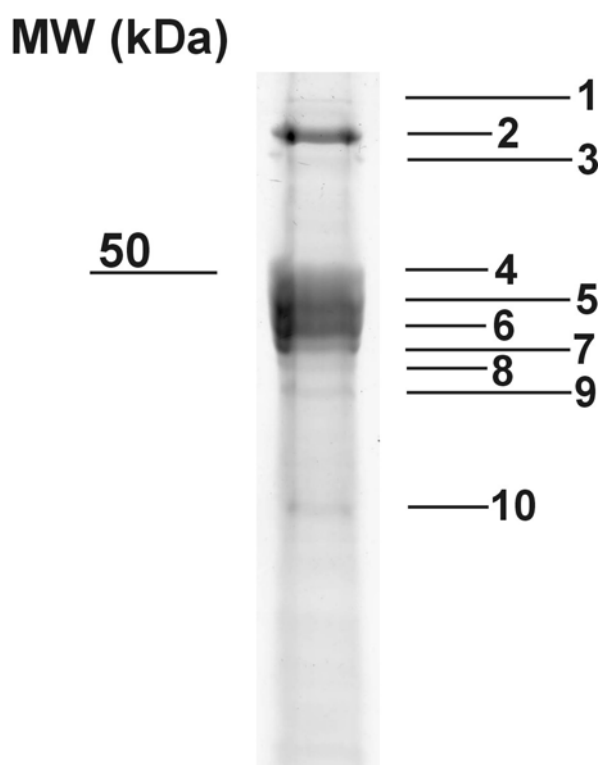
Fig. 30: Outer membrane vesicle proteins separated on a SDS-PAGE gel stained with Coomassie Blue and analyzed by MALDI-TOF-MS. Identified proteins from the gel bands were given in numbers.

The analysis of protein bands resulted in the identification of 5 different proteins summarized in table 16. Three of five identified proteins possess a secretion signal, whereas one of these proteins, a putative outer membrane lipoprotein (sce5067), occurs in 5 positions on the gel as isoforms. The putative outer membrane lipoprotein and the putative phosphate-selective porin O and P (sce7556) could possibly be enclosed from the outer membrane during OMV formation. This could be an explanation why membrane proteins occur in the extracellular environment. Only one protein could not be allocated to a functional group.

5 Discussion

In the present study a comprehensive proteome analysis of *Sorangium cellulosum* So ce56 was achieved under standardized conditions.

Sequencing of the *Sorangium cellulosum* So ce56 genome and subsequent sequence annotation was performed in parallel to this work with participation of the authors from the currently submitted So ce56 genome paper (Schneiker *et al.*, 2007). This comprehensive proteome analysis led to the detection in total 286 proteins with 247 distinguished proteins classified in COG categories (Tab. 22). The availability of this accumulated proteomic data concerning the identified proteins derived from the cytosol, extracellular, membrane, and outer membrane fractions has allowed proteomic verifications of the genome-based predictions of So ce56. Although 2-D gel-based approaches of total protein extracts only open a limited window to the proteome of So ce56, they provide plenty of information about cellular processes, protein expression differences as well as changes in protein modifications about the more abundant proteins.

5.1 Proteomic analysis of So ce56 cytosolic proteins resulted in the identification of enzymes involved in primary metabolism

From the 115 identified cytosolic proteins of the proteome map, specific proteins are involved in different important metabolic pathways. In the following the carbon, nitrogen and lipid metabolism were discussed. Despite its great potential, 2-D gel technology has its limitations. To work under standardized conditions and to set the proteomic basis for further analysis, the isoelectric focusing was carried out with IPG-strips ranging in a pH-value of 3 – 10 in a 12.5% SDS-PAGE gel, which allows the separation of proteins in a range of about 10 – 100 kDa. Therefore, the recovery of basic small and large proteins was negatively influenced. Additionally, numerous proteins were not expressed or only expressed in low concentrations during the early stationary phase. Since the high abundant proteins tend to mask the low abundant proteins with similar physiochemical properties, it is difficult to visualize them properly (Gygi *et al.*, 2000). The silver staining method used in So ce56 detects the low abundant proteins apparent in a number of 800 – 1,000 protein spots (data not shown), whereas the Coomassie staining protocols led to the detection of the more abundant proteins (300 proteins visualzed). Furthermore, membrane proteins are generally underrepresented on current 2-D gels due to their hydrophobic character, so that they are solubilized incompletely by the detergents that are compatible with isoelectric focusing. Moreover, the secretome of So ce56 is almost completely missing, as only whole cell extracts were used. Thus, efforts were made to overcome this problem by analyzing in addition, the membrane, outer membrane, outer membrane vesicle, and secreted proteins with different methods, e.g. BN-gels.

5.1.1 Growth in the early stationary phase of So ce56 leads to high expression of enzymes involved in carbon metabolism

The So ce56 cells were cultivated in a defined medium with glucose as carbon and asparagine as nitrogen source. The fact that glucose was the sole sugar source in the growth medium could explain the relative high abundance and completeness in identification of enzymes of the glycolytic pathway (Fig. 31).
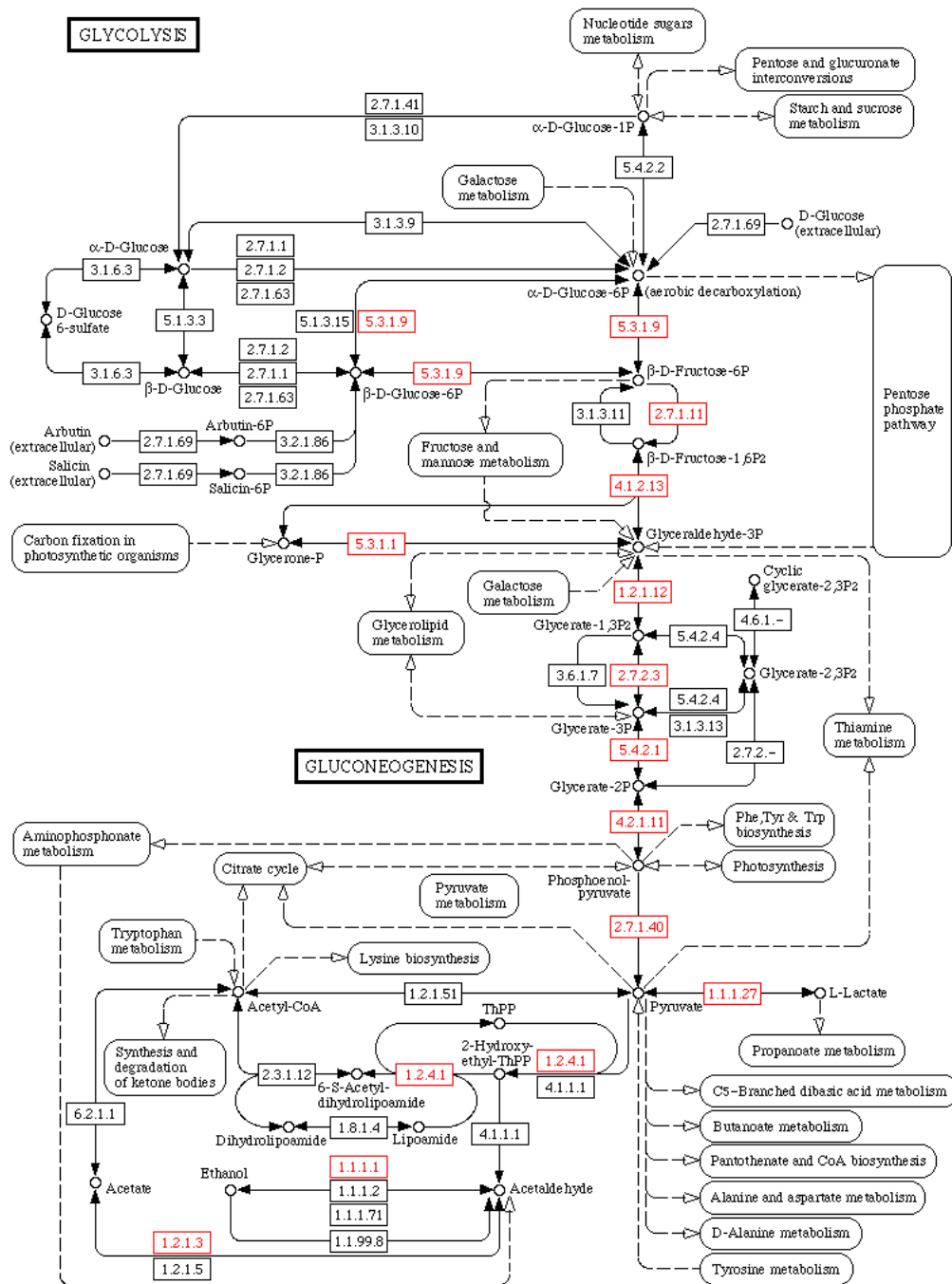
Fig. 31: Glycolysis KEGG-pathway scheme of *Sorangium cellulosum* So ce56. The red-colored EC numbers depict the identified proteins from So ce56 involved in the glycolysis and in the fermentation process. The identified proteins of the glycolysis are displayed in red: glucose-6-phosphate isomerase (sce5669, EC 5.3.1.9); 6-phosphofructokinase (sce3426, EC 2.7.1.11); fructose-bisphosphate aldolase (sce1923, EC 4.2.1.13); triose-phosphate isomerase (sce7348, EC 5.3.1.1); glyceraldehydes-3-phosphate dehydrogenase (sce7350, 1.2.1.12); phosphoglycerate kinase (sce7349, EC 2.7.2.3); phosphoglycerate mutase (sce4502, EC 5.4.2.1); phosphopyruvate hydratase (sce7698, EC 4.2.1.11); pyruvate kinase (sce4540, EC 2.7.1.40); pyruvate dehydrogenase (sce3800, sce3801, EC 1.2.4.1). Proteins from the fermentation process: alcohol dehydrogenase (sce3952, EC 1.1.1.1); lactate dehydrogenase (sce1050, EC 1.1.1.27); aldehyde dehydrogenase (sce0676, EC 1.2.1.3).

Proteins of the glucose uptake system could not be detected in the proteome analysis, but genome sequence annotations exhibit the sequences for a glucokinase (sce4351), which converts glucose in the cell, derived from the glucose-containing disaccharides (e.g. lactose, maltose or trehalose). Moreover, four compounds of a PTS-system (*pts*P, sce8622; *pts*H, sce5765; *pts*N, sce2509 and *pts*I, sce5764) were revealed by the genome sequence, which are responsible for transport and activation of glucose to form glucose-6-phosphate for the glycolytic pathway, and thus eliminating the need for glucokinase (Saier *et al.*, 1995; Meyer *et al.*, 1997). The end-products of glycolysis, phosphoenol-pyruvate and pyruvate build the link to the tricarboxylic acid (TCA) cycle as to fatty acid synthesis and other central metabolic steps (Fig. 32). The TCA cycle serves as a major converter to supply the cell with usable energy from carbohydrates, proteins or fatty acids (Voet *et al.*, 2006). This could explain the high abundance of the putative TCA pathway proteins, e.g. isocitrate dehydrogenase (sce5773) or aconitase hydratase (sce8137) in the cytosolic proteome.
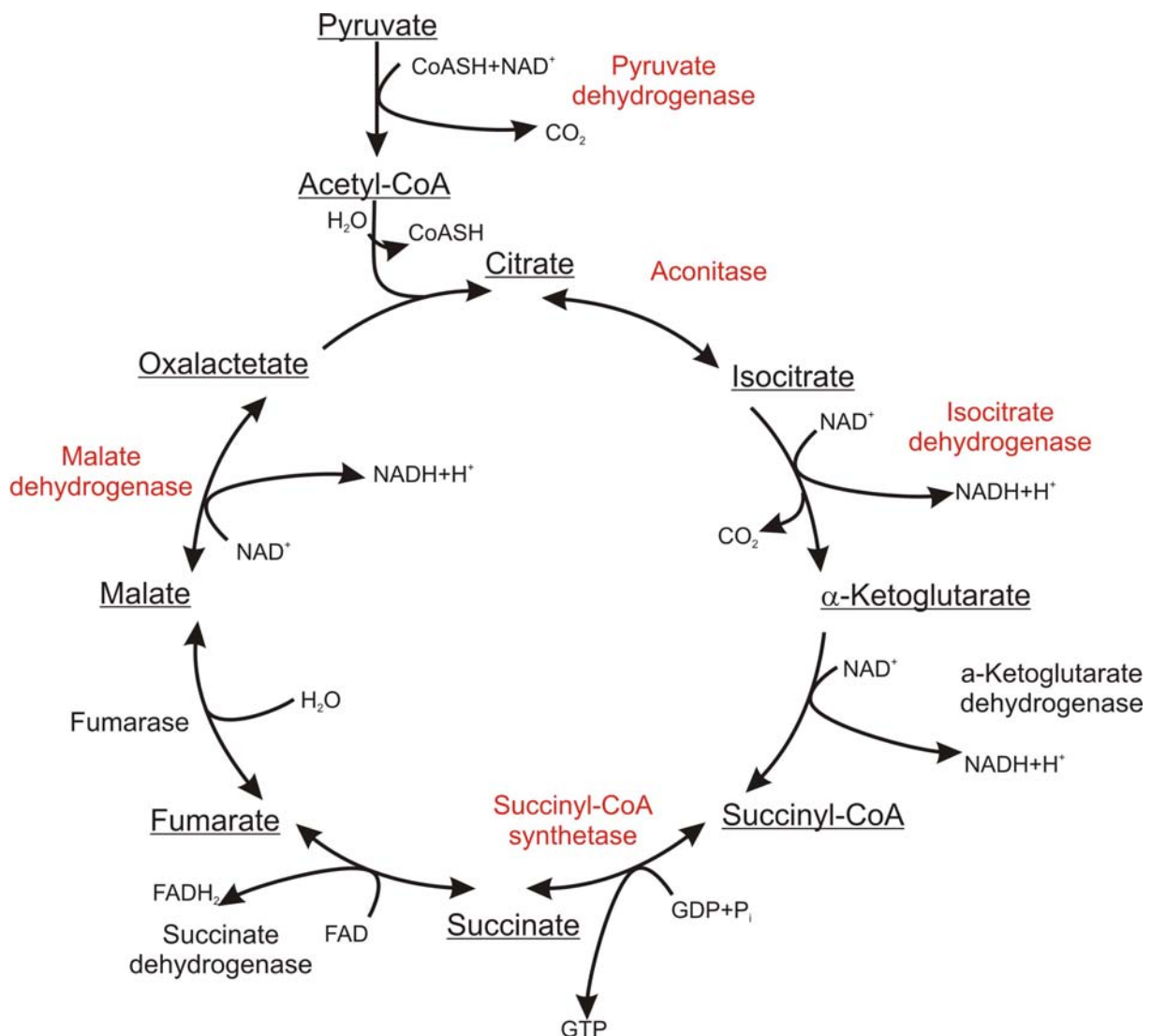
Fig. 32: TCA cycle scheme of So ce56. The identified enzymes are written in red. Pyruvate dehydrogenase (sce3800, sce3801, EC 1.2.4.1); Isocitrate dehydrogenase (sce5773, EC 1.1.1.41); aconitate hydratase (sce8137, EC 4.2.1.3); succinate-CoA ligase (sce9141, EC 6.2.1.5); malate dehydrogenase (sce1050, EC 1.1.1.37).

Between the TCA cycle and the glycolysis metabolic pathway, the intermediary enzyme complex pyruvate dehydrogenase (sce3800, sce3801) is required to convert the end product of glycolysis phosphoenolpyruvate for further processes. Detection of proteins most probably coding for a lactate-dehydrogense (sce1050) and for an alcohol-dehydrogenase (sce3952), could indicate that *S. cellulosum* So ce56 undergoes fermentation at the point of harvest due to an oxygen limitation in the culture (Fig. 31). Pyruvate is oxidized and decarboxylated in a complex reaction involving NAD, coenzyme A and pyruvate dehydrogenase, forming a central molecule in metabolism, the acetyl-CoA. Acetyl-CoA not only forms the first stable

intermediate of the TCA cycle, but it also plays a main role in the fatty acid biosynthesis (Voet *et al.*, 2006).

The significant identification of a putative xylose isomerase (sce5429) from the cytosolic fraction and the identification of a putative ABC-type xylose transport glucose (sce6008) from the outer membrane protein fraction of So ce56 is surprising since no xylose was present in the medium. Further on, xylose can not be used as a sole carbon source by *S. cellulosum* So ce56 (Müller & Gerth, 2006). Xylose isomerase converts xylose to xylulose, but is also usually referred to as glucose isomerase converting glucose into fructose (Asboth & Naray-Szabo, 2000). The identification of a putative ABC-type xylose transport system leads to the assumption that during the stationary phase when glucose is nearly depleted So ce56 possibly use alternate sugar uptake systems. Presumably, the xylose transport protein is constitutively expressed to activate further components for a functional high affinity to xylose during growth on glucose (Gonzales *et al.*, 2002). As cellulose and hemicellulose are components of plants, degradation of these biopolymers by microorganisms like So ce56, leads to the release of xylose and glucose monomers. For example, the genome sequence reveals the occurrence of the putative endo-1.4-beta-xylanase (sce4601) enzyme, which degradates the plant cell wall component xylan to obtain the pentose sugar xylose (Prescott *et al.*, 2005). Another sugar of the plant polysaccharides is the pentose arabinose (Hespell, 1998), where genome sequences reveal two putative arabinose uptake systems (sce3306 or sce3310). Maybe these alternate sugar uptake systems of So ce56 were used under natural conditions, much likely under starvation conditions in soil.

5.1.2 Nitrogen metabolism and supply in So ce56 is indicated by the identification of various enzymes involved in amino acid metabolism

The constantly abundant metabolic enzyme glutamate-ammonia ligase (sce7210) represents another interesting enzyme in So ce56. The central role of this enzyme in nitrogen metabolism is the ATP consuming condensation of ammonia with glutamate to yield glutamine (Voet *et al.*, 2006). Glutamine is important for further amino acid biosynthesis reactions. As asparagine is the main nitrogen source in the S-medium and a good reservoir for chemically fixed aspartate and ammonia, it could be

processed in further pathways, like the glutamine synthesis and the tricarboxylic acid cycle. In addition, three proteins were identified, which are involved in alanine and aspartate metabolism: argininosuccinate synthase (sce5046), adenylosuccinate synthase (sce8895) and aspartate transaminase (6239). Aspartate and glutamate as sole nitrogen sources are not useful substrates for growth of So ce56 (Müller & Gerth, 2006).

Furthermore the histidine (urocanate hydratase sce8010, histidinol-phosphate transaminase sce8855) and the purine (IMP dehydrogenase sce0088: ribonucleoside-diphosphate reductase sce3875; nucleoside diphosphate kinase sce 2949; phosphoribosylamine-glycine ligase sce9014; adenylosuccinate synthase sce8895) metabolic pathways were highly active during this growth phase. Histidine biosynthesis is a metabolic cross-road and plays an important role in cellular metabolism being interconnected to both the *de novo* synthesis of purines and nitrogen metabolism. The connection to purine biosynthesis results from an enzymatic step catalyzed by imidazole glycerol phosphate (IGP) synthase. The important connection to nitrogen metabolism is due to a glutamine molecule, the source of the final nitrogen atom of the imidazole ring of IGP (Fani *et al.*, 2007). Nucleotides are components of some central metabolic cofactors, including FAD, NAD$^+$, and coenzyme A probably supporting the various metabolic pathways in So ce56 (Voet *et al.*, 2006).

The branched chain amino acids valine and isoleucine are synthesized from the central intermediary metabolite pyruvate, using nearly the same biosynthetic pathway and enzymes (Fig. 33). However, the leucine biosynthetic pathway branches off from the valine pathway at the branchpoint 2-oxoisovalerate, which is required for the biosynthesis of coenzyme A and branched chain fatty acids.
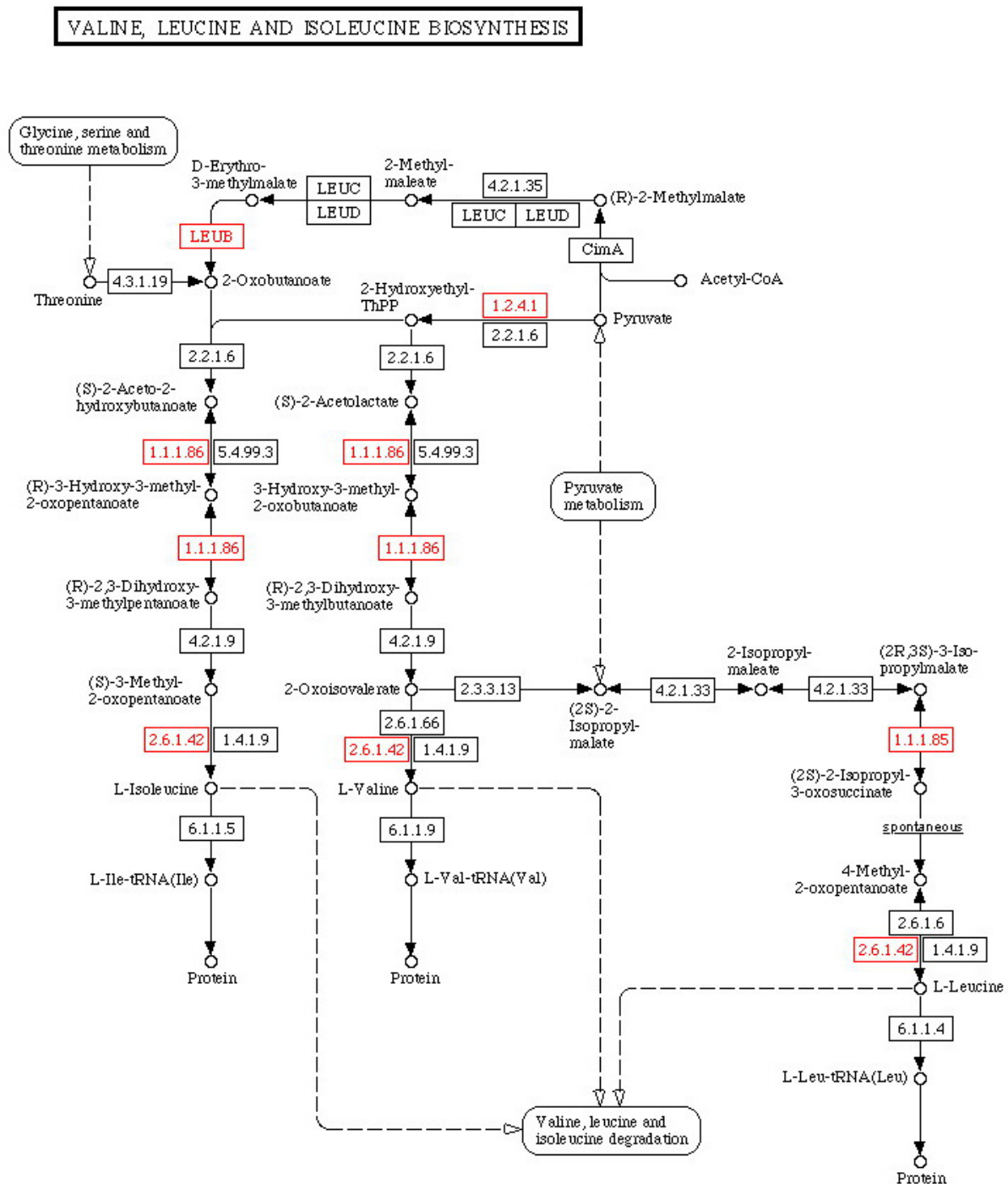
Fig. 33: Valine, leucine and isoleucine biosynthesis KEGG pathway scheme of So ce56. The red highlighted EC numbers correspond to the identified enzymes from the cytosolic fraction of So ce56. Branched-chain-amino-acid transaminase (sce6015, EC 2.6.1.42); ketol-acid reductoisomerase (sce3732, EC 1.1.1.86); 3-isopropylmalate dehydrogenase (sce3735; 1.1.1.85); pyruvate dehydrogenase (sce3800, sce3801, EC 1.2.4.1).

Similar to the β-oxidation, degradation of these amino acids delivers CoA derivatives and intermediates, which could be used in metabolic pathways. Experiments by

Müller and Gerth (2006) showed that addition of leucine and isoleucine has negative effects on the production of secondary metabolite whereas valine increases the yield of chivosazol production. This might be explained by synergistic effects on the pantetheine biosynthesis. Pantothenic acid is a precursor of coenzyme A, which is required for the synthesis of the secondary metabolites (Fig.34) (Jansen *et al.*, 1997; Müller & Gerth, 2006).
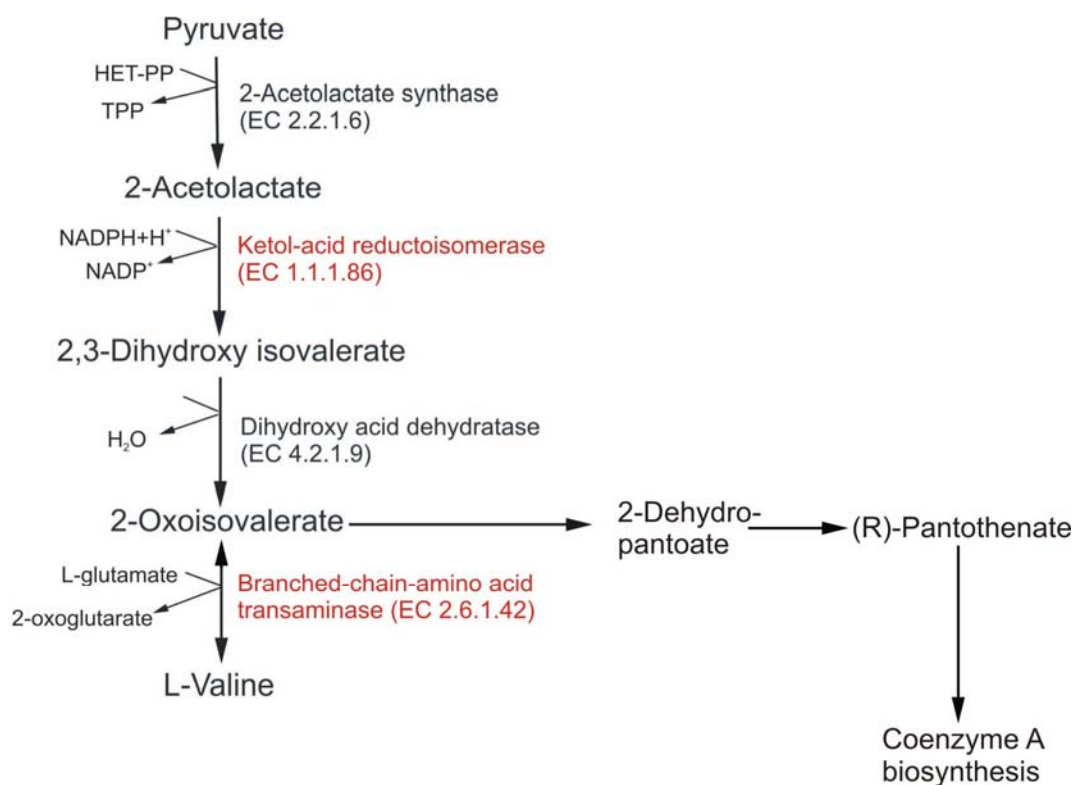
Fig. 34: A valine biosynthesis pathway scheme of the identified enzymes involved in the valine synthesis from *S.cellulosum* So ce56. The identified enzymes are colored in red: Ketol-acid reductoisomerase (sce3732) and branched-chain amino acid transaminase (sce6015). The intermediate 2-oxoisovalerate from the valine biosynthesis is necessary for the construction of the vitamin (R)-pantothenate, which is used in turn as substrate for the coenzyme A biosynthesis (based on KEGG pathway schemes).

5.1.3 Identified enzymes involved in the lipid metabolism are mainly participating in the β-oxidation of fatty acids

Proteomic analysis resulted also in the identification of various proteins of So ce56 that are involved in the fatty acid metabolism. For example the enzymes acyl-CoA dehydrogenase (sce2853), acetyl-CoA C-acetyltransferase or thiolase (sce7554) and the enoyl-CoA dehydratase (sce0250) are important for the fatty acid degradation (β-

oxidation) shown in figure 35 (Michal, 1999). Butyryl-CoA dehydrogenase (sce1166 and sce3575) belongs, like the acyl-CoA dehydrogenase, to the family of flavoproteins and differ only in the preference of substrates (Battaile *et al.*, 2002).
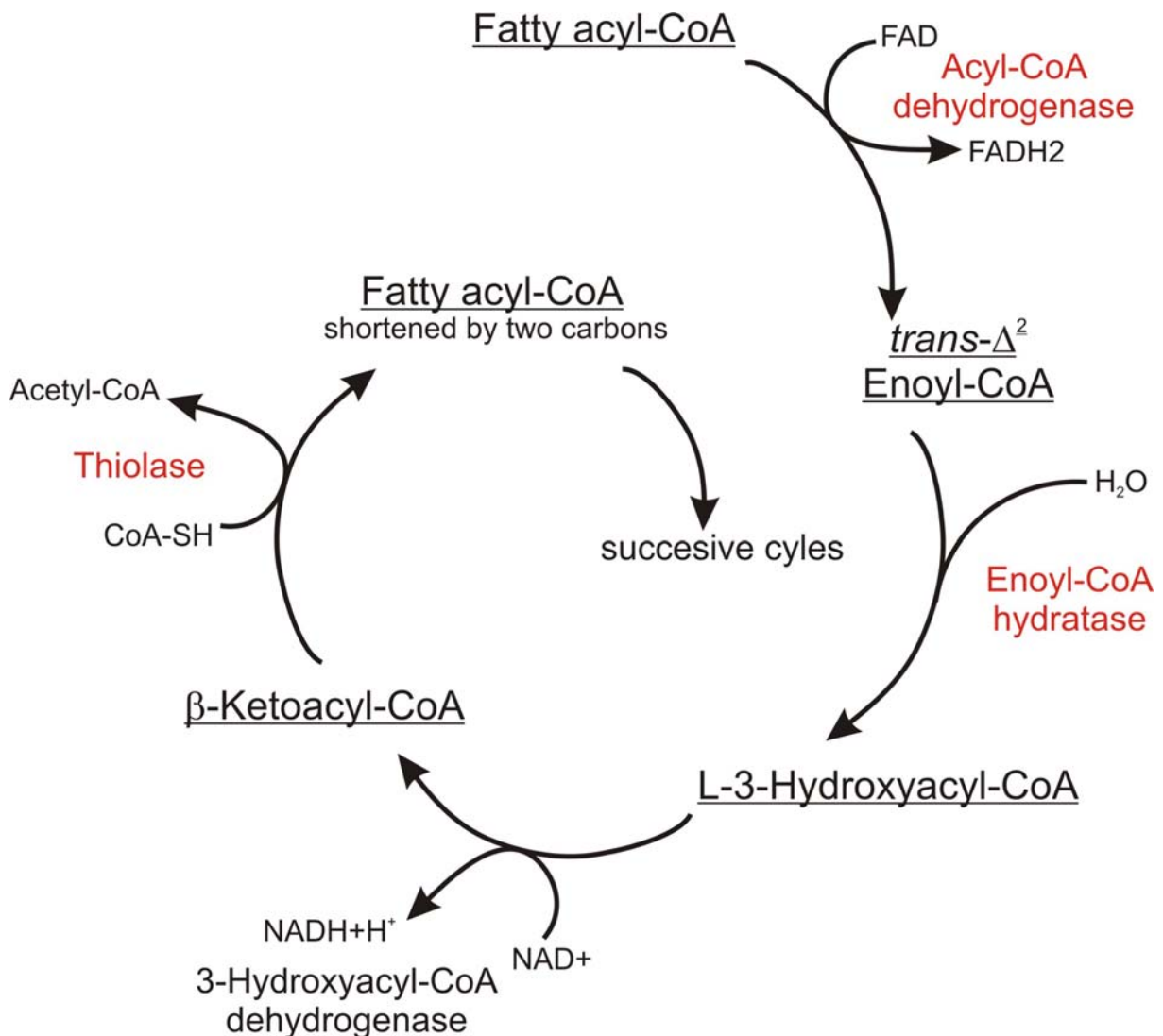
Fig. 35: The β-oxidation of a fatty acyl CoA of So ce56 illustrated in a diagram (based on Michal, 1999, Biochemical pathways). The identified enzymes are coloured in red.

The β-oxidation pathway provides the bacterial cell with acetyl-CoA fed in different metabolic pathways and with cell energy produced in the form of $FADH_2$ and NADH (Nyström, 2004). The identified enzyme 3-oxoid CoA-transferase (sce5785) catalyzes the reversible transfer of CoA from CoA-thioesters, e.g. the endproduct of the β-oxidation: acetoacetyl-CoA, to free acids. In contrast to the fatty acid degradation, chain elongation of the fatty acids is catalyzed by several individual enzymes associated into a large complex with acetyl-CoA and malonyl-CoA as

substrates and NADPH as electron donor. To summarize, fatty acid chain elongation is carried out stepwise by adding two-carbon units deriving from acetyl-CoA over and over until a fatty acid of the appropriate length has been made (Prescott *et al.*, 2005). The focus of So ce in this growth phase might be to supply the cell with energy and metabolic intermediates by the degradation of fatty acids for further cellular processes.

5.1.4 Differential Gel Electrophoresis (DIGE) from the exponential and early stationary phase of So ce56 cytosolic proteins reveals different regulation of metabolic enzymes

The study of So ce56 cell cycle-regulated protein expression by using differential gel electrophoresis has provided insights into the complexity of the myxobacterial cell cycle. Even though only 28 proteins could be detected significantly, it gives a first impression how So ce56 utilizes resources and maintains the functioning of the cell cycle. The majority of identified proteins in both growth phases are involved in cellular nutrient uptake and energy supply (14 proteins of 28 identified proteins). The data reveal that enzymes in the carbohydrate metabolism involved in glycolysis, like the triose-phosphate isomerase (sce7348), xylose isomerase (sce5429), phosphoglycerate kinase (sce7349) and fructose-bisphosphate aldolase (sce1923), are assumed to be more abundant in the exponential phase than in the stationary phase (Grünenfelder *et al.*, 2001). These enzymes are necessary for increased cell growth during exponential phase to provide the bacteria with energy for further cellular processes. Moreover, it might be also an indication for the depletion of carbon, i.e. the depletion of one energy source during the early stationary phase. This assumption is supported by the identification of the enzyme thiolase (sce 7554) involved in the β-oxidation during the early stationary phase. It has been suggested that So ce starts to provide itself with carbon and energy by generating fatty acids from the degradation of membrane lipids (see 5.1.3; Nyström, 2004). Furthermore, the detection of xylose isomerase in the exponential phase supports the presumption that this enzyme converts glucose into fructose during glycolysis (Asboth & Naray-Szabo, 2000). Therefore, it could be excluded that xylose isomerase acts as an alternative sugar uptake system. Metabolic conversions lead to the generation of radicals like superoxides during oxidative phosphorylation of metabolic products (NADH, FADH) (Schaechter, 2007). This might explain the expression of antioxidants

like superoxide dismutases (SodA, sce0071; SodB, sce4167) in the exponential phase, which are needed to protect the bacterial cell from the increasing toxic side products during nutrient conversion. These enzymes catalyze the reaction of free oxygen radicals produced during the aerobic respiratory chain reaction into oxygen and hydrogen peroxide, which in turn is used by a catalase. Normally, it is expected that the production level of superoxide dismutases is higher in the stationary phase than in the exponential phase, as the cell is entering a stress phase (starvation) as described in *E.coli* (Nyström, 2004; Barriere *et al.*, 2001). Another protective protein is the organic hydrogen peroxide resistance protein (sce0181).

A further protection system is the degradation of misfolded proteins in the cytoplasm with a putative endopeptidase (sce3147). Identification of a relatively low number of metabolic proteins, especially for carbohydrate metabolism, during the early stationary phase leads to the assumption that the bacterial cell down-regulates the metabolism as a consequence of nutrient depletion during this phase (Kolter *et al.*, 1993). Additionally, a high number of synthesized proteins were of unknown function in both growth phases (6 proteins of 28 identified proteins) and represent candidates for putative regulators of the *Sorangium* cell cycle.

5.1.5 Identification of enzymes involved in primary metabolism were detected via Western Blot analysis of serine and tyrosine phosphorylated proteins

Since the discovery of eukaryotic-like serine/threonine kinase in *Myxococcus xanthus* (Munoz-Dorado *et al.*, 1991), *M. xanthus* becomes an excellent model system to study bacterial signal transduction and developmental processes, where many interesting findings followed. For example, a novel bacterial signaling system with a combination of a two-component system and a serine/threonine kinase cascade was discovered, which is involved in the fine tune regulation of developmental processes (Lux & Shi, 2005). Moreover, the characterization of a complete functional protein serine/threonine kinase signaling cascade in a prokaryotic organism was performed with *M. xanthus* (Nariya & Inouye, 2005). The recent completion of the So ce56 genome with 9367 CDSs revealed about 498 predicted serine/threonine/tyrosine kinases (eukaryotic-like kinases) and histidine kinases involved in regulatory processes (Schneiker *et al.*, 2007). Therefore, serine and tyrosine phosphorylation in

So ce56 were investigated via Western Blot analysis using Immunoblot methods leading to the identification of 23 serine-phosphorylated and 28 tyrosine-phosphorylated proteins, whereby 12 proteins are assumed to be serine and tyrosine phosphorylated. So far, no detailed information about So ce phosphorylation and their cellular functions was reported. Thus, this work introduces possible functional roles of different biological processes in So ce56.

As phosphorylation plays an important role in the regulation of several metabolic key enzymes in different organisms (Kennelly & Potts, 1999), it is not unusual to find a high number of serine or tyrosine phosphorylated enzymes involved in the metabolic pathways of So ce56 (e.g. glycolysis and TCA, assigned as COG G and COG C). Protein phosphorylation on tyrosine residues in bacteria was discovered more recently and was long considered specific for eukaryotes (Cozzone *et al.*, 2004). The detection of tyrosine phosphorylation involved in the regulation of the developmental cycle in *M. xanthus* (Frasch & Dworkin, 1996), lead to the assumption that So ce56 also uses tyrosine phosphorylation to control different regulatory processes such as multicellular development or diverse metabolic pathways. Tyrosine phosphorylation of enolase (phosphopyruvate hydratase, sce7698) was described by Cooper *et al.* (1984) in virally transformed chicken fibroblasts, where the phosphorylation sites from enolase and lactate dehydrogenase was utilized by tyrosine protein kinases encoded by Rous sarcoma virus. In another experiment with [^{32}P]-labeled proteins in *E.coli*, Dannelly *et al.* (1989) demonstrated the presence of phosphoserine in enolase. In both cases phopshorylated enolase might play an important role as a possible control mechanism of glycolysis and gluconeogenesis. In contrast, Bergmann *et al.* (2003) reported that the export of enolase in *E. coli* to the extracellular medium is dependent on the modification of this enzyme, but it does not change the glycolytic activity.

Tyrosine phosphorylation on thiolase (sce7554), an enzyme of the fatty acid β-oxidation cycle, was reported by Fukao *et al.* (2003) occurring in glyoxysomes from etiolated cotyledons of *Arabidopsis*. The degradation of triglycerides is an important reaction in early post-germinative seedlings growth to produce sucrose as energy source, because the etiolated seedlings cannot produce energy autotrophically by photosynthesis. They suggest that protein phosphorylation is required during β-oxidation to regulate the overproduction of sucrose, i.e. not to waste energy in early

post-germinative seedlings. In So ce56 tyrosine phosphorylation on thiolase might also be needed to control fatty acid degradation and possibly to regulate the energy production between nutrient depletion for the availability of nutrient during cell growth.

Furthermore, the tyrosine phosphorylated protein UDP-glucose dehydrogenase (sce2793) identified in So ce56 were also found to be tyrosine phosphorylated by protein tyrosine kinases (PTKs) in several other bacterial UDP-glucose dehydrogenases, like *E.coli* and *Bacillus subtilis* (Grangeasse *et al.*, 2003; Mijakovic *et al.*, 2003, 2005). The UDP-glucose dehydrogenase converts UDP-glucose to UDP-glucuronate for the synthesis of acidic polysaccharides. In other organisms tyrosine phosphorylation is involved in exopolysaccharide (EPS) synthesis and assembly, especially for virulence (Vincent *et al.*, 2000), e.g. pathogenic *E. coli*. The PTK in *E. coli* is membrane-associated and is expressed specifically by pathogenic strains of *E. coli* (Ilan *et al.*, 1999). The role of the EPSs is the formation of a capsule that protects the pathogen (Ofek *et al.*, 1993). *Sorangium cellulosum* is regarded as a nonpathogenic bacterium, but it is assumed that tyrosine phosphorylation in So ce56 might be involved only in the EPS production, e.g. to protect them against competitors.

An unknown tyrosine phosphorylated protein in So ce56 was detected which contains a forkhead-associated (FHA) domain (sce8329). The FHA domain is a phosphopeptide-binding domain identified in a wide variety of proteins such as protein kinases, phosphatases, adenylate cyclases and proteases from eukaryotes and prokaryotes to coordinate diverse cellular processes (Li *et al.*, 2000). These domains vary also in their binding specifities, they can interact with phosphothreonine, phosphoserine and phosphotyrosine. It is assumed that this domain represents a new class of dual specificity phosphoprotein-binding domain (Liao *et al.*, 1999).

The first protein serine/threonine kinase (PSTK) in *M. xanthus*, the Pkn1, was characterized by Munoz-Dorado *et al.* (1991) playing a key role in cellular differentiation. Since then several PSTKs characterizations followed, which are involved in the *M. xanthus* life cycle like Pkn2 (Udo *et al.*, 1995) and Pkn5/Pkn6 (Zhang *et al.*, 1996), whose expression levels are needed for fruiting body formation and sporulation. Two putative serine kinases and a putative serine specific

phosphatase (sce7256) were found in So ce56. The kinases are involved in the carbon metabolism (sce7349; sce7348) and the phosphatase is assumed to be regulating the ATP biosysnthesis.

The superoxide dismutase SodA (sce0071) is serine phosphorylated in So ce56, whereas the SodB (sce4167) is assumed to be phosphorylated on serine and tyrosine sites. In *Listeria monocytogenes,* a facultative intracellular pathogen causing severe food-borne disease in humans and animals, the manganese-superoxide dismutase (MnSOD) is phosphorylated on serine/threonine residues during stationary phase down-regulating the activity. In contrast, the nonphosphorylated form of MnSOD is highly active secreted via the Sec-pathway. This post-translational modification plays a critical role in intracellular survival in macrophages and is required for full virulence of *L. monocytogenes* (Archambaud *et al.*, 2006).

It is striking that many reported phosphorylations of specific proteins are mainly used for pathogenicity or still not investigated in prokaryotes. *Sorangium* is regarded as non-pathogenic, thus, these informations can only give assumptions to the putative roles of some of the listed phosporylated proteins identified in So ce56 (Tab. 10). In addition, numerous enzymes in So ce56 were phosphorylated on tyrosine and serine residues, indicating that these phosphoproteins have multiple phosphorylation sites (Roach, 1991). The neural network Netphospho 2.0 (Blom *et al.*, 1999; www.expasy.ch) predicted that these proteins contain a serine and a tyrosine site, which supports the assumption of multiple phosphorylation sites. The differences in spot intensity between the tyrosine and serine blots might also reflect the changing signal intensity between tyrosine and serine phosphorylation in the myxobacterial cell. Putatively two different kinases (serine and tyrosine kinases) are involved in this regulation process cooperating possibly together as a complex in So ce56 (Gompert *et al.*, 2004). Nariya and Inouye (2005) described a complex of serine/threonine kinase network in *M. xanthus* that share common modulating factors, the multi-kinase associated proteins (Mkaps) for signal transduction required for fruiting body formation.

5.1.6 The analysis of So ce56 cytosolic proteins by Blue-Native PAGE led to the detection of enzymes involved in the primary and secondary metabolic pathways

A 2-D Blue-Native/SDS-PAGE was used to analyze protein complexes of the cytosolic fraction in So ce56 in order to elucidate their putative functional role in myxobacteria. The main focus was to detect the large polyketide synthases, which are responsible for synthesis of secondary metabolites. In this method, Coomassie Blue G-250 is added to the solubilized proteins introducing a negative charge-shift that enhances the migration of the proteins in a gradient native gel system without dissociating them according to their size and shape (Schägger & Jagow, 1991). The so resolved protein complexes were further separated in a second dimension (SDS-PAGE) after soaking the gel in denaturing SDS buffer. MALDI-TO-MS analysis of the proteins from the BN gel lead to the identification of additionally 14 different cytosolic proteins (in total 32 proteins were identified) additionally coming to the already described 115 identified proteins of the cytosolic proteome. The majority of identified proteins are involved in the lipid, carbon and amino acid metabolism. These findings are coincident with the results of the proteome map, where the majority of detected proteins can be assigned to the primary metabolism. One protein of the chivosazol secondary metabolic pathway was identified in the second dimension of the BN gel, the polyketide synthase ChiF (sce4133). It can be expected that further chivosazol PKSs of the multienzyme complex appeared in this gel, but the MALDI-TOF-MS analysis revealed no other corresponding enzymes. Rather components of the fatty acid metabolism complex/group could be detected like 3-hydroxybutyryl-CoA dehydratase (sce0250). It is not clear, if these enzymes (sce1166; sce3575), are also involved in the secondary metabolism providing substrates (e.g. CoA) required for polyketide biosynthesis.

Moreover, large proteins like the putative serine/threonine kinase two component sensor domain (sce5838), which reveals a molecular mass of 201 kDa, could be detected with this BN method. Presumably, the serine/threonine kinase is combined with the two component signaling system to achieve fine-tune regulation of central signaling events described in Lux & Shi (2005).

The heat shock protein GroEL requires for proper folding the help of the co-chaperonine GroES (Rye *et al.*, 1999). As the GroEL complex is composed of fourteen identical 60 kDa subunits arranged in two stacked rings, and GroES of seven identical 10 kDa subunits, therefore it is not unusual to find in the BN-analysis of So ce56 GroEL subunits (sce5911).

The membrane-bound succinate dehydrogenase (sce6554) was also found in the cytosolic fraction of So ce56, which is involved in the TCA cycle transferring electrons from succinate to ubiquinone during respiration (Fuchs, 2007). Succinate dehydrogenase forms a complex (II) with four so far known subunits: the flavoprotein subunit, the iron-sulfur subunit, subunit III and subunit IV (Eubel *et al.*, 2003; Yankovskaya *et al.*, 2003). It is assumed that the flavoprotein subunit (70 kDa) was detected, but the other three smaller subunits could not be identified. As the Blue-Native method is applied for the first time on myxobacteria, these results gave primary impressions of So ce56 protein:protein interactions.

5.2 The identification of exoenzymes achieved by proteomic analysis of the secretome of So ce56

The analysis of the extracellular proteins of So ce56 from the cell culture supernatant was carried out to find proteins or enzymes involved in (i) polymer degradation, (ii) protection against enemies in soil and (iii) protein signaling functions.

The identification of a cellulase in the extracellular fraction (sce8953) is interesting, due to the fact that So ce56 was cultivated in S-medium with glucose and harvested in the early stationary phase without exposure to cellulose supplements. This phenomenon could be explained by the fact that *Sorangium* cells start to produce these exoenzymes in the early stationary phase when glucose is nearly depleted to mobilize the reserves avoiding starvation. It is supposed that the depletion of readily metabolisable glucose monomers in the medium induces the production and release of extracellular enzymes to hydrolyse organic polymers like cellulose into monomeric substrates (glucose) (Ali & Sayed, 1992). Low concentrations of glucose might act as inducers for cellulase synthesis. For example, the cellulose degrading actinomycete *Thermomonosporata curvata* and the fungi *Aspergillus terreus* might be controlling their cellulase biosynthesis via this catabolite repression system (Fennington *et al.*,

1984). Other putatively secreted proteins identified from the extracellular fraction might have proteolytic activities like the putative peptidase (sce4529) and the exoprotease (sce3910). These enzymes probably hydrolyze nutritional polymers to protect *Sorangium* from probable competitors or to provide themselves with substrates (Müller & Gerth, 2006). The PRIAM enzyme database classified the sce3910 enzyme as xanthomonalisin, which is normally secreted by *Xanthomonas* sp. for the degradation of casein. It is assumed that this exoprotease also belongs to the peptidase family S53, which might have a proteolytic activity. Five putative extracellular proteins are predicted as exported or secreted (sce8614; sce2969; sce0172; sce7128; sce3202), but they have no concrete functional categories. The twin-arginine motif of the putative secreted protein sce8614 indicates that this protein may be transported in a folded state over the twin-arginine translocation pathway (Tat-pathway). It is assumed that some of them might be involved in enzymatically activities or have signaling functions outside the cell. The identified and putatively secreted protein sce4161 shows sequence similarities to the secreted VasA-L protein encoded by the *vas* gene (<u>v</u>irulence-<u>a</u>ssociated <u>s</u>ecretion) of *Vibrio cholerae* (TC database query). The VasA-L is transported via the "type VI" secretion system, as it is distinct from the secretion systems type III and type IV (Pukatzki *et al.*, 2006). This new system does not require the presence of a hydrophobic N-terminal signal sequence for secretion into the extracellular medium, and possibly into eukaryotic cells. Many Gram-negative bacteria seem to have homologous genes to these *vas* genes and potential effector proteins secreted by this pathway, such as hemolysin-coregulated protein (Pukatzki *et al.*, 2006). However, the function of sce4161 in So ce56 is still unclear. Maybe it is used for defence against enemies or competitors in the soil. Moreover, this example explains why so many proteins of So ce56 are secreted without having a signal P in their N-terminus.

Furthermore, a putative UDP-glucuronosyltransferase (sce3098) was reported in the extracellular proteome of So ce56, which might be involved in the teichoic acid biosynthesis (Ginsberg *et al.*, 2006) or in the changing of polyketide activity in the bacterial cell (Bode & Müller, 2007). BLASTP information reveals a significant identity of 57% to a putative teichoic acid biosynthesis related protein from the Gram-negative myxobacterium *Stigmatella aurantiaca*. Interestingly, teichoic acid normally occurs in Gram-positive bacteria (Ginsberg *et al.*, 2006). Another possible functional role of this putative UDP-glucuronosyltransferase could be the probable self-

resistance mechanism of macrolide-producing organisms. This was observed in the actinomycete *Streptomyces antibioticus*, where glycosylation of a hydroxyl group using UDP-glucose as cofactor inactivates the macrolide oleandomycin (Hernandez *et al.*, 1993). The conversion of the inactive oleandomycin into an active antibiotic was carried out by a glycosidase outside the cell (Quiros *et al.*, 1998, 2000). But glycosylation of a natural compound means not always inactivating of antibiotic effects. It is also possible that some secondary metabolites gain changed specifities after glycosylation (Bode & Müller, 2007). In contrast, the glycosides chivosazoles A - E have the same antibiotic and cytotoxic activity as the aglycon chivosazol F shown in figure 36 (Jansen *et al.*, 1997; Perlova *et al.*, 2006), i.e. in this case no changes could be detected after glycolysation with a putative glycosyltransferase.

Chivosazol	R₁	R₂	R₃	R₄
A	Me		Me	Me
A₁	Me		Me	Me
B	H		Me	Me
C	Me		H	H
D	H		H	Me
E	H		H	H
F	Me	H	-	-
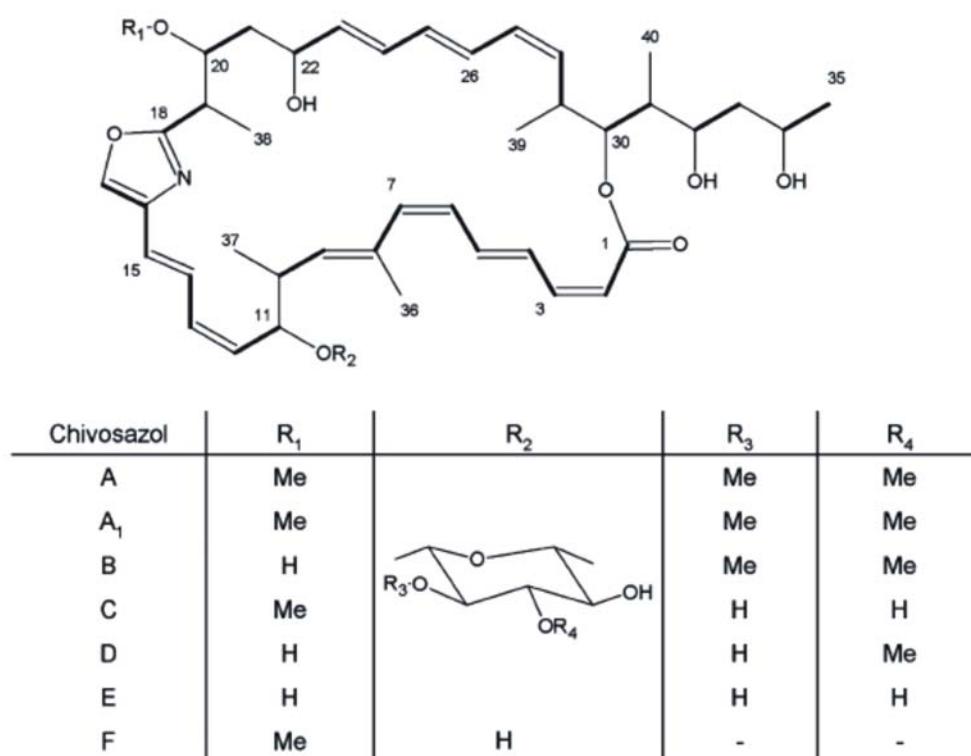
Fig. 36: The chemical structure of chivosazoles A – F (Irschik *et al.*, 1995; Jansen *et al.*, 1997; Perlova *et al.*, 2006).

A high number of proteins (22%) from the inner membrane, outer membrane and from the periplasm designated to the group "membrane/periplasmic proteins" were detected in the extracellular fraction. It raises the question, how these proteins get into the outside of the cell. Unfortunately, no detailed information for comparison

about further transport processes, signaling and motility from *Sorangium cellulosum* are available so far, since many experiments and results derived from the bacteria preying *Myxococcus xanthus* (Nicaud *et al.*, 1984; Yang *et al.*, 1998; Kaiser, 2004; Kimura *et al.*, 2006). Even though there are many homologous expressed proteins between these two strains, many proteins remained undefined or poorly defined in So ce56 (Schneiker *et al.*, 2007).

The membrane and membrane-associated proteins were analyzed by the TC database query to find possible transport proteins or structures, which might be involved in transport processes. This database search resulted in the identification of two putative ABC transporters: a cyanate or an aromatic sulfonate porter (sce5488) and an aromatic sulfonate porter (sce1321). ABC transport proteins are mainly located in the inner membrane, but periplasmic components of the ABC transporter were translocated through the cytoplasmic membrane. As the putative ABC transporter sce1321 contains a signal sequence with a twin-arginine motif, it is assumed that this protein might be translocated in a folded state by the Tat-signaling pathway. Further periplasmic components, which are transported via this system, are the putative hydrogen/potassium exchanging ATPase (sce5843) and the putative phosphohydrolase (sce0969). It is assumed that not a whole ABC and ATPase complex will be transported to the periplasmic side, but periplasmic components of these proteins complexes. The putative periplasmic superoxide dismutase SodC (sce8431) protects the cell from incoming radicals and is putatively transported by the sec-translocation system. Two putative lipoproteins with signal sequences (sce5067, sce4343) were recognized by the DOPOL database. It is not clear, how these proteins are translocated outside the cell and above all, what might be their functions. It is possible that these lipoproteins might be involved in sensory signaling systems (Sutcliffe & Russell, 1995). Three proteins, the chaperone protein DnaK (Hsp70) (sce9025), the chloroplast GrpE protein (sce0004) and the probable DnaJ molecular chaperone (0617) were identified and also detected in the TC database as transport proteins. The Hsp70 in *E.coli* and its co-chaperones (DnaJ and GrpE) are involved in several cellular processes including folding accompanying protein synthesis, remodeling of protein complexes (Liberek *et al.*, 1988), regulation of the heat shock response and also translocation through membranes (Arispe & De Maio, 2000; Zietkiewicz *et al.*, 2006). As heat shock proteins are highly conserved families, it is also expected that these proteins have the same functions in So ce56 (Fenton &

Horwich, 1997). A large number of identified proteins, which also occur in the extracellular fraction, were proteins involved in metabolic pathways (e.g. glycolysis), or interaction with DNA. These proteins should be normally located in the cytoplasm or associated to the cytoplasmic membrane. Secretome approaches of *Xanthomonas campestris* (Watt *et al.*, 2005) and *Bacillus subtilis* (Tjalsma *et al.*, 2004) showed that the secretion of cytoplasmic proteins, e.g., enolase (sce7698), is not very unusual. Extracellular enolase of numerous bacterial and fungal pathogens has a plasmin (ogen) binding function (e.g. *Streptococcus pneumoniae*), but the role for non-pathogenic organisms like So ce56 are still not determined (Bergmann *et al.*, 2003). The transport of enolase might be carried out via the type I secretion system, which implies an ABC transporter and an outer membrane porin, such as TolC (Boël *et al.*, 2003) as no specific export signalings in enolase exist.

5.3 Comprehensive proteomic analysis of membrane proteins yields the detection of a high number of transport proteins in So ce56

The envelope of *Sorangium cellulosum* So ce56 consists, like other Gram-negative bacteria, of two distinct lipid bilayers, the inner membrane (IM) and the outer membrane (OM), separated by a dynamic aqueous peptidoglycan-containing periplasm (Duong *et al.*, 1997). Proteomic analyzes of the myxobacterium *Myxococcus xanthus* resulted in the identification of membrane proteins involved in social gliding motility (Kaiser, 2000; Simunovic *et al.*, 2003), cell-cell signalling (Kaiser, 1998) and polyketide biosynthesis (Rosenberg & Dworkin, 1996).

5.3.1 Identification of membrane proteins participating in transport processes are located mainly in the inner membrane

Thus, it is much likely that So ce56 also shows this typical myxobacterial membrane proteome. The combination of membrane isolation techniques, SDS-PAGE and nanoLC-ESI-MS/MS proved to be a powerful tool to analyze membrane proteins (Wu *et al.*, 2003). Mass spectra analyzes of the membrane protein fraction resulted in the detection of 66 different proteins revealing a high number of membrane and membrane associated proteins in So ce56 (Tab. 13).

The majority of the identified membrane proteins belong to different transport systems. Some identified proteins are probably localized in the inner membrane and periplasm using ATP hydrolysis for substrate translocation or providing the cell with ATP via H^+-transporting, e.g. ABC transport systems (sce7548) and H^+-transporting two-sector ATPases (sce4444; sce9361), respectively (Schneider & Hunke, 1998; Yuriy, 2005)). The ATPase uses the ion flow to catalyze the reaction $ADP + P_i \rightarrow ATP$. Further enzymes integrated in the cytoplasmic membrane such as the putative NADH dehydrogenase (sce0528) and the putative molybdopterin oxidoreductase (sce7585) are involved in the electron transfer system during bacterial respiration to transfer electrons from the substrates to oxygen. Three identified proteins assumed to be integrated in the OM, like the maltoporin (sce7619) the outer membrane protein (sce5128) and the efflux transporter (sce8709), which mediates the export of heavy metal cations (cobalt, zinc, cadmium) and probably function in conjunction with a primary cytoplasmic membrane transporter (e.g. ABC transporter or RND superfamily). Efflux proteins are mainly responsible for the extrusion of toxic substances, e.g., detergents, antibiotics or heavy metals as mentioned before (Poole, 2004). Another two identified efflux pumps belong to the drug resistance-nodulation-division (RND) family transport system (sce2988; sce1628). The RND proteins need three components for antibiotic translocation including a periplasmic membrane fusion protein and an outer membrane protein, e.g. in *E. coli* the AcrBA - TolC system (Klebba, 2005; Nikaido, 1996). The detection of these proteins might explain the high resistance of So ce56 towards kanamycin, as sce1628 putatively exports this antibiotic and various other antibiotics (e.g. nalidixic acid, norfloxacin) (Tab.19). Another possible function of the putative RND efflux proteins in So ce56 might be the export of self-produced secondary metabolites that have an antimicrobial activity directed against competitors. For example *Mycobacterium tuberculosis* probably uses the drug-proton antiporter RND transporter (MmpL7) to excrete the polyketide phthiocerol dimycocerosate (PDIM) for infection processes (Jain & Cox, 2005). The authors propose that the RND transporter MmpL7 interacts with the PDIM synthetic machinery to form a complex that coordinately synthesize and translocate PDIM somehow across the cell membrane. The investigation of *Myxococcus xanthus* DK1622 membrane proteins lead to the discovery of a Ta-1 PKS, which is assumed to be membrane-associated and facilitates the safe export of the final product (Simunovic *et al.*, 2003). The PKS Ta-1 is involved in the production of myxovirescin

A, which inhibits the peptidoglycan synthesis of Gram-negative cells (Rosenberg & Dworkin, 1996). It is proposed that So ce56 could secrete the self-produced secondary metabolites via a similar transport mechanism connecting the PKS biosynthesis machinery with a transport protein.

The putative MglA protein (sce7249) found in the membrane fraction of So ce56 might be involved in the adventurous or social gliding motility and is containing a Ras-like GTPase active site, which has a high similarity to the MglA proteins of the myxobacterial strains *Myxococcus xanthus* and *Aneromyxobacter dehalogenans* (> 80%). This protein is involved in fruiting body formation and sporulation showed in the experiment of Zirkle *et al.* (2004), who created the first *mglA* mutant in a *Sorangium* strain (So ce26) exhibiting similar non-swarming defects like in *M. xanthus,* presumably due to their inability to conduct developmental signals, like the C-signal (Spormann, 1999). Genome predictions reveal a putative *mglB* gene located close to the *mglA* gene of *S. cellulosum*, which encodes a putative MglB protein (sce7248) with a probable Ca^{2+} binding motif (Womack *et al.*, 1989). Another identified protein (sce5071) from the membrane fraction might be a putative biopolymer transport protein (TolQ). Youderian *et al.* (2003) defined 30 new genes in *M. xanthus* required for A-motility, whereby six of the genes encode different homologues of the TolR, TolB and TolQ transport proteins, suggesting that adventurous motility is dependent on biopolymer transport. As no detailed investigations have been carried out in So ce56 about gliding motility proteins, it is assumed that So ce56 might also use these transport proteins, consistent with a model in which A motility is powered by the secretion of polyelectrolyte (Wolgemuth *et al.*, 2002). Another subset of genes that may encode structural components of a secretory apparatus involved in A motility includes those encoding proteins with TPR motifs. The putative AgmK proteins (sce0252, sce2921 and sce2920) found in So ce56, contain TPR motifs and might interact with proteins that form a β-propeller structure such as that predicted for the WD-repeat proteins AglU (TolB homologue 1) and AglW (TolB homologue 2) described for *M. xanthus* (White & Hartzell, 2000; Youderian *et al.*, 2003).

5.3.1.1 Blue-Native PAGE of membrane proteins led to the identification of metabolic enzymes and transport proteins attached to the membrane

In this approach hydrophobic membrane protein complexes in So ce56 were investigated with the Blue-Native PAGE method in order to find membrane-associated proteins involved in transport processes or in diverse metabolic pathways. As described in 6.1.6 many detected proteins belong to the protein complex of fatty acid oxidation in So ce56 (e.g. sce7555; 7905). Therefore, it is not clear, if these enzymes occur in the cytoplasm or in the inner membrane of So ce56 or act in both compartments. The identified cyclopropane-fatty-acyl phospholipid synthase (sce2529), which is associated to the cytoplasmic membrane, catalyzes the modification of the acyl chains of phospholipid bilayers through methylation (S-adenosylmethionine (SAM)) of unsaturated fatty acyl chains to their cyclopropane derivatives (Taylor & Cronan, 1979) for the cell wall biogenesis. For example, in *E. coli* this modification plays an important role in resistance to acidic conditions (Cronan, 2002). Furthermore, the detection of the Na^+/ H^+ antiporter (sce3269) located in the inner membrane playing a central role in the internal pH homeostasis and in the extrusion of Na^+, which is toxic at high concentrations (Hunte *et al.*, 2005; Padan *et al.*, 2004). Hayes *et al.* (2006) reported that *E. coli* upregulates the expression of Na^+/ H^+ antiporter and the cyclopropane-fatty-acyl phospholipid synthase, thus preparing the cell to survive future exposure to more extreme pH conditions. Therefore, it is possible that So ce56 also activates this resistance machinery towards stressing pH decreasion in the medium.

The detection of a cytochrome P450 (sce2191), which might be involved in the secondary metabolite production leads to the conclusion that BN-PAGE is a good method to analyze enzymes of the secondary biosynthesis. Maybe it requires further methods or higher protein concentrations for the detection of more polyketide synthases or proteins involved in the secondary metabolism. The active site of the membrane-attached microsomal P450 oxidizes hydrophobic compounds, which are dissolved in the membrane and could enter the P450 acces channel directly from the membrane (Peterson &Graham-Lorence, 1995).

Striking is also the identification of many proteins involved in the translation process, in particular the ribosomal proteins (sce7953; sce7939; sce7958). These proteins are

major components of polyribosomes. The membrane extraction method supposed to solubilize also ribosomal complexes putatively located in the cytosol.

5.3.2 Many outer membrane receptor proteins and transport proteins are found in the outer membrane protein analysis of So ce56

The analysis of the outer membrane proteins were carried out to find transport proteins and cell surface structures integrated in the outer membrane for the social gliding motility (type IV pili or fibrils) as described in 2.3.1. From the 35 identified proteins, two putative OMP β-barrel autotransport proteins (sce1186; sce7537) involved in translocation processes of So ce56 were detected. Autotransport proteins use sec-dependent type V secretion systems, where proteins mediate their own translocation across the outer membrane by forming a pore structure. This system was first described for the protease IgA1 from *Neisseria gonorrhoeae,* which destroys human immunoglobulin A1 (IgA1) (Pohlner *et al.*, 1987). The autotransport protein contains an N-teminal signal peptide responsible for the translocation from the inner membrane to the periplasm. The next domain is the functional N-passenger domain, which could be exposed to the cell-surface or released into the extracellular milieu. These domains might obtain enzymatic activities (like the IgA1 protease), adhesion functions, actin-promoted motility or cytotoxic effects (Yen *et al.*, 2002). Finally, the C-terminal domain of autotransporters is predicted to consist of β-pleated sheets in the form of a β-barrel, which is inserted into the outer membrane to export the rest of the peptide (Desvaux *et al.*, 2004; Henderson *et al.*, 2004). This might explain the occurrence of the OMP β-barrel proteins in the outer membrane fraction of So ce56. They could be probably involved in the autotransport processes of cell-surface motility proteins of So ce56. A putative identified pilus assembly protein (sce0254) might be involved in the type IV pilus biogenesis, which is possibly translocated at the cell surface.

Porins like the putative maltoporin (sce7619) or the putative phosphate selective porin (sce7966) are responsible for the uptake of soluble substrates from the medium, whereas a probable outer membrane efflux protein (sce3619) was determined for the extrusion. Three probable TonB dependent receptors were identified for the import of ferric-siderophore complexes. One of them (sce4255) might be involved in cellular adhesion reactions during fruiting body formation or in

the adventurous gliding motility system (Youderian *et al.*, 2003). DOPOL database search lead to the identification of two putative lipoproteins, the sce2691 and the sce4176, the latter is a protein kinase transported by the Tat-signaling pathway.

Strikingly, a putative ABC-type xylose transport system (sce6008) was identified. As the medium contains only glucose as sole carbon source and xylose, which is a predominant pentose in hemicellulose, is not supplemented. Glucose and xylose are the dominant monosaccharides in plant material decayed from this soil-living bacterium. It is possible that the enzymes for xylose uptake and turnover are constantly present in the cell or that they are produced during the depletion of an alternate sugar source (glucose).

Surprising is also the identification of proteins involved in secondary metabolite production in the outer membrane fraction since no secretion signal could be detected. Due to their resemblance to the fatty acid biosynthesis, it can be assumed that these PKSs mainly appear in the cytosol. The identified putative type I PKS is encoded by the *chiF* gene (sce4133), belonging to the charcterized chivosazol biosynthetic gene cluster in So ce56 (Perlova *et al.*, 2006). The PKS ChiF contains a C-terminal thioesterase domain and it is assumed that the *chiF* is the last gene in the core biosynthetic gene cluster probably responsible for the release and concomitant cyclization of the fully processed polyketide chain (Perlova *et al.*, 2006).

A putative 390 kDa polyketide synthase (sce3190) could be identified, which has similarities to a putative polyketide synthase pksM (sce_20050509_9622, identity 58%). In other experiments, the putative PKS sce3190 was isolated from the extracellular fraction revealing a MOWSE score of 66% and sequence coverage of 8% (data not shown). Interestingly, membrane proteome analysis of the micropredatory model strain *Myxococcus xanthus* DK1622 lead to the discovery of a PKS which might be membrane-associated probably facilitating the safe export of the final product myxovirescin A (Simunovic *et al.*, 2003). It is assumed that the PKSs sce3190 and sce4133 of So ce56 might be located at the membrane to carry out membrane-associated functions.

The biochemical function of sce3190 is still unknown. The genome annotation of So ce56 reveals that this putative protein/enzyme is an etnangien PKS (Schneiker *et al.*, 2007). The characteristic domains and modules of this PKS are still not available.

5.3.3 BLASTP comparisons of So ce56 protein sequences lead to the detection of further putative genes, which might be involved in the jerangolid/ambruticin biosynthesis

The identification of a putative sensor histidine kinase in So ce56 reveals an identity of 85% to the putative sensor kinase Jer3 and an identity of 81% to the putative sensor kinase Amb3, which is encoded by the jerangolid or ambruticin biosynthetic gene cluster, respectively (Julien *et al.*, 2006). This lead to the assumption that further proteins of the characterized jerangolid/ ambruticin biosynthetic gene clusters exist in *Sorangium cellulosum* So ce56. The NCBI protein BLAST screenings expose more proteins in So ce56 which have a high identity to the proteins of the jerangolid/ ambruticin secondary metabolite clusters that occur near the identified sensor kinase. The discovery of a putative new secondary metabolite biosynthetic gene cluster in *Sorangium cellulosum* So ce56 would help further investigations to reveal this PKS secret.

Ambruticin and jerangolid are structurally related with similar antifungal activity and cluster organization, many proteins of So ce56 show a high identity to genes of both compounds: a putative LysR-family transcriptional regulator (sce7797) similar to Jer1/ Amb1 with an identity of 84%/ 85%, respectively; a sensor histidine kinase (sce7799) identical to Jer3/ Amb3 (85%/ 81%); a sigma-54 dependent response regulator (sce7800) identical to Jer4/ Amb4 (92%/ 93%); a sensor histidine kinase (sce7107) identical to Jer5/ Amb5 (73%/ 72%); a conserved hypothetical protein (sce7805) identical to Jer6/ Amb6 (95%/ 95%); a two-component hybrid sensor and regulator (sce7807) identical to Jer7/ Amb7 (62%/ 62%). Only a few proteins of the ambruticin and jerangolid gene cluster are not related to each other, but nevertheless they occur with a high homology in the genome sequence of So ce56: a hypothetical protein (sce7798) with 80% identity to Jer2; a putative regulatory protein (sce7810) showing 75% identity to Amb8 and a putative xenobiotic reductase (sce7811) with 84% identity to Amb9. Moreover, three putative genes encoding hypothetical proteins without any assignation to a functional group reveal a high identity to genes discovered near the putative jerangolid/ ambruticin biosynthetic gene cluster in the So ce56 genome sequence: sce7795 (88% identity); sce7796 (64% identity) and

sce7812 (87% identity). The putative thioesterase sce0390 of So ce56 has a 40% similarity to the PKS JerE, which also contains a thioesterase for the release of the secondary metabolite product.

5.3.4 The electron microscope detection of outer membrane vesicles and the proteome analysis of outer membrane vesicle proteins indicate vesicles as a new transport system in So ce56

A large number of Gram-negative bacteria naturally produce spherical bilayered outer membrane vesicles (OMVs). Here, such structures could also be identified for So ce56 via electron micrograph measurements (Fig. 29). MALDI-TOF-MS analysis of the OMV proteins lead to the identification of putative outer membrane components probably enclosed during OMV formation (Mashburn-Warren & Whiteley, 2006). Putative porins (sce7619; sce7966) and putative outer membrane lipoproteins (sce5067) are normally integrated into the outer membrane. It is possible that not only outer membrane proteins were entrapped within these vesicles but also periplasmic proteins like the putatively predicted phosphatase (sce0936) and degradative enzymes such as the putative Clp protease (sce7556). Outer membrane vesicles were used mainly from pathogens to transport virulence factors to the host (Kuehn & Kesty, 2005). The pathogen *Pseudomonas aeruginosa* uses OMVs to export enzymes like alkaline phosphatase, phospholipase C, proelastase, protease and peptidoglycan hydrolase, where several of these components act as virulence or lytic factors (Li *et al.*, 1998; Beveridge *et al.,* 1997, 1999). Furthermore, the release of a cytolysin A (ClyA) protein from *Escherichia coli* was also mediated by outer membrane vesicle. This cytotoxic protein is translocated without cleavage of any signal sequence to affect eukaryotic cells (Wai *et al.*, 2003). Kadurugamuwa and Beveridge (1998) developed a model test to deliver the non-membrane-permeative antibiotic gentamycin via OMVs of *Shigella flexneri* into mammalian cells. These examples indicate that the OMVs in So ce56 might be a new transport system for exoenzymes, secondary metabolites or maybe for signaling proteins, which are secreted to degrade nutritional polymers, protect them from competitors in soil (Reichenbach & Dworkin, 1992) or to communicate (Kaiser, 2004).

5.4   Summary of the discussion

The aim of this work was the establishment of a proteomic map of *Sorangium cellulosum* So ce56 encompassing cytosolic, membrane, outer membrane and extracellular proteins. The annotated genome sequences (Schneiker *et al.*, 2007) could be verified and complemented at the proteome level. The extensive proteomic analyzes led to the identification of 247 unique proteins (Tab. 22), which are mainly involved in primary metabolism (e.g. carbon, amino acid and lipid metabolism). Nearly all enzymes of the central metabolic pathways, like glycolysis and the TCA cycle could be identified with these approaches. Moreover, the detection of proteins involved in the fatty acid degradation, histidine metabolism, valine, isoleucine and leucine biosynthesis reveals that these pathways and their intermediates were mainly required to support the central metabolic processes. Additionally, the membrane protein analyzes reveal that So ce56 uses different transport systems to maintain the metabolic pathways. Identifications of proteins involved in fruiting body formation, gliding motility and secondary metabolisms were underrepresented in the proteome analyzes. Reasons therefore could be the major use of one growth phase (early stationary phase) and the defined growth medium. The genome sequence of So ce56 reveals a high number of potential proteins, which might be expressed under natural conditions, but not under the chosen *in vitro* conditions. Therefore it would be interesting and necessary to make proteome approaches under different conditions. However, a basis for further proteomic approaches was achieved with this study.

6 References

Aebershold, R. and M. Mann (2003): Mass spectrometry-based proteomics. Nature 422, 198-207

Ali, S. and A. Sayed (1992): Regulation of cellulose biosynthesis in *Aspergillus terreus.* World J Microbiol Biotechnol 8, 73-75

Archambaud, C., M.A. Nahori, J. Pizarro-Cerda, P. Cossart, O. Dussurget (2006): Control of Listeria superoxide dismutase by phosphorylation. J Biol Chem 281, 31812-31822

Arispe, N. and A. De Maio (2000): ATP and ADP modulate a cation channel formed by Hsc70 in acidic phospholipids membranes. J Biol Chem 275, 30839-30843

Asboth, B. and G. Naray-Szabo (2000): Mechanism of action of *D*-xylose isomerase. Current protein and peptide science 1, 237-254

Austin, M. B. and J. P Noel (2003): The chalcone synthase superfamily of type III polyketide synthases. Nat Prod Rep 20, 79-110.

Babu, M.M., M.L. Priya, A.T. Selvan, M. Madera, J. Gough, L. Aravind, K. Sankaran, K. (2006): A database of bacterial lipoproteins (DOLOP) with functional assignments to predicted lipoproteins. J Bacteriol 188, 2761-2773

Bairoch, A. (2000): the ENZYME database in 2000. Nucleic Acids Research 28, 304-305

Barriere, C., S. Leroy-Setrin, R. Talon (2001): Characterization of catalase and superoxide dismutase in Staphylococcus carnosus 833 strain. J Appl Microbiol 91, 514-519

Battaile, K.P., T.V. Nguyen, J. Vockley, J.J. Kim (2004): Structures of isobutyryl-CoA dehydrogenase and enzyme-product complex: comparison with isovaleryl- and short-chain acyl-CoA dehydrogenase. J Biol Chem 279, 16526-16536

Berggren, K.N., B. Schulenberg, M.F. Lopez, T.H. Steinberg, A. Bogdanova, G. Smejkal, A. Wang, W.F. Patton (2002): An improved formulation of SYPRO Ruby protein gel stain: comparison with the original formulation and with a ruthenium II tris (bathophenan-thrdine disulfonate formulation). Proteomics 2, 486-498

Bergmann, S., D. Wild, O. Diekmann, R. Frank, D. Bracht, G.S. Chhatwal and S. Hammerschmidt (2003): Identification of a novel plasmin (ogen) binding motif in surface displayed α-enolase of *Streptococcus pneumoniae.* Mol Microbiol 49, 411-423

Berkeley, M.J. (1857): Introduction to Cryptogamic Botany (on *Stigmatella* and *Chondromyces*), pp. 313-315. H. Bailliere Publishers, London

Beveridge, T.J., S.A. Makin, J.L. Kadurugamuwa, Z. Li (1997): Interactions between biofilms and the environment. FEMS Microbiol Rev 20, 291-303

Beveridge, T.J. (1999): Structures of Gram-negative cell walls and their derived membrane vesicles. J Bacteriol 181, 4725-4733

Blackhart, B.D. and D.R. Zusman (1985): Frizzy genes of *Myxococcus xanthus* are involved in control of frequency of reversal of gliding motility. Proc Natl Acad Sci USA 82, 8767-8770

Blom, N., S. Gammeltoft, S. Brunak (1999): Sequence and structure-based prediction of eukaryotic protein phosphorylation sites. J Mol Biol 294, 1351-1362

Bode, H.B. and R. Müller (2006): Analysis of myxobacterial secondary metabolism goes molecular. J Ind Microbiol Biotechnol 33, 577-588

Bode, H. and R. Müller (2007): Reversible sugar transfer by glycosyltransferases as a tool for natural product (bio) synthesis. Angew Chem Int Ed, 46, 2147-2150

Boël, G., V. Picherau, I. Mijakovic, A. Mazé, S. Poncet, S. Gillet, J.-C. Giard, A. Hartke, Y. Auffray, J. Deutscher (2003): Is 2-phosphoglycerate-dependent automodification bacterial enolase implicated in their export? J Mol Biol 337, 485-496

Bollag, D.M., P.A. McQuency, J. Zhu, O. Hensens, L. Koupal, J. Liesch, M. Goetz, E. Lazarides, C.M. Woods (1995): Epothilones, a new class of microtubule-stabilizing agents with a taxol-like mechanism of action. Cancer Res 55, 2325-2333

Claudel-Renard, C., C. Chevalet, T. Faraut, D. Kahn (2003): Enzyme-specific profiles for genome annotation: PRIAM. Nucleic Acids Research 31, 6633-6639

Collgan, J.E., B.M. Dunn, H.L. Ploegh, D.W. Speicher, P.T. Wingfield (Eds.) (1995): Current Protocols in Protein Science, John Wiley & Sons, New York, 1, 10.5.11

Colditz, F., O. Nyamsuren, K. Niehaus, H. Eubel, H.-P. Braun, F. Krajinski (2004): Proteomic approach: Identification of *Medicago truncatula* proteins induced in roots after infection with pathogenic oomycete *Aphanomyces euteiches*. Plant Mol Biol 55, 109-120

Cooper, J.A., F.S. Esch, S.S. Taylor, T. Hunter (1984): Phosphorylation sites in enolase and lactate dehydrogenase utilized by tyrosine protein linases *in vivo* and *in vitro.* J Biol Chem 259, 7835-7841

Corbett, J.M., M.J. Dunn, A. Posch and A. Görg (1994): Positional reproducibility of protein spots in two-dimensional polyacrylamide gel electrophoresis using immobilised pH-gradient isoelectric focusing in the first dimension: an interlaboratory comparison. Electrophoresis 15, 1205-1211

Cozzone, A.J. (1998): Post-translational modification of proteins by reversible phosphorylation in prokaryotes. Biochimie 80, 43-48

Cozzone, A.J., C. Grangeasse, P. Doublet, B. Duclos (2004): Protein phosphorylation on tyrosine in bacteria. Arch Microbiol 181, 171-181

Cronan J.E. (2002): Phospholipid modifications in bacteria. Curr Opin Microbiol 5, 202-205

Dannelly, H.K., J.-C. Cortay, A.J. Cozzone, H.C. Reeves (1989): Identification of phosphoserine in in Vivo-labeled enolase from *Escherichia coli.* Current Microbiol 19, 237-240

Dawid, W. (1987): Myxobacteria in anarctic soils. In modern approaches in the biology of terrestrial microorganisms and plants in the antarctic. First Symposium (Sept. 7-11, 1987), Kiel.

Dawid, W. (2000): Biology and global distribution of myxobacteria in soils. FEMS Microbiol Rev 24, 403-427

Desvaux, M., N.J. Parham, I.R. Henderson (2004): Type V protein secretion: simplicity gone awry? Curr Issues Mol Biol 6, 111-124

Duong, F., J. Eichler, A. Price, M.R. Leonard, W. Wickner (1997): Biogenesis of the Gram-negative bacterial envelope. Cell 91, 567-573.

Dworkin, M. (1996): Recent advances in the social and developmental biology of the myxobycteria. Microbiol Rev 60, 70-102

Epperson, E., J. Kirby (2006): Characterization of the Che7 system of *Myxococcus xanthus* through a yeast two-hybrid assay. Honor thesis, Georgia Instititute of Technology, School of Biology, Atlanta, GA 30332

Eubel, H., H.P. Braun, A.H. Miller (2005): Blue-native PAGE in plants: a tool in analysis of protein-protein interactions. Plant Methods 1, 11

Eubel, H., L. Jänsch, H.P. Braun (2003): New insights into the respiratory chain of plant mitochondria. Supercomplexes and a unique composition of complex II. Plant Physio 133, 274-286

Fani, R., M. Brilli, M. Fondi, P. Lio (2007): The role of gene fusions in the evolution of metabolic pathways: the histidine biosynthesis case. BMC Evolutionary Biol 7 (Suppl 2):S4

Fenton W.A. and A.L. Horwich (1997): GroEL-mediated protein folding. Protein Sci 6, 743-760

Fenn, J.B., M. Mann, C.K. Meng, S.F. Wong, C.M. Whitehouse (1989): Electrospray ionization for mass spectrometry of large biomolecules. Science 246, 64-71

Fennington, G., D. Neubauer, F. Stutzenberger (1984): Cellulase biosynthesis in a catabolite repression-mutant of *Thermomonospora curvata.* Appl Environ Microbiol 47, 201-204

Frank, B. (2007): Polyketidbiosynthese in Myxobakterien. PhD thesis, University Saarland, Saarbrücken

Frasch, S.C. and M. Dworkin (1996): Tyrosine phosphorylation in *Myxococcus xanthus*, a multicellular prokaryote. J Bacteriol 178, 4084-4088

Fraser, C.M., J.A. Eisen, S.L. Salzberg (2000): Microbial genome sequencing. Nature 406, 799-803

Fuchs, G. (2007): Allgemeine Mikrobiologie, 8th Ed. Georg Thieme Verlag, Stuttgart

Fukao, Y., M. Hayashi, I. Hara-Nishimura, M. Nishimura (2003): Novel glyoxysomal protein kinase, GPK1, identified by proteomic analysis of glyoxysomes in etiolated cotyledons of *Arabidopsis thaliana*. Plant Cell Physiol 44, 1002-1012

Gaitatzis, N., B. Kunze, R. Müller (2005): Novel insights into siderophore formation in myxobacteria ChemBioChem 6, 365-374

Gerth, K., N. Bedorf, H. Irschik, G. Höfle, H. Reichenbach (1993): The soraphens: A family of novel antifungal compounds from *Sorangium cellulosum* (Myxobacteria). J Antibiot 47, 23-31

Gerth, K., N. Bedorf, G. Höfle, H. Irschik, H. Reichenbach (1996): Epothilones A and B: Antifungal and cytotoxic compounds from *Sorangium   cellulosum* (Myxobacteria). J Antibiot 49, 560-563

Gerth, K., S. Pradella, O. Perlova, S. Beyer, R. Müller (2003): Myxobacteria: proficient producers of novel natural products with various biological activities-past and future biotechnological aspects with the focus on the genus *Sorangium.* J Biotechnol 106, 233-253

Ginsberg, C., Y. - H. Zhang, Y. Yuan, S. Walker (2006): In vitro reconstitution of two essential steps in wall teichoic acid biosynthesis. ACS Chem Biol 1, A-D

Görg, A., C. Obermaier, G. Boguth, A. Harder, B. Scheibe, R. Wildgruber, W. Weiss (2000): The current state of two-dimensional electrophoresis with immobilized pH gradients. Electrophoresis 21, 1037-1053

Görg, A., W. Postel, S. Gunther (1988): The current state of two-dimensional electrophoresis with immobilized pH gradients. Electrophoresis 9, 531-546

Goldman, B.S. *et al.* (2006): Evolution of sensory complexity recorded in a myxobacterial genome. Proc Natl Acad Sci USA 103, 15200-15205

Gompert, B.D., I.M. Kramer, P.E.R. Tatham (2004): Signal Transduction. Academic Press, San Diego, USA

Grangeasse, C., B. Obadia, I. Mijakovic, J. Deutscher, A.J. Cozzone, P. Doublet (2003): Autophosphorylation of the *Escherichia coli* protein kinase WzC regulates tyrosine phosphorylation of Ugd, a UDP-glucose dehydrogenase. J Biol Chem 278, 39323-39329

Gonzalez, R., H. Tao, K.T. Shanmugam, S.W. York, L.O. Ingram (2002): Global gene expression differences associated with changes in glycolytic flux and growth rate in *Escherichia coli* during the fermentation of glucose and xylose. Biotechnol Prog 18, 6-20

Grabley, S. and S. Thiericke (Eds.) (1999): Drug discovery from nature. Springer-Verlag Berlin Heidelberg New York

Graves P.R. and T.A. Haystead (2002): Molecular biologist's guide to proteomics. Microbiol Mol Biol Rev 66, 39-63

Grünenfelder, B., G. Rummel, J. Vohradsky, D. Röder, H. Langen, U. Jenal (2001): Proteomic analysis of the bacterial cell cycle. PNAS 98, 4681-4686

Gross, F., N. Luniak, O. Perlova, N. Gaitatzis, H. Jenke-Kodama, K. Gerth, D. Gottschalk, E. Dittmann, R. Müller (2006): Bacterial type III polyketide synthases: phylogenetic analysis and potential fort he production of novel secondary metabolites by heterologous expression in pseudomonads. Arch Microbiol 185, 28-38

Gygi, S.P., G. Corthals, Y. Zhang, Y. Rochon, R. Aebersold (2000): Evaluation of two-dimensional gel electrophoresis-based proteome analysis technology. Proc Natl Acad Sci USA 97, 9390-9395

Hartzell, P. and D. Kaiser (1991): Function of MglA, 22-kilodalton protein essential for gliding in *Myxococcus xanthus*. J Bacteriol 173, 7615-7624

Hayes, E.T., J.C. Wilks, P. Sanfilippo, E. Yohannes, D.P. Tate, B.D. Jones, M.D. Radmacher, S.S. BonDurant, J.L. Slonczewski (2006): Oxygen limitation modulates pH regulation of catabolism and hydrogenases, multidrug transporters, and envelope composition in *Escherichia coli* K-12. BMC Microbiol 6:89

Henderson, I.R., F. Navarro-Garcia, M. Desvaux, R.C. Fernandez, D.A. Aldeen (2004): Type V protein secretion pathway: The autotransporter story. Microbiol Mol Biol Rev 68, 692-744

Hernandez, C., C. Olano, C. Mendez, J. A Salas (1993): Characterization of a *Streptomyces antibioticus* gene cluster encoding a glycosyltransferase involved in oleandomycin inactivation. Gene 134, 139-140

Hespell, R. B. (1998): Extraction and characterization of hemicellulose from the corn fiber produced by corn wet-milling processes. J Agric Food Chem 46, 2615-2619

Höfle, G. (1995): Isolation, structure elucidation and chemistry, GBF (Ed.) Braunschweig, Scientific Annual Report 80-83

Hopwood, D. A. (1997): Genetic contributions to understand polyketide synthases. Chem. Rev. 97, 2465-2497

Hunte, C., E. Screpanti, M. Venturi, A. Rimon, E. Padan, H. Michel (2005): Structure of a Na^+/H^+ antiporter and insights into mechanism of action and regulation by pH. Nature 435, 1197-1202

Hunter, T. (1995): Protein kinases and phosphatases: The Yin and Yang of protein phosphorylation and signaling. Cell 80, 225-236

Ilan, O., Y. Bloch, G. Frankel, H. Ulrich, K. Geider, I. Rosenshine (1999): Protein tyrosine kinases in bacterial pathogens are associated with virulence and production of exopolysaccharide. EMBO 18, 3241-3248

Irschik, H., R. Jansen, K. Gerth, G. Höfle, H. Reichenbach (1995): Chivosazol A, a new inhibitor of eukaryotic organisms isolated from myxobacteria. J Antbiot 48, 962-966

Jain, M. and J.S. Cox (2005): Interaction between polyketide synthase and transporter suggests coupled synthesis and export of virulence lipid in *M. tuberculosis*. PLoS Pathogens 1, 12-19

Jänsch, L. V. Kruft, H.P. Braun (1996): New insights into the composition, molecular mass and stoichiometry of the protein complexes of plant mitochondria. Plant J 9, 357-368

Jansen, R., H. Irschik, H. Reichenbach, G. Höfle (1997): Chivosazoles A-F: Novel antifungal and cytotoxic Macrolides from *Sorangium* cellulosum (Myxobacteria). Liebigs Ann, 1725-1732

Julien, B., Z.Q. Tian, R. Reid, C.D. Reeves (2006): Analysis of the ambruticin and jerangolid gene clusters of the *Sorangium cellulosum* reveals unusual mechanisms of polyketide biosynthesis. Chem Biol 13, 1277-1286

Kadurugamuwa, J. L., T.J. Beveridge (1998): Delivery of the non-membrane-permeative antibiotic gentamycin into mammalian cells by using *Shigella flexineri* membrane vesicles. Antimicrobial Agents and Chemotherapy 42, 1476-1483

Kaiser, D., C. Manoil (1979): Myxobacteria: cell interactions, genetics, and development. Ann Rev Microbiol 33, 595-639

Kaiser, D. (1998): How and why myxobacteria talk to each other. Curr Opin Microbiol 1, 663-668

Kaiser, D. (2000): How do pili pull? Current Biology 10, R777-R780

Kaiser, D. (2004): Signaling in myxobacteria. Annu Rev Microbiol 58, 75-98

Karas M. and F. Hillenkamp (1988): Laser desorption ionization of proteins with molecular masses exceeding 10,000 daltons. Anal Chem 60, 2299-2301

Karas, M., M. Gluckmann, J. Schäfer (2000): Ionization in matrix-assisted laser desorption/ionization: singly charged molecular ions are the lucky survivors. J Mass Spectrom 35, 1-12

Kearns, D.B. and L.J. Shimkets (1998): Chemotaxis in a gliding bacterium. Proc Natl Acad Sci USA 95, 11957-11962

Kearns, D.B., B.D. Campell, L.J. Shimkets (2000): *Myxococcus xanthus* fibril appendages are essential for excitation by a phospholipids attractant. Proc Natl Acad Sci USA 97, 11505-11510

Kearns, D.B., A. Venot, P.J. Bonner, B. Stevens, G.J. Boons, L.J. Shimkets (2001): Identification of a developmental chemoattractant in *Myxococcus xanthus* through metabolic engineering. Proc Natl Acad Sci USA 98, 13990-13994

Kegler, C., K. Gerth, R. Müller (2006): Establishment of a real-time PCR protocol for expression studies of secondary metabolite biosynthetic gene cluster in the G/C-rich myxobacterium *Sorangium cellulosum* So ce56. J Biotechnol 121, 201-212

Kennelly, P.J. (2001): Protein phosphatases – aphylogenetic perspective. Chem Rev 101, 2291-2312

Kennelly, P.J. and M. Potts (1999): Life among primitives: protein O-phosphatases in prokaryotes. Frontiers in Bioscience 4, d372-385

Kim, S.-H., S. Ramaswamy, J. Downard (1999): Regulated exopolysaccharide production in *Myxococcus xanthus.* J Bacteriol 181, 1496-1507

Kimura, Y., H. Saiga, H. Hamanaka, H. Matoba (2006): *Myxococcus xanthus* twin-arginine translocation system is important for growth and development. Arch Microbiol, 184, 387-396

Kirby J.R. and D.R. Zusman (2003): Chemosensory regulation of developmental gene expression in *Myxococcus xanthus*. Proc Natl Acad Sci USA 100, 2008-2013

Klose, J. (1975): Protein mapping by combined isoelectric focusing and electrophoresis of mouse tissues: a novel approach to test induced point mutations in mammals. Humangenetik 26, 231-243

Klose, J. (1995): Protein mapping by combined isoelectric focusing and electrophoresis of mouse tissues-novel approach to testing for induced point mutations in mammals. Humangenetik 26, 231-243

Klose, J. and U. Kobalz (1995): Two-dimensional electrophoresis of proteins: an updated protocol and implications for a functional analysis of the genome. Electrophoresis 16, 1034-1059

Klebba, P.E. (2005): The porinologist. J Bacteriol 187, 8232-8236

Kobayashi, N., K. Nishino, A. Yamaguchi (2001): Novel macrolide-specific ABC-type efflux transporter in *Escherichia coli*. J Bacteriol 183, 5639-5644.

Kobayashi, N., K. Nishino, T. Hirata, A. Yamaguchi (2003): Membrane topology of ABC-type macrolide exporter MacB in *Escherichia coli*. FEBS 546, 241-246.

Kolter, R., D.A. Siegele, A. Tormo (1993): The stationary phase of the bacterial cell cycle. Annu Rev Microbiol 47, 855-874

Kopp, M., H. Irschik, F. Gross, O. Perlova, A. Sandmann, K. Gerth, R. Müller (2004): Critical variations of conjugational DANN transfer into secondary metabolite multiproducing *Sorangium cellulosum* strains So ce12 and So ce56: development of a *mariner*-based transposon mutagenesis system. J Biotechnol 107, 29-40

Kopp, M., H. Irschik, S. Pradella, R. Müller (2005): Production of the tubulin destabilizer disorazol in *Sorangium cellulosum*: Biosynthetic machinery and regulatory genes. Chem Bio Chem 6, 1277-1286

Krogh, A., B. Larsson, G. von Heijne, E.L. Sonnhammer (2001): Predicting Transmembrane Protein Topology with a Hidden Markov Model: Application to Complete Genomes. J Mol Biol 305, 567-580

Krzemieniewska H. and S. Krzemieniewski (1937): Die zellulosezersetzenden Myxobakterien. Bull Acad Polon Sci Lettr Classe Sci Math Nat, Ser B (I): 11-31

Kühlwein, H. (1950): Beiträge zur Biologie und Entwicklungsgeschichte der Myxobakterien. Arch Mikrobiol 14, 678-704

Kuehn, M.J. and N.C. Kesty (2005): Bacterial outer membrane vesicles and the host-pathogen interaction
Genes and Dev 19, 2645-2655

Kussmann, M. and P. Roepstorff (2000): Sample preparation techniques for peptides and proteins analyzed by MALDI-MS. Methods Mol Biol 146, 405-424

Laemmli, U.K. (1970): Cleavage of structural proteins during assembly of the head of bacteriophage T4. Nature 227, 680-685

Lancero, H.L., S. Castaneda, N.B. Caberoy, X. Ma, A.G. Garza, W. Shi (2005): Analysing protein-protein interactions of the *Myxococcus xanthus* Dif signalling pathway using two-hybrid system. Microbiol 151, 1535-1541

Li, J., G. Lee, S.R. Van Doren, J.C. Walker (2000): The FHA domain mediates phosphoprotein interactions. J Cell Sci 113, 4143-4149

Li, Z., Clarke, A. J., Beveridge, T. J. (1998): Gram-negative bacteria produce membrane vesicle which are capable of killing other bacteria. J Bacteriol 180, 5478-5483

Liao, H., I.J. Byeon, M.D. Tsai (1999): Structure and function of a new phosphopeptide-binding domain containing FHA2 of Rad53. J Mol Biol 294, 1041-1049

Liberek, K., C. Georgopoulos, M. Zylicz (1988): Proc Natl Acad Sci USA 85, 6632-6636

Link, V. (2006): Identification of protein controlling gastrulation movements by a proteomic approach in zebrafish. Dissertation, Technische Fakultät Dresden

Lohaus, C., H.E. Meyer (1998): Proteomforschung. Biospektrum 5, 32-43

Lottspeich, F. (1999): Proteome analysis: A pathway to the functional analysis of proteins. Angew Chem Int Ed 38, 2476-2492

Lottspeich, F. (2006): Bioanalytik, Spektrum Akademischer Verlag

Ludwig, W., K.H. Schleifer, H., Reichenbach, E. Stackebrandt (1983): A phylogenetic analysis of the myxobacteria *Myxococcus fulvus*, *Stigmatella aurantiaca*, *Cystobacter fuscus*, *Sorangium cellulosum* and *Nannocystis exedens.* Arch Microbiol 135, 58-52

Lux, R., W. Shi (2005): A novel bacterial signalling system with a combination of a Ser/Thr kinase cascade and a His/Asp two-component system. Mol Microbiol 58, 345-348

Mann, M., R.C. Hendrickson, A. Pandey (2001): Analysis of proteins and proteomes by mass spectrometry. Annu Rev Biochem 70, 437-473

Mann, M., P. Hoirup, P. Roepstorff (1993): Use of mass spectrometric molecular weight information to identify proteins in sequence databases. Biol Mass Spectrom 22, 338-345

Marouga, R., S. David, E. Hawkins (2005): The development of the DIGE system: 2D fluorescence difference gel analysis technology. Anal Bioanal Chem 382, 669-678

Mashburn-Warren, L. M. and M. Whitely (2006): Special delivery: Vesicle trafficking in prokaryotes. Mol Microbiol 61, 839-846

Meyer, D., C. Schneider-Fresenius, R. Horlacher, R. Peist, W. Boos (1997): Molecular characterization of glucokinase from *Escherichia coli* K-12. J Bacteriol 179, 1298-1306

Meyer, F., A. Goesmann, A. C. McHardy, D. Bartels, T. Bekel, J. Clausen, J. Kalinowski, B. Linke, O. Rupp, R. Giegerich, A. Pühler (2003): GenDB - An open source genome annotation system for prokaryote genomes. Nucl Acids Res 31, 2187-2195

Michal, G. (1999): Biochemical Pathways. Spektrum Akademischer Verlag GmbH, Heidelberg, Berlin.

Mijakovic, I., S. Poncet, G. Boël, A. Mazé, S. Gillet, E. Jamet, P. Decottignies, C. Grangeasse, P. Doublet, P. Le Marechal, J. Deutscher (2003): Transmembrane modulator-dependent bacterial tyrosine kinase activates UDP-glucose dehydrogenase. EMBO 22, 4709-4718

Mijakovic, I., L. Musumeci, L. Tautz, D. Petranovic, R.A. Edwards, P.R. Jensen, T. Mustelin, J. Deutscher, N. Bottini (2005): In vitro characterization of the Bacillus subtilis protein tyrosine phosphatase YwqE. J Bacteriol 187, 3384-3390

Moore, B.S. and J.N. Hopke (2001): Discovery of a new bacterial biosynthetic pathway. Chem Bio Chem 2, 35-38

Mootz, H.D., D. Schwarzer, M.A. Marahiel (2002): Ways of assembling complex natural products on modular nonribosomal peptide synthetases. Chem Bio Chem 3, 490-504

Müller, R. and K. Gerth (2006): Development of simple media which allow investigations into the global regulation of chivosazol biosynthesis with *Sorangium cellulosum* So ce56. J Biotechnol 121, 192-200

Munoz-Dorado, J., S. Inouye, M. Inouye (1991): A gene encoding a protein serine/threonine kinase is required for normal development of *M. xanthus*, a gram-negative bacterium. Cell 67, 995-1006

Nariya, H., S. Inouye (2005): Modulating factors for the Pkn4 kinase cascade in regulating 6-phosphofructokinase in Myxococcus xanthus. 56, 1314-1328

Neuhoff, V., R. Stamm, H. Eibl (1985): Clear backround and highly sensitive protein staining with Coomassie Blue dyes in polyacrylamide gels: A systematic analysis. Electrophoresis 6, 427-448

Nicaud, J.-M., A. Breton, G. Younes, J. Guespin-Michel (1984): Mutants of *Myxococcus xanthus* impaired in protein secretion: an approach to study of a secretory mechanism. Appl Microbiol Biotechnol, 20, 344-350

Nielsen, H., J. Engelbrecht, S. Brunak, G. von Heijne (1997): Identification of prokaryotic and eukaryotic signal peptides and prediction of their cleavage sites. Protein Engineering 10, 1-6

Nikaido, H. (1996): Multidrug efflux pumps of Gram-negative bacteria. J Bacteriol 178, 5853-5859

Nock, S. and Wagner (2000): Proteomics: Die post-genomische Revolution. Chemie in unserer Zeit 34, 348-354

Nyström, T. (2004): Stationary-phase physiology. Annu Rev Microbiol 58, 161-181

O'Farrell, P.H. (1975): High resolution two-dimensional electrophoresis of proteins. J Biol Chem 250, 4007-4021

Ofek, J., K. Kabha, A. Athamna, G. Frankel, D.J. Wozniak, D.L. Hasty, D.E. Ohman (1993): Genetic exchange of determinants for capsular polysaccharide biosynthesis between *Klebsiella pneumoniae* strains expressing serotypes K2 and K21a. Infect Immun 61, 4208-4216

Padan, E., T. Tzubery, K. Herz, L. Kozachkov, A. Rimon, L. Galili (2004): NhaA of *Escherichia coli*, as a model of a pH-regulated Na^+/H^+ antiporter. Biochim Biophys Acta 1658, 2-13

Palmer, T. and B.C. Berks (2003): Moving folded proteins across the bacterial cell membrane. Microbiol 149, 547-556

Pandey, A. and M. Mann (2000): Proteomics to study genes and genomes. Nature 405, 837-846

Pappin, D.J.C., P. Hoirup, (1993): Rapid identification of proteins by peptide-mass fingerprinting. Current Biology 3, 327-332.

Pennington, S.R., M.R. Wilkins, D.F. Hochstrasser, M.J. Dunn (1997): Proteome analysis. From protein characterization to biological function. Trends in Cell Biology 7, 168-173

Perkins, D.N., D.J. Pappin, D.M. Creasy, J.S. Cotrell (1999): Probality-based protein identification by searching sequence databases using mass spectrometry data. Electrophoresis 20, 3551-3567

Perlova, O., K. Gerth, O. Kaiser, A. Hans, R. Müller (2006): Identification and analysis of the chivosazol biosynthetic gene cluster from, the myxobacterial model strain *Sorangium cellulosum* So ce56. J Biotechnol 121, 174-191

Peterson, J.A. and S.E. Graham-Lorence (1995): Bacterial P450s:Structural similarities and functional differences. Cytochrome P450: Structure, Mechanism, and Biochemistry (2nd Ed.), edited by P.R. Oritz de Montellano. Plenum Press, New York

Pohlner, J., R. Halter, K. Beyreuther, T.F. Meyer (1987): Gene structure and extracellular secretion of *Neisseria gonorrhoeae* IgA protease. Nature 325, 458-462

Poole, K. (2004): Efflux-mediated multiresistance in Gram-negative bacteria. European Society of Clinical Microbiology and Infectious Diseases 10, 12-26

Pradella, S., A. Hans, C. Spröer, H. Reichenbach, K. Gerth, S. Beyer (2002): Characterisation, genome size and genetic manipulation of the myxobacterium *Sorangium cellulosum* So ce56. Arch Microbiol 178, 484-492.

Prescott, L., J. Harley, D. Klein (2005): Microbiology. 6th Ed., the McGraw Hill Companies, New York.

Pukatzki, S., A.T. Ma, D. Sturtevant, B. Krastins, D. Sarracino, W.C. Nelson, J.F. Heidelberg, J.J. Mekalanos (2006): Identification of a conserved bacterial protein secretion system Vibrio cholerae using the Dictyostelium host model system. PNAS 103, 1528-1533

Quiros, L. M., I. Aguirezzabalaga, C. Olano, C. Mendez, J.A. Salas (1998):
Mol Microbiol 28, 1177-1186

Quiros, L. M., R. J. Carbajo, A.F. Brana, J.A. Salas (2000):
Glycolisation of macrolide antibiotics. J Biol Chem 275, 11713-11720

Rawlings, B.J. (1999): Biosynthesis of polyketides (other than actinomycete macrolides). Nat Prod Rep 16, 425-484

Reichenbach, H. (1974): Die Biologie der Myxobakterien. Biologie in unserer Zeit 4, 33-45

Reichenbach, H., M. Dworkin: The myxobacteria "The Prokaryotes" 2nd Edition Vol IV, 1992, Chapter 188

Reichenbach, H. and G. Höfle (1993): Biologically active secondary metabolites from myxobacteria. Biotech Adv 11, 219-277

Reichenbach, H. (1999): The ecology of the myxobacteria. Environ Microbiol 1, 15-21

Reichenbach, H. and G. Höfle (1999): Myxobacteria as producers of secondary metabolites. In *Drug Discovery from Nature*, pp. 149-179. Edited by S. Grabley & R. Thiercke. Berlin, Heidelberg: Springer.

Reichenbach, H. (2001): Myxobacteria, producers of novel bioactive substances. J Ind Microbiol Biotechnol 27, 149-156

Reichenbach, H. (2004): The Myxococcales. In: Garrity, G.M. (Ed.), Bergey`s Manual of Systematic Bacteriology. Springer-Verlag, New York, pp. 1059-1143

Roach, P.J. (1991): Multisiet and hierarchal protein phosphorylation. J Biol Chem 266, 14139-14142

Rosenberg, E., and M. Dworkin (1996): Autocides and a paracide, antibiotic TA, produced by *Myxococcus xanthus*. J Industrial Microbiol 17, 424-431

Rye, H.S., A.M. Roseman, S. Chen, K. Furtak, W.A. Fenton, H.R. Saibil, A.L. Horwich (1999): GroEL-GroES cycling: ATP and nonnative polypeptide direct alternation of folding-active rings. Cell 97, 325-338

Saier, M.H., S. Chaveaux, J. Deutscher, J. Reizer, J.-J. Ye (1995): Protein phosphorylation and regulation of carbon metabolism in Gram-negative versus Gram-positive bacteria. TIBS 20, 267-271

Saier, M.H., C.V. Tran, R.D. Barabote (2006): TCDB: the Transport Classification Database for membrane transport protein analyses and information. Nucleic Acids Research 34, D181-D186

Sandmann, A., F. Sasse, R. Müller (2004): Identification and analysis of the core biosynthetic machinery of tubulysin, a cytotoxin with potential anticancer activity. Chem Biol 11, 1071-1079

Schaechter, M. (2007): Microbe. Spektrum Akademischer Verlag, Elsevier GmbH, München.

Schägger, H. (2001): Blue native gels to isolate protein complexes from mitochondria. Methods Cell Biol 65, 231-244

Schägger, H. and Jagow, G. von (1991): Blue Native electrophoresis for isolation of membrane protein complexes in enzymatically active form. Analyt Biochem 199, 223-231

Schägger, H., W.A. Cramer, G. von Jagow (1994): Analysis of molecular masses and oligomeric states of protein complexes by blue native electrophoresis and isolation of membrane protein complexes by two-dimensional native electrophoresis. Anal Biochem 217, 220-230

Schneider, E. and S. Hunke (1998): ATP-binding-cassette (ABC) transport systems: Functional and structural aspects of the ATP-hydrolyzing subunits/domains. FEMS Microbiol Rev 22, 1-20

Schneiker, S. *et al.* (2007): Complete sequence of the largest known bacterial genome from the myxobacterium *Sorangium cellulosum*. Nat. Biotechnol.

Shevchenko, A., M. Wilm, O. Vorm, M. Mann (1996): Mass spectrometric sequencing of proteins from silver-stained polyacrylamide gels. Anal Chem 68, 850-858

Sieber, S.A. and M.A. Marahiel (2003): Learning from nature's drug factories: Nonribosomal synthesis of macrocylic peptides. J Bacteriol 185, 7036-7043

Shimkets, L.J., M. Dworkin, H. Reichenbach (2005): The myxobacteria. In: The Prokaryotes, third ed. Springer-Verlag, New York, NY, release 3.19

Simunovic, V., F.C. Gherardini, L.J. Shimkets (2003): Membrane localization of motility, signalling, and polyketide synthetase proteins in *Myxococcus xanthus*. J. Bacteriol 185, 5066-5075.

Sogaard-Andersen, L., M. Overgaard, S. Lobedanz, E. Ellehauge, L. Jelsbak, A.A. Rasmussen (2003): Coupling gene expression and multicellular morphogenesis during fruiting body formation in *Myxococcus xanthus*. Mol Microbiol 48, 1-8

Sonnhammer, E.L., G. von Heinje, A. Krogh (1998): A hidden Markov model for predicting transmembrane helices in protein sequences. Proc Int Conf Intell Syst Mol Biol 6, 175-182

Spormann, A.M. (1999): Gliding motility in bacteria: insights from studies of *Myxococcus xanthus*. Microbiol Mol Biol Rev 63, 621-641

Staunton, J., K.J. Weissman (2001): Polyketide biosynthesis: a millenium review. Nat Prod Rep 18, 380-416

Stenberg, F., P. Chovanec, S.L. Maslen, C.V. Robinson, L.L. Ilag, G.von Heijne, D.O. Daley (2005): Protein complexes of the *Escherichia coli* cell envelope. J Biol Chem 280, 34409-34419

Stephens, K., P. Hartzell, D. Kaiser (1989): Gliding motility in *Myxococcus xanthus: mgl* locus, RNA, and predicted protein products. J Bacteriol 171, 819-830

Sutcliffe, I.C. and R.R.B. Russell (1995): Lipoproteins of Gram-positive bacteria. J Bacteriol 177, 1123-1128

Taylor, F.R. and J.E. Cronan, Jr. (1979): Cyclopropane fatty acid synthase of *Escherichia coli*: stabilization, purification, and interaction with phospholipid vesicles. Biochem 15, 3292-3300

Thaxter, R. (1892): On the Myxobacteriaceae, a new order of Schizomycetes. Bot Gaz 17, 389-406

Thomasson, B., J. Link, A.G. Stassinopoulos, N. Burke, L. Plamann, P.L. Hartzell (2002): MglA, a small GTPase, interacts with a tyrosine kinase to control type IV pili-mediated motility and development of *Myxococcus xanthus*. Mol Microbiol 46, 1399-1413

Towbin, H., T. Staehelin, J. Gordon (1979): Electrophoretic transfer of proteins from polyacrylamide gels to nitrocellulose sheets. Procedure and some applications. Proc Natl Acad Sci USA 76, 4350-4354

Tjalsma, H., H. Antelmann, J.D.H. Jongbloed, P.G. Braun, E. Darmon, R. Dorenbos, J.-Y.F. Dubois, H. Westers, G. Zanen, W.J. Quax, O.P. Kuipers, S. Bron, M. Hecker, J.M. van Dijl (2004): Proteomics of protein secretion by *Bacillus subtilis*: Separating the "secrets" of the secretome. Microbiol Mol Biol Rev 68, 207-233

Udo, H., J. Munoz-Dorado, M. Inouye, S. Inouye (1995): Myxococcus xanthus, a gram-negative bacterium, contains a transmembrane protein serine/threonine kinase that blocks the secretion of beta-lactamase by phosphorylation. Genes Dev 9, 972-983

Unlu, M., M.E. Morgan, J.S. Minden (1997): Difference gel electrophoresis: a single gel method for detecting changes in protein extracts. Electrophoresis 18, 2071-2077

Vincent, C., B. Duclos, C. Grangeasse, E.Vaganay, M. Riberty, A.J. Cozzone, P. Doublet (2000): Relationship between exopolysaccharide production and protein-tyrosine phosphorylation in gram-negative bacteria. J Biol Chem 276, 2361-2371

Vlamakis, H.C., J.R. Kirby, D.R. Zusman (2004): The Che4 pathway of *Myxococcus xanthus* regulates type IV pilus-mediated motility. Mol Microbiol 52, 1799-1811

Voet, D., J.G. Voet, C.W. Pratt (2006): Fundamentals of biochemistry, 2nd edn, New York: John Wiley & Sons Inc.

Wai, S.N., A. Takade, K. Amako (1995): The release of outer membrane vesicles from the strains of enterotoxogenic *Escherichia coli*. Microbiol Immunol 39, 451-456

Wai, S. N., B. Lindmark, T. Söderblom, A. Takade, M. Westermark, J. Oscarsson, J. Jass, A. Richter-Dahlfors, Y. Mizunoe, B.E. Uhlin (2003): Vesicle-mediated export and assembly of pore-forming oligomers of the enterobacterial ClyA cytotoxin.
Cell 115, 25-35

Washburn, M.P. and J.R. Yates (2000): 3rd Analysis of the microbial proteome. Curr Opin Microbiol 3, 292-297

Watt, S.A., A. Wilke, T. Patschkowski, K. Niehaus (2005): Comprehensive analysis of the extracellular proteins from *Xanthomonas campestris* pv. *campestris* B100.
Proteomics 5, 153-167

Welch, R. and D. Kaiser (2001): Cell behavior in travelling wave patterns of myxobacteria. Proc Natl Acad Sci USA 98, 14907-14012

White, D.J. and P.L. Hartzell (2000): AglU, a protein required for gliding motility and spore maturation of Myxococcus xanthus, is related to WD-repeat proteins. Mol Microbiol 36, 662-678

Wilke, A., C. Rückert, D. Bartels, M. Dondrup, A. Goesmann, A.T. Hüser, S. Kespohl, B. Linke, M. Mahne, A.C. McHardy, A. Pühler, F. Meyer (2003): Bioinformatics support for high-throughput proteomics. J Biotechnol 106, 147-156.

Wilkins, M.R., C. Pasquali, R.D. Appel, K.Ou, O. Golaz, J.C. Sanchez, J.X. Yan, A.A. Gooley, G. Hughes, I. Humphery-Smith, K.L. Williams and D.F. Hochstrasser (1996): From proteins to proteoms: Large-scale protein identification by two-dimensional electrophoresis and amino acid analysis. Bio Technology 14, 61-65

Wolgemuth, C., E. Hoiczyk, D. Kaiser, G. Oster (2002): How myxobacteria glide. Curr Biol 12, 369-377

Womack, B.J., D.F. Gilmore, D. White (1989): Calcium requirement for gliding motility in myxobacteria. J Bacteriol 171, 6093-6096

Wu, C.C., MacCoss, M.J., Howell, K.E., Yates, J.R. (2003): A method for the comprehensive proteomic analysis of membrane proteins. Nature Biotchnol 21, 532-538

Yang, Z., Y. Geng, D. Xu, H.B. Kaplan, W. Shi (1998): A new set of chemotaxis homologues is essential for *Myxococcus xanthus* social motility. Mol Microbiol 30, 1123-1130.

Yang, Z., X. Ma, L.Tong, H.B. Kaplan, L.J. Shimkets, W. Shi (2000): *Myxococcus xanthus dif* genes are required for biogenesis of cell surface fibrils essential for social gliding motility. J Bacteriol 182, 5793-5798

Yankovskaya, V., R. Horsefield, S. Tornroth, C. Luna-Chavez, H. Miyoshi, C. Leger, B. Byrne, G. Cecchini, S. Iwata (2003): Architecture of succinate dehydrogenase and reactive oxygen species generation. Science 299, 700-704

Yen, M., C.R. Peabody, S.M. Partovi, Y. Zhai, Y. Tseng, M.H. Saier (2002): Protein-translocating outer membrane porins of Gram-negative bacteria. Biochim Biophys Acta 1562, 6-31

Youderian, P., N. Burke, D.J. White, P.L. Hartzell (2003): Identification of genes required for adventurous gliding motility in *Myxococcus xanthus* with the transposable element mariner. Mol Microbiol 49, 555-570

Yuriy, C. (2005): Subunit topology in the V type ATPase and related enzymes. Dissertation, University of Groningen

Zhang, W., M. Inouye, S. Inouye (1996): Reciprocal regulation of the differentiation of *Myxococcus xanthus* by Pkn5 and Pkn6, eukaryotic-like Ser/Thr protein kinases. Mol Microbiol 20, 435-447

Zietkiewicz, S., A. Lewandowska, P. Stocki, K. Liberek (2006): Hsp70 chaperone machine remodels protein aggregates at the initial step of Hsp70-Hsp100-depending disaggregation. J Biol Chem 281, 7022-7029

Zirkle, R., J.M. Ligon, I. Molnar (2004): Heterologous production of the antifungal polyketide antibiotic soraphen A of *Sorangium cellulosum* So ce26 in *Streptomyces lividans*. Microbiol 150, 2761-2774

Acknowledgements

While working on my project I was delighted to get the support of different people. I cannot list them all but I would like to mention some of them:

First of all, I want to gratefully thank Prof. Dr. Pühler for giving me the opportunity to work in the Department of Genetics and for his trust.

I am extremely thankful to my advisor, Prof. Dr. Karsten Niehaus, for his encouragement, mentoring and great support during all the time.

I especially thank Prof. Dr. Hans-Peter Braun from the University of Hannover for kindly reviewing this thesis and for assistance in the Blue-Native method.

Furthermore, I am deeply indebted to Dr. Klaus Gerth, Diana Telkemeyer and Claus Conrad from the Helmholtz Institute in Braunschweig for providing me with happy So ces and for helping me.

I also thank Prof. Dr. Rolf Müller and Dr. Olena Perlova from the Pharamceutical Biotechnology at the University of Saarland in Saarbrücken.

Sincere thanks also to Dr. Anke Treuner-Lange, Dr. Tina Knauber and Sabrina Doß from the Institute of Microbiology at the University of Giessen for their help.

Special thanks to Dr. Raimund Hoffrogge and Marc Wingens from the Faculty of Technical Sciences and Andreas Unger from the Biochemical Cellbiology at the University of Bielefeld.

Sincere thanks to my colleagues in the lab for supporting me during this time and for giving me good advices whenever there was a problem to be solved and for encouraging me. Especially, I would like to thank Frank Colditz, Thomas Patschkowski, Steven Watt, Nadine Küpper, Vishaldeep Kaur Sidhu and Mila Bellanco-Spädt, Martina Brecht, Prachumporn Nounurai.

I also thank the Bioinformatic group (BRF) at the University of Bielefeld for their kindness of helping me handling my data, for valuable suggestions and for nice and encouraging discussions, in particular Andreas Wilke, Stefan Albaum, Sebastian

Appendix

Tab. 8: The identified proteins of the cytoplasmic fraction and the Differential Gel Electrophoresis of *Sorangium cellulosum* So ce56 were categorized according to their Clusters of Orthologous Groups of proteins (COG) classification scheme. The numeration corresponds to the protein spot numbers in Figure 17 and 19. Also given are the accession numbers and the functions of the identified proteins from the So ce56 database (GenDB), the observed and theoretical Mr and pl values, the sequence coverage and the MOWSE score.

Spot	Protein (Accession)	MW(calc/gel)	p*l*(calc/gel)	Score	Coverage
Lipid transport and metabolism (I):					
7; 80-82	**Acyl-CoA dehydrogenase** (EC 1.3.99.3) sce2853	41728 / 41000	6 / 6.9	92	18
12; 36; 37	**Butyryl-CoA dehydrogenase (**EC 1.3.99.2) sce3575	67254 / 68000	5.87 / 5.5	94	17
71	**Acetyl CoA C-acyltransferase**[TMH] **Thiolase** (EC 2.3.1.9) sce7554	40727 / 40000	9.03 / 9.1	102	18
84	**Butyryl-CoA dehydrogenase** (EC 1.3.99.2) sce1166	42149 / 42000	5.4 / 6.2	76	14
115; 143	**3-hydroxybutyryl-CoA dehydratase** (EC 4.2.1.55) and **Enoyl-CoA dehydratase** (EC 4.2.1.17) sce0250	28510 / 23000	6.19 / 7.1	127	31
138	**3-oxoid CoA-transferase subunit B** (EC 2.8.3.5) sce5785	23335 / 22000	4.7 / 5.1	84	30
Carbohydrate transport and metabolism (G):					
32; 33	**Pyruvate kinase 1** (EC 2.7.1.40) sce4540	50721 / 52000	6.29 / 7.2	138	28
27	**Transketolase** (EC 2.2.1.1) sce3987	71063 / 69000	6.22 / 7.2	128	9
26	**4-alpha-glucanotransferase homolog** (EC 2.4.1.25) sce0351	73407 / 75000	6.31 / 7	134	16
34	**Glucose-6-phosphate isomerase** (EC 5.3.1.9) sce5669	58980 / 57000	5.97 / 6.9	135	20
35	**Phosphoglycerate mutase** (EC 5.4.2.1) sce4502	59882 / 59000	5.94 / 6.8	125	20

13	**Phosphomannomutase** (EC 5.4.2.8) sce4837	63114 / 63000	4.83 / 5.4	59	6
50-57; 125	**Phosphopyruvate hydratase Enolase** (EC 4.2.1.11) sce7698	45912 / 45000	5.14 / 5.6	204	34
59	**Phosphoglycerate kinase** (EC 2.7.2.3) sce7349	43679 / 43000	5.55 / 5.4	89	21
60; 61	**Xylose isomerase** (EC 5.3.1.5) sce5429	49930 / 48000	5.8 / 6.6	165	59
70	**6-Phosphofructokinase** (EC 2.7.1.11) sce3426	44256 / 42000	8.98 / 9.5	78	12
73; 74	**Glyceraldehyde-3-phosphate dehydrogenase** (EC 1.2.1.12) sce7350	36939 / 36000	7.71 / 8.1	100	29
76	**Fructose-bisphosphate aldolase** (EC 4.1.2.13) sce1923	39122 / 39000	6.46 / 7.5	67	24
127	**Triose-phosphate isomerase** (EC 5.3.1.1) sce7348	28490 / 25000	4.74 / 5.4	112	43

Energy production and conversion (C):

99	**Alcohol dehydrogenase** (EC 1.1.1.1) sce3952	39841 / 38000	6.16 / 6.9	67	15
101	**Pyruvate dehydrogenase** (EC 1.2.4.1) sce3800	36222 / 39000	5.82 / 6.5	105	25
121	**Pyruvate dehyrogenase (acetyl-transferring)** (EC 1.2.4.1) sce3801	35930 / 35000	5.2 / 5.9	112	32
106	**Isocitrate dehydrogenase** (EC 1.1.1.41) sce5773	40919 / 36000	9.79 / 7.4	92	18
108; 109; 114	**Lactate dehydrogenase** (EC 1.1.1.27) **Malate dehydrogenase** (EC 1.1.1.37) sce1050	33184 / 33000	8.55 / 8.7	108	35
112	**Succinate—CoA ligase (ADP-forming)** (EC 6.2.1.5) sce9141	30013 / 25000	8.65 / 7.9	148	32
16; 21; 22; 122; 148	**Aconitate hydratase** (EC 4.2.1.3) sce8137	98774 / 83000	5.74 / 6.7	114	12
64	**Aldehyde dehydrogenase** (EC 1.2.1.3) sce0676	51881 / 51000	6.52 / 7.3	83	15
163	**Sulfotransferase** (TC 2.A.53.9.1) sce2035	23956 / 17000	5.22 / 5.6	87	27

179	**Thioredoxin Thiol-disulfide isomerase** (EC 5.3.4.1) sce7351	11520 / 9000	7.27 / 7.9	53	28
15	**H$^+$-transporting two-sector ATPase (atpD)** (EC 3.6.3.14/ TC 3.A.2.1.3) sce4444	50722 / 51500	4.88 / 5.5	70	18
25	**H$^+$-transporting two-sector ATPase F$_0$F$_1$-type (atpG)** (TC 3.A.2.1.1) sce9360	34917 / 78000	9.37 / 6.9	62	11
159	**Conserved hypothetical protein Electron transport protein yjeS** sce4434	42072 / 21000	7.67 / 6.3	56	26
168; 169	**Rubrerythrin** sce1753	15552 / 16000	5.37 / 6.1	116	62

Inorganic ion transport and mechanism (P):

19; 20; 140; 157; 160	**Superoxide dismutase sodA** (EC 1.15.1.1) sce0071	22805 / 22000	6.17 / 5.9	97	32
154	**Superoxide dismutase sodB** (EC 1.15.1.1) sce4167	21115 / 20000	6.32 / 7.5	53	17
162; 170	**Probable DNA-binding stress protein Dps family (starvation inducible)** sce6807	17634 / 17500	5.65 / 6	105	46
72	**Phosphate ABC transporter PstS**[SignalP] (TC 3.A.1.7.1) sce2946	38892 / 38000	8.47 / 8.4	65	20

Secondary metabolites transport and metabolism (Q):

14	**ABC transporter ATP-binding protein,** (TC 3.A.1.27.1) sce3697	27561 / 56000	6.25 / 5.5	64	29
90	**Putative SAM domain protein Methyltransferase slr 0309** sce0689	56275 / 37000	8.74 / 6.5	67	9
119	**Fumarylacetoacetase family protein** sce8243	30959 / 27000	5.07 / 5.9	53	16

Amino acid transport and metabolism (E):

43; 45; 46; 67; 92; 117; 132-135	**Glutamate-ammonia ligase** (EC 6.3.1.2) sce7210	52171 / 52000	5.84 / 6.6	167	38
44	**Urocanate hydratase** (EC 4.2.1.49) sce8010	60527 / 57000	5.85 / 6.6	54	16
63	**Argininosuccinate synthase** (EC 6.3.4.5) sce5046	49631 / 50000	6.07 / 7	71	13

68	**Glycine hydroxymethyltransferase** (EC 2.1.2.1) sce6587	45527 / 44000	7.08 / 7.9	138	21
75; 105	**Aspartate-semialdehyde dehydrogenase** (EC 1.2.1.11) sce5347	36930 / 36000	6.72 / 7.6	67	23
18	**Oligopeptidase A Zn-dependent** (EC 3.4.24.70) sce6973	76268 / 74000	5.51 / 6.3	53	9
86	**Agmatinase** (EC 3.5.3.11) sce4400	43276 / 39000	6.79 / 5.6	78	18
88	**Histidinol-phosphate transaminase** (EC 2.6.1.9) sce8855	40190 / 40000	5.58 / 6.4	65	16
89	**3-isopropylmalate dehydrogenase** (EC 1.1.1.85) sce3735	37426 / 38000	5.7 / 6.5	112	20
95	**Agmatinase** (EC 3.5.3.11) sce0044	34310 / 34000	6.03 / 6.7	72	20
98	**Ketol-acid reductoisomerase** (EC 1.1.1.86) sce3732	36352 / 37000	6.09 / 7	134	35
103	**Branched-chain-amino-acid transaminase (ilvE)** (EC 2.6.1.42) sce6015	40834 / 39000	6.21 / 7.2	88	19
113	**Dihydrodipicolinate synthase** (EC 4.2.1.52) sce8027	31167 / 24000	7.51 / 7.5	110	22
28; 30; 31	**ABC-type dipeptide transport system**[Signal P] (TC 3.A.1.5.6) sce7548	63508 / 60000	8.87 / 7.6	105	13

Coenzyme transport and metabolism (H):

107	**Naphthoate synthase Dihydroxynaphthoic acid synthase** (EC 4.1.3.36) sce5310	33145 / 35000	6.51/ 7.5	106	29
152	**Pyridoxine-5-phosphate synthase, Vitamin B6** (EC 2.6.99.2) sce5839	26933 / 20000	6.45 / 8.1	85	28
153; 174	**Riboflavin synthase beta chain, Vitamin B2** (EC 2.5.1.9) sce7268	16258 / 18000	7.64 / 8.5	80	38
97	**Glutathione synthase (gshB)** (EC 6.3.2.3) sce7568	34950 / 35000	6.58 / 7	134	36
62	**Adenosylhomocysteinase** (EC 3.3.1.1) sce2963	47785 / 48000	5.91 / 6.7	55	10

Nucleotide transport and metabolism (F):

29	**IMP dehydrogenase/ GMP reductase** (EC 1.1.1.205) sce0088	56506 / 58000	6.15 / 7.2	135	25
42	**Dihydroorotase** (EC 3.5.2.3) sce4269	46665 / 49000	5.47 / 6.4	98	22
78	**Ribonucleoside-diphosphate reductase** (EC 1.17.4.1) sce3875	92960 / 41000	6.95 / 7.2	84	10
128	**Phosphoribosylamine-glycine ligase** (EC 2.7.4.6) sce9014	45271 / 24000	6.22 / 5.5	65	14
173	**Nucleoside diphosphate kinase** (EC 2.7.4.6) sce2949	15608 / 14000	7.5 / 8.3	144	65
66; 77	**Adenylosuccinate synthase** (EC 6.3.4.4) sce8895	45339 / 45000	6.29 / 7.2	87	19

Posttranslational modifications (O):

141; 144; 165; 166	**Glutathione transferase** (EC 2.5.1.18) sce4509	30236 / 22000	9.86 / 6	78	34
94	**Thioredoxin-disulfide reductase** (EC 1.8.1.9) sce7636	34005 / 35000	5.88 / 6.7	82	21
8; 9; 17; 123; 124	**Chaperone protein dnaK** (TC 1.A.33.1.2) sce9025	68892 / 54000	5.22 / 5.4	140	24
38-40	**Heat shock protein groEL (HSP 60 family)** sce5911	57987 / 59000	5.45 / 6.2	131	21
131; 136	**Chloroplast GrpE protein** (TC 3.A.8.1.1) sce0004	21074 / 22000	4.82 / 5	61	16
150; 151; 158	**Peptidyl-prolyl cis-trans isomerase** (EC 5.2.1.8) sce0374	20646 / 20000	8.81 / 9.1	171	58
172	**Organic hydroperoxide resistance protein** sce0181	14487 / 14000	7.41 / 8	87	45
182; 185	**GroES-like protein (HSP 10)** sce5844	10687 / 10000	5.3 / 6	95	62
137	**Putative peroxiredoxin 2 family/ glutaredoxin** sce0905	26548 / 21000	5.62 / 4.8	52	12
156	**Peroxidase** (EC 1.11.1.7) sce6959	20612 / 20000	6.5 / 7	82	35
129	**ATP-dependent protease La (Lon)** (EC 3.4.21.53) sce5003	90380 / 23000	5.6 / 5.5	57	5
142	**Endopeptidase Clp**	24210 / 22000	6.4 / 6.5	123	31

	ATP-dependent (EC 3.4.21.92) sce3147				
100	**Peptide methionine sulfoxide reductase**[Signal P] (EC 1.8.4.11) sce7999	42467 / 39000	7.64 / 6.8	157	30
175; 177	**Heavy metal ATPase** (TC 3.A.3.6.5) sce2780	10663 / 18500	9.42 / 9.5	112	63

Replication (L):

85	**DNA polymerase III β-subunit** (EC 2.7.7.7) sce8164	39990 / 42000	5.23 / 6.1	80	16

Translation (J):

87	**Elongation factor – GTPases (EF-Tu)** (EC 3.6.5.3) sce0402	43373 / 39000	6.47 / 6	89	18

Transcription (K):

161	**Transcription elongation factor GreA** sce3595	17498 / 18000	5.01 / 6.4	76	32
183	**Transcriptional regulator** sce6445	34069 / 11000	4.75 / 5.9	57	14

Cellwall biogenesis (M):

65	**UDP-glucose 6-dehydrogenase** (EC 1.1.1.22) sce2793	46492 / 49000	6.12 / 7	93	18

Signal transduction mechanisms (T):

110	**Putative protein phosphatase Diadenosine tetraphosphatase** sce7256	27907 / 30000	5.38 / 8.7	80	26
126	**Phosphoprotein phosphatase** (EC 3.1.3.16) sce2784	29871 / 25000	4.4 / 4.7	82	26
146; 147	**FHA domain protein** sce8329	38420 / 24000	8.94 / 7.6	104	19

General function prediction only (R):

1	**Secreted endonuclease/ exonuclease/ phosphatase family**[Signal P] sce0688	120231 / 90000	4.12 / 4.2	98	8
2-4; 6	**Hypothetical protein**[Signal P] **Phosphatase** sce0936	85860 / 85000	4.37 / 4.5	163	19

10; 11; 139	**Putative secreted protein**[Signal P] sce4014	68792 / 68000	4.65 / 5.4	114	23
41	**Peptidase U62 Zn-dependent** sce6446	51116 / 52000	5.52 / 6.4	112	19
49	**PE-PGRS family protein probable cell surface protein** sce2648	60274 / 41000	4.03 / 4.5	53	10
79	**Hippurate hydrolase** (EC 3.5.1.32) sce8630	42318 / 42000	6.22 / 7.1	59	8
91	**Conserved hypothetical protein** sce5499	36215 /36000	6.16 / 6.5	59	20
102	**Putative phosphoesterase Phosphohydrolases** sce3464	30420 / 40000	6.05 / 6.9	52	31
116; 118	**Conserved hypothetical protein Metallo β-lactamase family protein** sce0859	30520 / 24000	5.56 / 6.3	86	28
120	**SphH pore forming hemolysin** (TC 1.C.67.1.1) sce4785	31223 / 27000	5.68 / 5.6	153	40

Function unknown (S):

48	**Icm/Dot protein secretion system** (TC 3.A.7.9.1) sce6785	104637 / 51000	4.23 / 4	67	10
58	**Conserved hypothetical protein** sce0425	44693 / 45000	5.5 / 5.3	86	17
155	**Secreted protein Hcp Hemolysin** sce4994	18797 / 21000	6.22 / 7.1	108	44

No functional category (X):

5	**Hypothetical protein ATPase**[Signal P, Tat] sce5843	183013 / 85000	4.6 / 5.3	62	5
23; 24	**Hypothetical protein Clp protease** sce7556	10456 / 80000	10.22 / 7.4	53	6
47	**Putative outer membrane lipoprotein**[Signal P] sce5067	49276 / 51000	3.78 / 3.9	63	13
83	**BNR repeat domain protein glycosyl hydrolase**[TMH] sce7527	42577 / 40000	5.74 / 6.6	52	11
93	**Hypothetical protein** sce6147	44631 / 25000	6.29 / 7	54	19
111; 130; 164	**Hypothetical protein Phycocyanin α lyase** sce8617	24189 / 24000	3.97 / 8.5	87	23
69	**Aspartate transaminase** (EC 2.6.1.1) sce6239	45916 / 47000	7.71 / 8.3	131	22

96; 104	**Putative nucleotide binding protein (membrane protein) SRPI protein** sce4642	33383 / 34000	6.19 / 6.9	90	17
145; 149	**Hypothetical protein Chlorite dismutase** sce4838	28556 / 23000	6.51/ 7.4	130	34
167	**Hypothetical protein glyoxalase family protein** sce3094	16097 / 15000	5.05 / 5.6	45	23
171	**Hypothetical protein Secreted protein**[Signal P] sce9092	16074 / 14000	6.1 / 7.5	54	22
176	**Hypothetical protein** sce0142	18954 / 18500	11.41 / 9.5	52	23
178	**Conserved hypothetical protein** sce7128	10543 / 18000	9.37 / 9.8	105	67
180; 181	**Hypothetical protein Exported protein** sce3202	10374 / 8000	5.49 / 6.3	70	47
184	**Hypothetical protein** sce8445	13068 / 10000	10.2 / 5.5	62	49

Tab. 9: List of CyDye labeled identified proteins of the cytosolic fraction from So ce56. 16 proteins were up-regulated in the exponential and 9 proteins were up-regulated in the stationary phase. The spot numbers correspond to Figure 19, but following the numeration of Fig. 17 and Tab.8.

Spot No.	Cy3[TM] labeled proteins from the exponential phase are marked with red arrows (red protein spots)	Spot No.	Cy5[TM] labeled proteins from the stationary phase (green protein spots, marked with green arrows)
36	**Butyryl-CoA dehydrogenase** Sce3575 (I)	71	**Thiolase** Sce7554 (I)
27	**Transketolase** Sce3987 (G)	70	**Phosphofructokinase** Sce3426 (G)
59	**Phosphoglycerate kinase** Sce7349 (G)	97	**Glutathione synthetase** Sce7568 (H)
61	**Xylose isomerase** sce5429 (G)	72	**Phosphate ABC transporter PstS**[SignalP] sce2946 (P)
76	**Fructose-bisphosphate aldolase** sce1923 (G)	159	**Conserved hypothetical protein** Sce4434 (C)
127	**Triose-phosphate isomerase** Sce7348 (G)	9	**Chaperone protein dnaK** Sce9025 (O)
183	**Transcriptional regulator** Sce6445 (K)	2	**Hypothetical protein / Phosphatase** Sce0936 (R)
169	**Ruberythrin** Sce1753 (C)	155	**Secreted protein Hcp** Sce4994 (R)
157; 160	**Superoxide dismutase sodA** Sce0071 (P)	171	**Hypothetical protein** Sce9029 (X)
154	**Superoxide dismutase sodB** Sce4167 (P)		
142	**Endopeptidase Clp** Sce3147 (O)		
165	**Glutathione-S-transferase** sce4509 (O)		
172	**Organic hydroperoxide resistance protein** sce0181 (O)		
58	**Conserved hypothetical protein** sce0425 (R)		
96	**Putative nucleotide binding protein (membrane protein) SRPI protein** sce4642 (X)		
11; 139	**Putative secreted proteins** Sce4014 (R)		

Tab. 10: The serine and tyrosine phosphorylated proteins detected in So ce56. 23 serine phosphorylated proteins and 28 tyrosine phosphorylated proteins were detected (Fig. 20). The spot numbers were the same as given in table 8. The COG categories letters were given in in brackets.

Spot No.	Serine phosphorylated proteins	Spot No.	Tyrosine phosphorylated proteins
59	**Phosphoglycerate kinase** sce7349 (G)	56	**Phosphopyruvate hydratase Enolase** sce7698 (G)
127	**Triose-phosphate isomerase** sce7348 (G)	61	**Xylose isomerase** sce5429 (G)
95	**Agmatinase** sce0044 (E)	68	**Glycine hydroxymethyltransferase** sce6587 (E)
98	**Ketol-acid reductoisomerase** sce3732 (E)	89	**3-isopropylmalate dehydrogenase** sce3735 (E)
128	**Phosphoribosylamine-glycine ligase** sce9014 (F)	21	**Glutathione synthase (gshB)** sce7568 (H)
152	**Pyridoxine-5-phosphate synthase, Vitamin B6** sce5839 (H)	62	**Adenosylhomocysteinase** sce2963 (H)
94	**Thioredoxin-disulfide reductase** sce7636 (O)	29	**IMP dehydrogenase/GMP reductase** sce0088 (F)
156	**Peroxidase** sce6959 (O)	173	**Nucleoside diphosphate kinase** sce2949 (F)
157	**Superoxide dismutase sodA** sce0071 (P)	71	**Acetyl CoA C-acyltransferase[TMH]** sce7554 (I)
110	**Putative protein phosphatase Diadenosine tetraphosphatase** sce7256 (T)	72	**Phosphate ABC transporter PstS[SignalP]** sce2946 (P)
11	**Putative secreted protein[Signal P]** sce4014 (R)	147	**FHA domain protein** sce8329 (T)
		172	**Organic hydroperoxide resistance protein** sce0181 (O)
		65	**UDP-glucose 6-dehydrogenase** sce2793 (M)
		102	**Putative phosphoesterase Phosphohydrolases** sce3464 (R)
		111	**Hypothetical protein Phycocyanin α lyase** sce8617 (X)
		155	**Secreted protein Hcp Hemolysin** sce4994 (S)
Phosphorylated proteins in So ce56, which have might have serine and tyrosine sites.			
32	**Pyruvate kinase 1** sce4540 (G)	32; 33	**Pyruvate kinase 1** sce4540 (G)
74	**Glyceraldehyde-3-phosphate dehydrogenase** sce7350 (G)	74	**Glyceraldehyde-3-phosphatedehydrogenase** sce7350 (G)
76	**Fructose-bisphosphate aldolase** sce1923 (G)	76	**Fructose-bisphosphate aldolase** sce1923 (G)
64	**Aldehyde dehydrogenase** sce0676 (C)	64	**Aldehyde dehydrogenase** sce0676 (C)
112	**Succinate-CoA ligase (ADP-forming)** sce9141 (C)	112	**Succinate-CoA ligase (ADP-forming)** sce9141 (C)
108; 109; 114	**Malate dehydrogenase** sce1050 (C)	108; 109; 114	**Malate dehydrogenase** sce1050 (C)
45	**Glutamate-ammonia ligase** sce7210 (E)	45	**Glutamate-ammonia ligase** sce7210 (E)
75	**Aspartate-semialdehyde dehydrogenase** sce5347 (E)	75	**Aspartate-semialdehyde dehydrogenase** sce5347 (E)
103	**Branched-chain-amino-acid transaminase (ilvE)** sce6015 (E)	103	**Branched-chain-amino-acid transaminase (ilvE)** sce6015 (E)
66	**Adenylosuccinate synthase** sce8895 (F)	66	**Adenylosuccinate synthase** sce8895 (F)
154	**Superoxide dismutase sodB** sce4167 (P)	154	**Superoxide dismutase sodB** sce4167 (P)
96	**Putative nucleotide binding protein (membrane protein) SRPI protein** sce4642 (X)	96	**Putative nucleotide binding protein (membrane protein) SRPI protein** sce4642 (X)

Tab. 11: Blue-Native PAGE from cytosolic proteins. 5 proteins in the first dimension and 33 proteins of the second dimension were identified (Fig. 21). The identified of the second dimension were given in numbers, the identified proteins of the first dimension depicted letters.

Spot	Protein (Accession)	MW(calc)	p*I*(calc)	Score	Coverage

Second dimension (SDS-Tricine-PAGE):

Lipid transport and metabolism (I):

20	**Butyryl-CoA dehydrogenase** (EC 1.3.99.2) sce1166	42149	5.4	74	14
26	**3-hydroxybutyryl-CoA dehydratase** (EC 4.2.1.55) sce0250	28510	6.19	119	27
28	**Butyryl-CoA dehydrogenase** (EC 1.3.99.2) sce3575	67254	5.87	72	19

Carbohydrate transport and metabolism (G):

6	**Glucose-6-phosphate isomerase** (EC 5.3.1.9) sce5669	58980	5.97	60	10
9	**Xylose isomerase** (EC 5.3.1.5) sce5429	49930	5.8	165	59
10; 11	**Glycogen phosphorylase** (EC 2.4.1.1) sce4388	97724	5.9	88	16

Energy production and conversion (C):

8	**Succinate dehydrogenase** (EC 1.3.99.1) sce6554	70465	8.98	74	8

Amino acid transport and metabolism (E):

2-5	**Glutamate--ammonia ligase** (EC 6.3.1.2) sce7210	52139	5.89	56	16
13; 14	**Aspartate transaminase** (EC 2.6.1.1) sce6239	45916	7.71	79	23
16	**Aryl-alcohol dehydrogenase** (EC 1.1.1.91) sce5264	49357	10.29	55	12
17; 29; 30	**Lactate dehydrogenase** (EC 1.1.1.27) **Malate dehydrogenase** (EC 1.1.1.37) sce1050	33184	8.55	69	13
18	**4-aminobutyrate transaminase** (EC 2.6.1.19) sce9194	51002	6.89	107	25

| 23 | **Agmatinase** (EC 3.5.3.11) sce0044 | 34310 | 6.03 | 59 | 21 |

Nucleotide transport and metabolism (F):

| 7 | **Aspartate carbamoyltransferase** (EC 2.1.3.2) sce3822 | 34648 | 10.07 | 70 | 15 |

Posttranslational modifications (O):

| 1 | **Heat shock protein groEL (HSP 60 family)** sce5911 | 57987 | 5.45 | 102 | 18 |
| 32 | **Endopeptidase Clp ATP-dependent** (EC 3.4.21.92) sce3147 | 24210 | 6.4 | 50 | 15 |

<u>Secondary metabolites transport and metabolism (Q):</u>

| 19 | **Polyketide synthase chiF** (EC 2.3.1.41) sce4133 | 626946 | 6.17 | 51 | 7 |

Signal transduction mechanisms (T):

| 22 | **Serine/threonine protein kinase two-component sensor domain** (EC 2.7.11.1) sce5838 | 201467 | 6.15 | | |

Inorganic ion transport and mechanism (P):

| 33 | **Superoxide dismutase sodA** (EC 1.15.1.1) sce0071 | 22805 | 6.17 | 72 | 16 |

Hypothetical proteins (X/S/R):

12	**Conserved hypothetical protein** sce1792	36931	7.62	52	8
15	**Conserved hypothetical protein** sce4374	38447	5.34	97	25
21	**Hypothetical protein** sce0278	21255	10.26	48	26
24	**Conserved hypothetical protein** sce0859	30520	5.56	61	18
27	**Hypothetical protein**[SignalP, Tat] **Phosphatase** sce0936	85810	4.66	62	9

<u>First dimension (BN-PAGE):</u>

| a) | **Conserved hypothetical protein** sce0860 | 25990 | 12.73 | 50 | 14 |
| b) | **Glutamate--ammonia ligase** (EC 6.3.1.2) (COG E) sce7210 | 52139 | 5.89 | 62 | 13 |

c)	**Endopeptidase Clp ATP-dependent** (EC 3.4.21.92) (COG O) sce3147	24210	6.4	79	13
d)	**Maltoporin precursor**[SignalP, Tat] (TC 1.B.3.1.1) (COG G) sce7619	52055	6.23	92	21
e)	**Putative Phosphomethylpyrimidin kinase** (COG H) (EC 2.7.4.7) sce0656	28018	7.66	47	36

Tab. 12: Identified extracellular proteins of So ce56 analyzed via MALDI-TOF-MS. The 41 identified proteins are sorted according to their predicted function and cellular location relating to the numeration in figure 22. Furthermore, it includes the Signal P results. The figures MW(calc) and pI(calc) were calculated by the MASCOT software, whereas the MW(gel) and pI(gel) values were observed spot position in the 2-D gel.

Spot	Protein (Accession)	MW(calc/gel)	pI(calc/gel)	Score	Coverage
Extracellular proteins:					
1; 2; 9; 11; 12; 25; 26; 27	**Cellulase**[SignalP] (EC 3.2.1.4) sce8953	86962 / 71000	4.6 / 4.7	197	24
8	**Putative secreted protein**[SignalP, Tat] sce8614	88530 / 51000	4.36 / 4.0	108	21
16	**Putative peptidase** sce4529	29790 / 51000	6.8 / 5.7	53	14
34; 68	**Putative Xanthomonalisin**[SignalP] (EC 3.4.21.101) sce3910	55609 / 30000	4.35 / 4.4	50	14
45; 64; 75	**Hypothetical protein Secreted cytotoxin** sce2967	18668 / 16000	6.19 / 6.2	114	73
52	**Conserved hypothetical protein**[SignalP] **Large extracellular α-helical protein** sce4409	202861 / 25000	6.51 / 5.3	52	5
61; 62	**Hypothetical protein**[SignalP] **Secreted protein** sce0172	20997 / 21000	4.4 / 4.1	92	52
70	**Putative typeVI secreted protein** (TC 9.A.34.1.1) sce4161	49851 / 20000	9.13 / 3.3	57	10
72; 80	**Hypothetical protein Possibly exported** sce7128	10708 / 10000	9.37 / 9.4	96	75
73; 74	**Hypothetical protein Exported protein** sce3202	10425 /13000	5.48 / 6.5	89	72
Membrane proteins:					
3; 4; 13; 14; 17; 18; 19; 21; 22; 30	**Hypothetical protein**[SignalP, Tat] **Phosphohydrolase** sce0969	60093 / 62000	5.1 / 5.2	105	24
7; 29; 32; 33; 37; 60	**Putative outer membrane lipoprotein**[SignalP] sce5067	49703 / 50000	3.78 / 3.1	84	23
10	**Putative ATPase**[SignalP, Tat] (EC 3.6.3.10) sce5843	183013 / 51000	4.6 / 4.3	55	5
31	**Hypothetical protein**[SignalP] **Lipoprotein** sce4343	60042 / 41000	3.52 / 3.1	76	14

43	**ABC transporter substrate binding**[SignalP, Tat] **nitrate/sulfonate/bicarbonate transporter** (TC 3.A.1.17.2) sce1321	39093 / 49000	9.83 / 9.1	53	19
58	**ABC transporter** **Putative cyanate porter** (TC 3.A.1.16.2) **Putative aromatic sulfonate porter** (TC 3.A.1.17.2) sce5488	29428 / 27000	6.2 / 3.6	54	23
24	**Hypothetical protein**[TMH] **Quinoprotein** sce1365	44081 / 35000	9.75 / 5.2	52	10
59; 69	**Conserved hypothetical protein**[TMH] **Cell surface protein** sce1531	40423 / 25000	4.38 / 4.1	68	16
77	**Secreted superoxide dismutase**[SignalP] **sod C** (EC 1.15.1.1) sce8431	21907 / 23000	5.7 / 8.4	67	27

Secondary metabolism:

71	**Hypothetical UDP-glucuronosyltransferase** sce3098	40353 / 12000	8.52 / 3.5	50	22

Metabolic enzymes:

40; 41; 47; 53	**Phosphoglycerate kinase** (EC 2.7.2.3) sce7349	43938 / 30000	5.55 / 5.5	103	31
5; 49; 57	**Phosphopyruvate hydratase Enolase** (EC 4.2.1.11) sce7698	45912 / 52000	5.14 / 5.3	77	23
42; 50; 51	**Pyruvate kinase** (EC 2.7.1.40) sce4540	51032 / 27000	6.29 / 5.4	111	27
48	**Pyruvate dehydrogenase (acetyl transferring)** (EC 1.2.4.1) sce3800	36314 / 23000	5.82 / 5.7	103	26
65	**Pyruvate dehydrogenase** (EC 1.2.4.1) sce3801	35930 / 15000	5.2 / 5.5	71	21
56	**Glutamate—ammonia ligase** (EC 6.3.1.2) sce7210	52367 / 22000	5.84 / 5.0	59	15
54	**Hypothetical protein Glyoxalase family protein** sce3094	15372 / 20000	5.05 / 5.4	62	35
66	**Lactate dehydrogenase** (EC 1.1.1.27) **Malate dehydrogenase** (EC 1.1.1.37) sce1050	33335 / 13000	8.55 / 4.3	72	18

Protein folding:

15	**Chaperone protein dnaK** (TC 1.A.33.1.2) sce9025	68908 / 51000	5.22 / 5.4	75	13
35	**Chloroplast GrpE protein** (TC 3.A.8.1.1) sce0004	21074 / 31000	4.82 / 4.5	70	24
44; 81; 82	**Peptidyl-prolyl cis-trans isomerase** (EC 5.2.1.8) sce0374	20748 / 25000	8.8 / 8.7	62	26
55	**Probable DnaJ molecular chaperone** (TC 3.A.5.8.1) sce0617	34546 / 21000	9.33 / 4.5	76	26
79	**GroES like protein (HSP10)** sce2780	10656 / 20000	9.42 / 9.9	132	56

DNA-interacting proteins:

20; 38; 78	**Elongation factor tufA** sce0841	43517 / 50000	6.46 / 6.5	89	20
23	**Conserved hypothetical protein** **Transposase (IS 1 family)** sce2831	41773 / 40000	10.13 / 5.2	52	18
36	**Transcriptional regulator**[HTH] **TetR family protein** sce3479	23548 / 29000	9.71 / 4.7	66	37

Protection:

39	**Putative Glutathione S-transferase** sce4509	30236 / 28000	9.86 / 6.4	69	25
46	**Thiol peroxidase** sce5724	17714 / 25000	5.74 / 6.5	81	42
63; 67	**Rubrerythrin** sce1753	15552 / 15000	5.37 / 4.7	72	47
76	**Organic hydroperoxide resistance protein** sce0181	14592 / 20000	7.41 / 7.6	85	48

Hypothetical protein:

28	**Conserved hypothetical protein** sce1224	15517 / 35000	6.31 / 4.3	65	40

Tab. 13: NanoLC-ESI MS/MS analysis of membrane proteins of So ce56.

List of the 66 identified membrane proteins of So ce56 analyzed with nanoLC-ESI-MS/MS. The identified membrane proteins numerated according to each gel-segment, shown in figure 24. The identified membrane proteins listed due to their predicted function and cellular location. The calculated MW was determined via a 10-150 kDa protein marker.

Spot	Protein (Accession)	MW(calc/gel)	p*I*(calc)	Score	Coverage
Membrane proteins:					
I	**Multidrug efflux protein**[SignalP, Tat] (TC 2.A.6.2.21) sce2988	59285/>80000	6.46	139	19
I	**Metal ion efflux outer membrane**[SignalP, Tat] **protein czcC exporter** (TC 1.B.17.2.2) sce8709	43114/>80000	8.85	126	24
I	**Maltoporin precursor**[SignalP, Tat] (TC 1.B.3.1.1) sce7619	52055/>80000	6.23	393	22
I	**RND family efflux transporter (AcrB)**[SignalP, Tat] (TC 2.A.6.2.14) sce1628	115380/>80000	6.46	51	3
I	**Hypothetical protein adventurous gliding motility protein AgmK** sce0252	416522/>80000	4.85	296	3
I	**TPR protein (7x) adventurous gliding motility protein** sce2921	237380/>80000	4.9	182	3
I	**TPR protein (2x) adventurous gliding motility protein** sce2920	196736/>80000	4.85	158	3
VIII	**Putative MglA1 protein gliding motility protein** sce7249	21939/>18000	7.68	86	13
II	**Putative outer membrane lipoprotein**[SignalP] sce5067	49247/>60000	4.09	53	4
II	**Hypothetical protein putative membrane protein** sce5122	66874/>60000	5.00	54	2
II	**Molybdopterin oxidoreductase iron-sulfur binding subunit** (TC 5.A.3.3.3) sce7585	107721/>60000	6.39	143	5
III	**ABC-type dipeptide transport system**[SignalP, Tat] (TC 3.A.1.5.6) sce7548	63470/>45000	8.43	178	7
III	**H$^+$-transporting two-sector ATPase** (TC 3.A.2.1.2) sce9361	68031/>45000	8.13	166	8

IV	H$^+$-transporting two-sector ATPase (TC 3.A.2.1.3) sce4444	50692/>35000	5.11	261	18
III; V	Hypothetical protein$^{SignalP, Tat}$ Surface DGF-1 protein sce3201	38745/>25000	4.66	205	15
VI	NADH dehydrogenase I chain I (nuo I) (EC 1.6.99.3 / TC 3.D.1.2.1) sce0528	25138/>25000	8.52	86	4
VI	GAF sensor domain protein sce1762	31108/>25000	5.22	123	15
VIII	Biopolymer transport protein$^{SignalP, Tat}$ (TC 1.A.30.2.2) sce5071	24579/>18000	9.16	116	8
IX	Conserved hypothetical protein^{TMH} sce0725	18618/>12000	6.73	100	12
X	Hypothetical protein^{3xTMH} Kef-type K+ transport systems sce0244	75209/>10000	5.80	43	5
VI	Outer membrane protein^{SignalP} (TC 1.A.30.1.3) sce5128	29508/>25000	8.69	121	12

Hypothetical proteins with Signal P:

II	Hypothetical protein^{SignalP} sce3203	79634/>60000	8.78	529	18
III	Conserved hypothetical protein TPR like protein^{SignalP} sce2914	64535/>45000	6.41	181	8

Extracellular protein:

II	putative secreted protein^{SignalP} sce2958	73837/>60000	8.59	141	5

Modifications:

V	TPR-like protein (2x) Similar to O-linked GlcNac transferase sce7919	54400/>25000	8.92	127	5

Degradative enzymes:

II	Predicted subtilisin-like protease sce3206	72356/>60000	6.22	59	1
II	ATP-dependent protease La (EC 3.4.21.53) sce5003	90327/>60000	5.71	285	10

Metabolic enzymes:

I	Carbamoyl-phosphate synthase (EC 6.3.4.16) sce2399	119512 />80000	5.92	204	7

II	**Protein kinase** (EC 2.7.1.37) sce6948	79282/>60000	6.23	194	7
III	**Glutamate – ammonia ligase** (EC 6.3.1.2) sce7210	52139/>45000	5.89	416	26
III	**Pyruvate kinase** (EC 2.7.1.40) sce4540	50691/>45000	6.32	272	16
III	**Phosphoenolpyruvate mutase** (EC 5.4.2.9) sce7305	60806/>45000	5.94	181	12
IV	**Glutamate dehydrogenase** (EC 1.4.1.3) sce6195	48499/>35000	8.45	86	2
IV	**Dihydrolipoyl dehydrogenase** (EC 1.8.1.4) sce8000	48957/>35000	7.12	100	7
IV	**Citrate synthase** (EC 2.3.3.1) sce8281	48140/>35000	7.26	110	8
IV	**Histidinol dehydrogenase** (EC 1.1.1.23) sce2464	47309/>35000	5.8	82	3
IV	**Methionine adenosyltransferase** (EC 2.5.1.6) sce7312	45848/>35000	8.77	117	9
IV	**Dihydrolipoyllysine-residue succinyltransferase** (EC 2.3.1.61) sce3802	45805/>35000	6.99	156	10
IV	**UDP-glucose-6-dehydrogenase** (EC 1.1.1.22) sce0875	48448/>35000	6.62	484	26
IV; V	**Phosphopyruvate hydratase Enolase** (EC 4.2.1.11) sce7698	45885/>35000	5.35	337	20
V	**Glyceraldehyde-3-phosphate dehydrogenase** (EC 1.2.1.12) sce7350	36917/>25000	7.14	477	26
V	**Ketol-acid reductoisomerase** (EC 1.1.1.86) sce3732	36352/>25000	6.09	307	21
V	**Lactate dehydrogenase** (EC 1.1.1.27) sce1050	33165/>25000	7.63	146	12
IV; V	**Agmatinase** (EC 3.5.3.11) sce0044	34290/>25000	6.03	221	16

DNA interaction proteins:

I	**DNA-directed RNA polymerase** **140 kDa subunit (rpo B)** (EC 2.7.7.6) sce0410	154949/>80000	5.4	142	4
I	**DNA-directed RNA polymerase** **β-subunit (rpo C)** (EC 2.7.7.6) sce0411	158729/>80000	7.36	260	5
IX	**50 ribosomal protein L7/L12** **(rpl L)** sce0409	13435/>12000	5.13	59	14
III; VI	**Conserved hypothetical protein** **Rhs element Vgr protein** sce6784	87435/>45000	8.82	188	8
VII	**Response regulator**[HTH] sce0622	22872/>20000	6.38	320	30
VII	**DNA-binding response regulator** sce5073	26281/>20000	5.57	133	16
V	**DNA-directed RNA polymerase** **alpha subunit** (EC 2.7.7.6) sce7936	38452/>25000	5.29	115	7
II	**Elongation factor (EF)** sce0644	76986/>60000	5.68	90	5
V	**Elongation factor (tuf A1)** sce0402	43347/>25000	6.44	217	14
IX	**Putative DNA binding protein** sce7400	16138/>12000	10.47	285	30
X	**Histone-like protein** **bacterial nucleoid** **DNA-binding protein** sce8278	12071/>10000	10.36	155	27
X	**Histone-like protein** **bacterial nucleoid** **DNA-binding protein** sce6591	11979/>10000	11.21	64	25

Proteinfolding:

III	**Heat shock protein groEL** **HSP60 family** sce5911	57952/>45000	5.61	380	19
VIII	**Peptidyl-prolyl cis-trans isomerase** (EC 5.2.1.8) sce0374	20634/>18000	7.83	58	13

Protection:

VI	**Glutaredoxin-like protein** sce6471	33476/>25000	5.35	122	15
VII	**Glutathione S-transferase** (EC 2.5.1.18) sce4509	30218/>20000	9.38	72	8

VII	**Peroxidase** (EC 1.11.1.7) sce0170	23687/>20000	6.3	115	13
VIII	**Peroxidase** (EC 1.11.1.7) sce6959	20600/>18000	6.44	96	29
VIII	**Conserved hypothetical protein Alkylhydroperoxidase AhpD core** sce5383	19140/>18000	7.93	65	7

Hypothetical proteins:

III	**Conserved hypothetical protein** sce4981	55324/>45000	5.49	163	12
IV	**Conserved hypothetical protein** sce0425	44667/>35000	5.59	76	10
IX	**Conserved hypothetical protein** sce0957	19091/>12000	7.93	237	24

Tab. 14: Blue-Native PAGE from membrane proteins. The identified proteins of the second dimension were given in numbers and the identified proteins of the first dimension were given in letters (Fig. 26).

Spot	Protein (Accession)	MW(calc)	p*I*(calc)	Score	Coverage

Second dimension (SDS-Tricine-PAGE):

Lipid transport and metabolism (I):

Spot	Protein (Accession)	MW(calc)	p*I*(calc)	Score	Coverage
5	**Butyryl-CoA dehydrogenase** (EC 1.3.99.2) sce3575	57254	5.86	151	27
13	**3-hydroxybutyryl-CoA dehydrogenase** (EC 4.2.1.55) sce0250	28510	6.19	80	27
16	**Butyryl-CoA dehydrogenase** (EC 1.3.99.2) sce1166	42149	5.4	170	35
22	**3-hydroxyacyl-CoA dehydratase** (EC 1.1.1.157) sce7905	32527	8.76	58	15
23	**Enoyl-CoA dehyrogenase** (EC 1.1.1.35) sce7555	85579	6.42	152	22

Carbohydrate transport and metabolism (G):

Spot	Protein (Accession)	MW(calc)	p*I*(calc)	Score	Coverage
7	**Transaldolase tal1** (EC 2.2.1.2) sce1460	36144	5.86	71	16
6	**4-alpha-glucanotransferase homolg** (EC 2.4.1.25) sce0351	73407	6.31	125	20
17	**Glyceraldehyde-3-phosphate dehydrogenase** (EC 1.2.1.12) sce7350	36939	7.71	179	54
14	**Beta-glucosidase bglX** (EC 3.2.1.21) sce2601	78220	4.99	119	19

Energy production and conversion (C):

Spot	Protein (Accession)	MW(calc)	p*I*(calc)	Score	Coverage
8	**Lactate dehydrogenase** (EC 1.1.1.27) **Malate dehydrogenase** (EC 1.1.1.37) sce1050	33184	8.55	53	15
24	**Aryl-alcohol dehydrogenase** (EC 1.1.1.91) sce5264	49357	10.29	85	18

Amino acid transport and metabolism (E):

Spot	Protein (Accession)	MW(calc)	p*I*(calc)	Score	Coverage
4	**Glycine hydroxymethyltransferase** (EC 2.1.2.1) sce6587	45527	7.07	127	26

28	**ABC-type dipeptide transport system**[Signal P] (TC 3.A.1.5.6) sce8424	63871	8.87	50	7
30	**Glutamate--ammonia ligase** (EC 6.3.1.2) sce7210	52139	5.89	104	23

Secondary metabolites transport and metabolism (Q):

3	**Cytochrome P450** sce2191	52423	9.42	50	15

Cellwall biogenesis (M):

15	**Cyclopropane-fatty-acyl phospholipid synthase** (EC 2.1.1.79) sce2529	33551	8.49	53	12

Signal transduction mechanisms (T):

1	**Serine/threonine kinase** (EC 2.7.11.17) sce1019	49942	9.63	49	14

Defense mechanism (V):

21	**ABC transporter ATP-binding putative lipooligosaccharide exporter** (TC 3.A.1.102.1) sce5573	33647	5.44	52	30

Inorganic ion transport and mechanism (P):

11	**Na^+/H^+ antiporter nhaA** (TC 2.A.33.1.1) sce3269	79773	11.65	59	13

Translation (J):

9	**50S ribosomal protein L14 rplN** sce7953	13323	10.58	58	29
18	**Polynucleotide phosphatase pnpA** (EC 2.7.7.8) sce4541	36854	5.63	50	16
25	**30S ribosomal protein S13 rpsM** sce7939	14426	11.22	50	25
31	**50S ribosomal protein L22 rplV** sce7958	12348	11.64	53	33

Coenzyme transport and metabolism (H):

19	**Adenosylhomocysteinase ahcY** (EC 3.3.1.1) sce2963	47785	5.91	111	27

Posttranslational modifications (O):

27	**Heat shock protein (HSP20 family)** sce0577	17224	9.41	98	45

26	**Probable serine protease** sce1673	98246	12.29	49	4

Hypothetical proteins (X/R/S):

2	**Conserved hypothetical protein**[SignalP] **α-2-macroglobulin-like protein** sce4409	202861	6.51	61	6
10	**Conserved hypothetical protein** sce4994	18797	6.22	162	58
12	**Hypothetical protein**[SignalP] sce0478	54580	4.00	34	6
20	**Hypothetical protein**[TMH] sce4257	46680	9.95	55	18
29	**TPR domain protein** sce1616	155131	9.66	59	5

First dimension (BN-PAGE):

a)	**50S ribosomal protein L14 rplN** (COG J) sce7953	13323	10.58	53	35
b)	**50S ribosomal protein L22 rplV** (COG J) sce7958	12348	11.64	53	33
c)	**Carboxyl-and carbamoyltransferase** (COG O) sce2401	63144	7.81	51	6
d)	**RHS family** (COG M) **carbohydrate binding protein** sce3545	60844	9.08	47	12

Tab. 15: Outer membrane proteins from Sorangium cellulosum So ce56 identified by nanoLC-ESI-MS/MS. Identification of 35 outer membrane proteins analyzed with nanoLC-ESI. The identified proteins of each segment (I-VII) correspond to the numeration in the outer membrane 1-D SDS-PAGE gel (Fig. 27). Moreover the calculated MW and p*l* values were given. The observed MW in the gel was estimated by using a protein marker between 10-150 kDA.

Spot	Protein (Accession)	MW(calc/gel)	p*l*(calc)	Score	Coverage
Outer membrane proteins:					
I	**Hypothetical protein**[SignalP, Tat] **accumulation-associated protein** sce5126	77922/>120000	5.08	48	1
II	**Probable tonB-dependent receptor**[SignalP, Tat] (TC 1.B.14.1.6) sce9157	113997/>70000	5.11	79	1
II	**Oar protein**[SignalP] **tonB dependent receptor cellular adhesion during fruiting body** sce4255	118450/>70000	5.02	78	2
II	**Putative lipoprotein**[SignalP, Tat] sce2691	47150/>70000	4.74	44	2
III; IV	**Conserved hypothetical protein OMP barrel autotransporter**[SignalP] sce1186	52268/>55000	4.49	178	9
III; IV	**Hypothetical protein**[SignalP] **phosphate selective porin O and P** sce7966	61246/>55000	5.29	238	11
III	**Probable tonB-dependent receptor fecA**[SignalP, Tat] (TC 1.B.14.1.5) sce8808	7401/>550005	5.68	44	2
I; IV; V; VI; VII	**Maltoporin precursor**[SignalP, Tat] (TC 1.B.3.1.1) sce7619	52055/>45000	6.23	559	27
IV	**OMP barrel autotransporter**[Signal P] (TC 1.B.12.1.1) sce7537	52047/>45000	4.38	94	3
IV	**Putative type VI secretory pathway**[Signal P] (TC 9.A.34.1.1) sce4985	139301/>45000	6.28	51	6
IV	**Protein kinase putative lipoprotein**[SignalP, Tat] (EC 2.7.11.1) sce4176	142981/>45000	6.80	48	6
IV	**OMP efflux protein**[SignalP, Tat] (TC 1.B.17.3.1) sce3619	53628/>45000	9.16	45	7
VI	**Unknown protein**[SignalP] **Pilus assembly protein** sce0254	28592/>35000	4.15	81	9

VI	**Hypothetical protein**[SignalP, Tat] **Surface DGF-1 protein** sce3201	38745/>35000	4.66	70	3

Extracellular proteins:

I; III; IV; V	**Putative secreted protein**[SignalP] sce4014	68751/>55000	4.9	231	13

Inner membrane and periplasmic proteins:

I; IV	**Hypothetical protein**[SignalP, Tat] **probable ATPase** sce5242	208040/>120000	5.79	246	12
II	**Conserved hypothetical protein**[TMH] **Fe^{2+}-dicitrate sensor membrane component** sce3657	44433/>70000	7.01	40	19
II	**Hypothetical protein**[SignalP, Tat] **Phosphatase** sce0936	85810/>70000	4.66	160	5
VII	**Secreted superoxide dismutase**[SignalP] **sodC** (EC 1.15.1.1) sce8431	21736/>30000	6.05	204	17
III	**ABC-type dipeptide transport system**[SignalP, Tat] (TC 3.A.1.5.6) sce7548	63470/>55000	8.43	221	11
III	**Cation transporting P-type ATPase**[10xTMH] (TC 3.A.3.2.4) sce2485	98954/>55000	5.83	52	4
I; V	**Branched-chain amino acid ABC transporter**[SignalP, Tat] (TC 3.A.1.4.6) sce8312	43095/>40000	8.22	103	6
V	**ABC-type xylose transport system xylF** (TC 3.A.1.2.4) sce6008	38721/>40000	6.07	57	4
VI	**Putative nucleotide binding protein SRPI** **(major membrane protein)** sce4642	33363/>35000	6.19	51	2
VII	**Putative membrane bound zinc metallopeptidase** (TC 3.A.16.1.2) sce0417	67483/>30000	7.86	43	3
VII	**Hypothetical protein**[SignalP] **Gluconolactonase precursor periplasma** sce9199	40244/>30000	5.35	45	7

Metabolic enzymes:

III; IV	**4-α-glucanotransferase glycogen debranching enzyme** (EC 2.4.1.25) sce2296	71744/>55000	5.42	60	8
IV	**Glutamate--ammonia ligase** (EC 6.3.1.2) sce7210	52139/>45000	5.89	59	7

Signal transduction:

I	**Serine/threonine protein kinase** (EC 2.7.1.37) sce0184	123037/>120000	6.36	55	6
IV	**Serine/threonine protein kinase** (EC 2.7.1.37) sce8728	139820 />45000	5.52	50	8

Secondary metabolism:

IV	**Polyketide synthase chiF** (EC 2.3.1.41) sce4133	626946/>45000	6.17	50	4
VI	**Sensor histidine kinase**[SignalP, Tat] **Jer3 (Jerangolid gene cluster, identity: 85%)** (TC 2.A.21.9.1) sce7800	54741/>35000	6.66	51	5
VI	**Polyketide synthase Etnangien-PKS** (EC 2.3.1.41) sce3190	389790/>35000	6.06	46	2

DNA-interacting proteins:

IV	**ATP-dependent DNA ligase** sce3523	82845/>45000	9.77	63	6

Hypothetical proteins:

IV; VII	**Hypothetical protein**[SignalP, Tat] sce4619	72613/>45000	6.23	52	6

Tab. 16: Isolated outer membrane vesicle proteins from So ce56 extracellular fraction. The 10 identified protein bands from the SDS-PAGE are listed after the numeration in figure 30. The score and the sequence coverage were given in percentages.

Spot	Protein (Accession)	MW(calc)	p*I*(calc)	Score	Coverage
1; 3	**Maltoporin precursor**[SignalP, Tat] sce7616	52086	6.24	82	17
2	**Hypothetical protein**[SignalP, Tat] predicted phosphatase sce0936	85860	4.37	161	20
4 – 8	**Putative outer membrane lipoprotein**[SignalP] sce5067	49276	3.78	80	16
9	**Hypothetical protein**[SignalP] phosphate selective porin O and P sce7966	61282	5.06	60	13
10	**Hypothtical protein** probable Clp protease sce7556	10456	10.22	78	20

Tab. 17: Identified proteins from the cytosol (see Tab. 8) involved transport processes based on TC database searches.

SoCe ID	TC number	Transporter name	E-value TCDB	TC superfamily/ TC family	
sce0004	3.A.8.1.1	Mitochondrial protein translocase	2.00E-016	3.A.8 The Mitochondrial Protein Translocase (MPT) Family	
sce0181	9.B.74.1.2	The putative ABC-2-like protein	0.66	9.B.74 The Phage Infection Protein (PIP) Family	
sce2035	2.A.53.9.1	SulP homologue with fused C-terminal STAS/Rhodanese domains	2.00E-009	2.A.53 The Sulfate Permease (SulP) Family	
sce2780	3.A.3.6.5	Mono- and divalent heavy metal (Cu+, Ag+, Zn2+, Cd2+) ATPase	5.00E-004	3.A.3 The P-type ATPase (P-ATPase) Superfamily	
sce2946	3.A.1.7.1	Phosphate porter	1.00E-072	3.A.1 The ATP-binding Cassette (ABC) Superfamily	3.A.1.7 The Phosphate Uptake Transporter (PhoT) Family
sce3697	3.A.1.27.1	The γ-hexachlorocyclohexane (γ-HCH) uptake permease	6.00E-035	The ATP-binding Cassette (ABC) Superfamily	The Carbohydrate Uptake Transporter-1 Family
sce4785	1.C.67.1.1	The pore-forming hemolysin	0.14	1.C.67 The SphH Hemolysin Family	
sce6785	3.A.7.9.1	The Icm/Dot protein secretion system	1.00E-008	3.A.7 The Type IV (Conjugal DNA-Protein Transfer or VirB) Secretory Pathway Family	
sce7548	3.A.1.5.6	The β-glucoside (cellobiose (β-1,4) uptake porter	7.00E-065	3.A.1 The ATP-binding Cassette (ABC) Superfamily	3.A.1.5 The Peptide/Opine/Nickel Uptake Transporter Family
sce9025	1.A.33.1.2	Heat shock protein-70 homologue, DnaK	0	1.A.33 The Cation Channel-forming Heat Shock Protein-70 (Hsp70) Family	
sce9360	3.A.2.1.1	H+-translocating F-type ATPase	8,00E-044	3.A.2 The H+- or Na+-translocating F-type, V-type and A-type ATPase (F-ATPase) Superfamily	

Tab. 18: Identified extracellular proteins (Tab. 12) involved in transport processes (TC database).

SoCe ID	TC number	Transporter name	E-value TCDB	TC superfamily TC family	
sce0004	3.A.8.1.1	Mitochondrial protein translocase	2.00E-016	3.A.8 The Mitochondrial Protein Translocase (MPT) Family	
sce0617	3.A.5.8.1	The general secretory pathway (Sec-SRP) complex	5,00E-008	3.A.5 The General Secretory Pathway (Sec) Family	
sce1321	3.A.1.17.2	Aromatic sulfonate porter	1,00E-017	3.A.1 The ATP-binding Cassette (ABC) Superfamily	3.A.1.17. The Taurine Uptake Transporter Family (Similar to 3.A.1.12 and 3.A.1.16)
sce4161	9.A.34.1.1	VasA-L of Vibrio cholerae (Pukatzki *et al.*, 2006)	2,00E-039	9.A.34 The Putative Type VI Symbiosis/Virulence Secretory Pathway (VISP) Family	
sce5488	3.A.1.16.2	Cyanate porter	4,00E-034	3.A.1 The ATP-binding Cassette (ABC) Superfamily	3.A.1.16. The Nitrate/Nitrite/Cyanate Uptake Transporter Family (Similar to 3.A.1.12 and 3.A.1.17)
sce5488	3.A.1.17.2	Aromatic sulfonate porter	6,00E-034	3.A.1 The ATP-binding Cassette (ABC) Superfamily	3.A.1.17. The Taurine Uptake Transporter Family (Similar to 3.A.1.12 and 3.A.1.16)
sce5488	3.A.1.16.1	Nitrate/nitrite porter	3,00E-033	3.A.1 The ATP-binding Cassette (ABC) Superfamily	3.A.1.16. The Nitrate/Nitrite/Cyanate Uptake Transporter Family (Similar to 3.A.1.12 and 3.A.1.17)
sce9025	1.A.33.1.2	Heat shock protein-70 homologue, DnaK	0	1.A.33 The Cation Channel-forming Heat Shock Protein-70 (Hsp70) Family	

Tab. 19: Identified membrane proteins (Tab. 13) involved in transport processes (TC database).

SoCe ID	TC number	Transporter name	E-value TCDB	TC superfamily TC family	
sce1628	2.A.6.2.14	Bile salt exporter	1.00E-117	2.A.6 The Resistance-Nodulation-Cell Division (RND) Superfamily	2.A.6.2.Hydrophobe/ Amphiphile Efflux-1 Family
sce2988	2.A.6.2.21	The multidrug (aminoglycosides, tetracycline, erythromycin, ofloxacin, etc.) efflux pump	2.00E-005	2.A.6 The Resistance-Nodulation-Cell Division (RND) Superfamily	2.A.6.2 The (Largely Gram-negative Bacterial) Hydrophobe/ Amphiphile Efflux-1 Family
sce4444	3.A.2.1.3	H+-translocating F-type ATPase	1.00E-170	3.A.2 The H+- or Na+-translocating F-type, V-type and A-type ATPase (F-ATPase) Superfamily	
sce5071	1.A.30.2.2	The TonB energy-transducing system	5.00E-018	1.A.30 The H+- or Na+-translocating Bacterial Flagellar Motor 1ExbBD Outer Membrane Transport Energizer (Mot-Exb) Superfamily	1.A.30.2 The TonB-ExbB-ExbD/TolA-TolQ-TolR (Exb) Family of Energizers for Outer Membrane Receptor (OMR)-Mediated Active Transport
sce5071	2.C.1.1.1	The TonB energy-transducing system	5.00E-018	2.C.1 The TonB-ExbB-ExbD/TolA-TolQ-TolR (TonB) Family of Auxiliary Proteins for Energization of Outer Membrane Receptor-mediated Active Transport	
sce5128	1.A.30.1.3	The flagellar motor (pmf-dependent) (MotAB)	4.00E-019	1.A.30 The H+- or Na+-translocating Bacterial Flagellar Motor 1ExbBD Outer Membrane Transport Energizer (Mot-Exb) Superfamily	1.A.30.1 The H+- or Na+-translocating Bacterial Flagellar Motor (Mot) Family
sce7585	5.A.3.3.3	Anaerobic dimethylsulfoxide/trimethylamine-N-oxide reductase	4.00E-035	5.A.3 The Prokaryotic Molybdopterin-containing Oxidoreductase (PMO) Family	
sce7619	1.B.3.1.1	LamB (MalL) maltoporin (maltose–maltoheptose)	9	1.B.3 The Sugar Porin Family	
sce8709	1.B.17.2.2	CzcC outer membrane exporter of Co2+, Cd2+, Zn2+	0.87	1.B.17 The Outer Membrane Factor (OMF) Family	
sce9361	3.A.2.1.2	Na+-translocating F-type ATPase	1.00E-110	3.A.2 The H+- or Na+-translocating F-type, V-type and A-type ATPase (F-ATPase) superfamily	

Tab. 20: Identified outer membrane proteins (Tab. 15) involved in transport processes (TC database).

SoCe ID	TC number	Transporter name	E-value TCDB	TC superfamily TC family	
sce0417	3.A.16.1.2	ER retrotranslocon (yeastl)	2.00E-037	3.A.16 The Endoplasmic Reticular Retrotranslocon (ER-RT) Family	
sce2485	3.A.3.2.4	Ca2+-ATPase (efflux)	1.00E-173	3.A.3 The P-type ATPase (P-ATPase) Superfamily	
sce3619	2.A.6.2.23	The multidrug (β-lactams, aminoglycerides (gentamycin and streptomycin) macrolides (erythromycin) and dye (acriflavin)) efflux pump	1.00E-008	2.A.6 The Resistance-Nodulation-Cell Division (RND) Superfamily	2.A.6.2. The (Largely Gram-negative Bacterial) Hydrophobe/Amphiphile Efflux-1 Family
sce4985	9.A.34.1.1	VasA-L of Vibrio cholerae	1.00E-051	9.A.34 The Putative Type VI Symbiosis/Virulence Secretory Pathway Family	
sce6008	3.A.1.2.4	Xylose porter	1.00E-086	3.A.1 The ATP-binding Cassette (ABC) Superfamily	3.A.1.2. The Carbohydrate Uptake Transporter-2 Family
sce7537	1.B.12.1.1	Autotransporter of adhesin involved in diffuse adherence	3.00E-005	1.B.12 The Autotransporter (AT) Family	
sce7548	3.A.1.5.6	The β-glucoside (cellobiose (β-1,4) uptake porter	7.00E-065	3.A.1 The ATP-binding Cassette (ABC) Superfamily	3.A.1.5. The Peptide/Opine/Nickel Uptake Transporter Family
sce7619	1.B.3.1.1	LamB (MalL) maltoporin (maltose–maltoheptose)	9	1.B.3 The Sugar Porin Family	
sce7800	2.A.21.9.1	The nitrogen sensor-receptor domain of the CbrA sensor kinase	5,00E-028	2.A.21 The Solute:Sodium Symporter Family	
Sce8312	3.A.1.4.6	The neutral amino acid permease, N-1 (transports pro, phe, leu, gly, ala, ser, gln and his)	4.00E-022	3.A.1 The ATP-binding Cassette (ABC) Superfamily	3.A.1.4. The Hydrophobic Amino Acid Uptake Transporter Family
sce8312	3.A.1.4.1	Leucine; leucine/isoleucine/valine porter (also transports phenylalanine and tyrosine)	5.00E-022	3.A.1 The ATP-binding Cassette (ABC) Superfamily	3.A.1.4. The Hydrophobic Amino Acid Uptake Transporter family
sce8808	1.B.14.1.5	IroN ferri-enterobactin (also ferricorynebactin) receptor	4.00E-010	1.B.14 The Outer Membrane Receptor Family	
sce9157	1.B.14.1.6	CirA colicin I/Fe3+ catecholate receptor	1.00E-012	1.B.14 The Outer Membrane Receptor Family	

Tab. 21: Identification of genes related to Jerangolid or Ambruticin biosynthesis clusters in the *Sorangium cellulosum* So ce56 genome by BLASTP. Moreover, putative polyketide synthases from So ce56 are also compared to the *Polyangium* database to look for putative jerangolid/ ambruticin sequence similarities. The identities are given in percentages.

Accession	(TC/EC No.)	Function prediction in So ce56	Ambruticin (%)/ Jerangolid(%)	other %
sce7795		hypothetical protein	- / -	88
sce7796		hypothetical protein [SignalP]	- / -	64
sce7797		LysR-transcriptional regulator[HTH]	amb1 (85)/ jer1(84)	-
sce_20050509_8912		cytochrome P450	amb2 (34)/ -	-
sce7798		hypothetical protein	- / jer2 (80)	-
sce7800	(TC 2.A.21.9.1)	sensor histidine kinase	amb3 (81)/ jer3 (85)	-
sce7801		sigma-54 dependent response regulator[HTH]	amb4 (93)/ jer4 (92)	-
sce7107	(TC 2.A.21.9.1)	sensor histidine kinase	amb5 (72)/ jer5 (73)	-
sce7805		conserved hypothetical protein	amb6 (95)/ jer6 (95)	-
sce7807	(TC 2.A.21.9.1)	two-component hybrid sensor and regulator	amb7 (62)/ jer7 (62)	-
sce7810	(EC 1.6.99.1)	putative regulatory protein	amb8 (75)/ -	-
sce7811		similar to xenobiotic reductase	amb9 (84)/ -	-
sce7812		hypothetical protein	- / -	87
sce0820	(EC2.3.1.41)	putative polyketide synthase	ambB (35)/ jerB (30)	-
sce3189	(EC 2.3.1.41)	putative polyketide synthase[HTH]	ambC (32)/ jerC (31)	-
sce0819	(EC 2.3.1.41)	putative polyketide synthase	ambD (35)/ -	-
sce0356	(EC 3.1.2.14)	putative thioesterase	- / jerE (40)	-
sce3188	(EC 2.3.1.41)	putative polyketide synthase	ambF (49)/ -	-
sce3192	(EC 2.3.1.41)	putative polyketide synthase	- / -	51

Tab. 22: Summarization of the identified proteins from each compartment of *Sorangium cellulosum* So ce56 compared to the predicted proteins of the So ce56 database and classified according to different COG categories. The identified/predicted proteins were given in numbers and percentages related to the total number of identified proteins from each compartment.

COG categories	Cytosolic proteins (129)	Membrane and periplasmic proteins (90)	Outer membrane proteins (35)	Outer membrane vesicle proteins (5)	Extracellular proteins (41)	Predicted proteins (9,367) (So ce genome)
E: Amino acid transport and metabolism	17 (13%)	9 (11%)	3 (8%)	-	1 (2%)	369 (4%)
G: Carbohydrate metabolism	15 (11%)	9 (11%)	3 (8%)	1 (20%)	4 (10%)	258 (3%)
C: Energy production and conversion	15 (11%)	9 (11%)	1 (3%)	-	4 (10%)	339 (3.6%)
P: inorganic ion transport and metabolism	4 (3%)	2 (2%)	5 (14%)	-	3 (7%)	217 (2.3%)
I: lipid transport and metabolism	6 (5%)	5 (5%)	-	-	-	204 (2.1%)
H: Coenzyme transport and metabolism	6 (4%)	2 (2%)	-	-	-	158 (1.7%)
F: Nucleotide transport and metabolism	7 (5%)	-	-	-	-	74 (1%)
Q: Secondary metabolite biosynthesis	4 (3%)	1 (1%)	2 (6%)	-	-	188 (2%)
B: Chromatin structure and dynamics	-	-	-	-	-	3 (0.03%)
L: Replication	1 (1%)	2 (2%)	1 (3%)	-	-	242 (2.6%)
K: Transcription	2 (2%)	6 (6%)	-	-	1 (2%)	775 (8%)
J: Translation	1 (1%)	7 (7%)	-	-	1 (2%)	191 (2%)
D: Cell cycle control	-	-	-	-	-	34 (0.4%)
N: Cell motility	-	1 (1%)	-	-	-	62 (0.7%)
M: Cell wall	1 (1%)	4 (4%)	2 (6%)	-	-	284 (3%)
V: Defense mechanism	-	2 (2%)	-	-	-	83 (0.9%)
U: Intracellular trafficking	-	1 (1%)	-	-	-	48 (0.5%)
O: Post-translational modification	14 (10%)	12 (13%)	1 (3%)	-	8 (20%)	237 (2.5%)
T: Signal transduction mechanisms	4 (3%)	2 (2%)	3 (8%)	-	1 (2%)	383 (4%)
S: Function unknown	3 (3%)	8 (8%)	1 (3%)	-	1 (2%)	514 (5.5%)
R: General function prediction only	13 (9%)	6 (6%)	1 (3%)	1 (20%)	1 (2%)	632 (6.7%)
X: No functional category	16 (12%)	8 (8%)	12 (34%)	3 (58%)	16 (39%)	4,068 (43.4%)
total Signal P number	4 (3%)	7 (7%)	11 (31%)	4 (80%)	8 (20%)	~1,296

Erklärung

Hiermit beantrage ich beim Promotionsausschuß der Fakultät für Biologie der Universität Bielefeld mit der vorliegenden Dissertation die Eröffnung des Promotionsverfahrens nach § 5 der Promotionsordnung (03. Juni 2002). Die Anfertigung der Dissertation mit dem Titel „ Comprehensive proteomics of *Sorangium cellulosum* So ce56" erfolgte unter der Betreuung von Prof. Dr. Alfred Pühler und Prof. Dr. Karsten Niehaus am Lehrstuhl für Genetik der Fakultät für Biologie der Universität Bielefeld.

Ich erkläre hiermit, dass ich die vorliegende Arbeit selbst angefertigt und nur angegebene Quellen und Hilfsmittel verwendet habe. Alle aus der Literatur entnommenen Zitate sind als solche kenntlich gemacht. Weiterhin erkläre ich, dass die vorliegende Dissertation weder vollständig noch in Auszügen einer anderen Fakultät mit dem Ziel vorgelegt worden ist, einen akademischen Titel zu erwerben. Ich bewerbe mich hiermit erstmalig um den Doktorgrad der Naturwissenschaften der Universität Bielefeld.

Bielefeld, den 31.10.2007

Aysel Alici